EFFECTS OF GAS METAL ARC WELDING PARAMETERS ON THE MECHANICAL AND CORROSION BEHAVIOUR OF AUSTENITIC STAINLESS STEEL IN SOME ENVIRONMENTS

BY

IBRAHIM MOMOH-BELLO OMIOGBEMI

(M.SC/ENG/11338/2011-2012)

DEPARTMENT OF MECHANICAL ENGINEERING

FACULTY OF ENGINEERING

AHMADU BELLO UNIVERSITY

ZARIA, NIGERIA

MAY, 2015

EFFECTS OF GAS METAL ARC WELDING PARAMETERS ON THE MECHANICAL AND CORROSION BEHAVIOUR OF AUSTENITIC STAINLESS STEEL IN SOME ENVIRONMENTS

BY

Ibrahim Momoh-Bello OMIOGBEMI, B.Eng (A.A.U, Ekpoma) 2008

(M.SC/ENG/11338/2011-2012)

A THESIS SUBMITTED TO THE SCHOOL OF POSTGRADUATE STUDIES,

AHMADU BELLO UNIVERSITY, ZARIA

IN PARTIAL FULFILLMENT OF THE REQUIREMENTS FOR THE AWARD

OF

MASTER DEGREE IN MECHANICAL ENGINEERING

DEPARTMENT OF MECHANICAL ENGINEERING

FACULTY OF ENGINEERING

AHMADU BELLO UNIVERSITY, ZARIA

NIGERIA

MAY, 2015

DECLARATION

I declare that the work in this thesisentitled **"Effects of Gas Metal Arc Welding Parameters on the Mechanical and Corrosion Behaviour of Austenitic Stainless Steel in Some Environments"**has been carried out by me in the Department of Mechanical Engineering, Faculty of Engineering, Ahmadu Bello University, Zaria, Nigeria under the supervision of Engr. (Dr.) D.S. Yawas and Engr. (Dr.) I. M. Dagwa. The information derived from literature has been duly acknowledged in the text and a list of references provided. No part of this thesis was previously presented for another degree or diploma at this or any other institution.

Ibrahim Momoh-Bello OMIOGBEMI Name of Student	…….....	……
	Signature	Date

CERTIFICATION

This thesisentitled **"EFFECTS OF GAS METAL ARC WELDING PARAMETERS ON THE MECHANICAL AND CORROSION BEHAVIOUR OF AUSTENITIC STAINLESS STEEL IN SOME ENVIRONMENTS"** meets the regulations governing the award of the degree of Master of Science of Mechanical Engineering, Ahmadu Bello University Zaria, and was approved for its contribution to knowledge and literary presentation.

Dr. D. S. Yawas		
Chairman, Supervisory Committee	(Signature)	(Date)
Dr. I. M. Dagwa		
Member, Supervisory Committee	(Signature)	(Date)
Dr. M. Dauda		
Head of Department	(Signature)	(Date)
Prof. A. Z. Hassan		
Dean, School of Postgraduate Studies	(Signature)	(Date)

DEDICATION

This work is dedicated to The Almighty GOD, my late lovely parents (Chief and Mrs. Bello Omiogbemi), my impeccable uncle and guardian (Engr. Kess Omiogbemi), my siblings and my beloved wife to be.

ACKNOWLEDGEMENT

This research would not have been possible without the help and support of many people. My profound gratitude will at first go to the Almighty God for the gift of life, good and the privilege to undertake this research.

I am indeed grateful to my supervisors; Engr. (Dr) D.S.Yawas and Engr. (Dr) I.M. Dagwa for their time, suggestions, contributions and interest in the research which has immensely contributed to the completion of this work.

My appreciation goes to Dr. F.G. Okibe of the Department of Chemistry, Ahmadu Bello University, Zaria for helping me with Design Expert Software. My appreciation to all member of staff of Mechanical Engineering Department, Ahmadu Bello University, Zaria for their support, especially Engr.(Dr) M. Afolayan, Engr. (Dr) F.O. Anafi, Engr. (Dr) G.Y. Pam, Engr. (Dr) D.M. Kullla and others for their suggestions and constructive criticisms which have made me a better researcher.

My gratitude to the management of Peugeot Automobile Company, Kaduna for their assistance during this research, especially Engr. Usifo Christian, Mr. David and Mr. Amadi.

I am indeed grateful to my beloved friends and colleagues Engr. I.A. Lucky, Mr. ObotMfun, Mr. Yakubu Michael, Mr. WadzaniDauda,Mr Sunday Alegbe, Engr. I.A. Amasa, Mr. A. Adegoke, Mr. Aderemi and Engr. S.A.Etukesssienand all my MSc colleagues, I am grateful for the esprit de corps you displayedand forall your moral support and encouragement during this study. I would like to thank everyone who contributed in one way or the other to make this work a success.

My spiritual fathers, Pastor W. F. Kumuyi, Pastor S. Dania, Pastor I. Zamdayu, Pastor E. Meshubi, Pastor L. Ejeh, late Pastor B. Longe, Pastor I. Elice, Pastor (Barr) J.J. Momoh, Pastor E.D. Akafyi and host of others, I will ever be appreciated of their prayers, spiritual nourishments, concern and encouragement. I am also indebted to the entire members of DLCF post graduate and staff and also for the entire members of DLCF Zaria region for their prayers and support during this research work.

I would like to express my deepest gratitude to all my siblings especiallyAliyu Bello, Juliet Ekhorose and Lucy Bello for their support and encouragement throughout the study. Last but not the least my heart sincere appreciation goes to my late parents Chief and Mrs. Bello Omiogbemi and also to my lovely caring uncle, Engr. (Chief) KessOmiogbemi for the training, support, encouragement and love I received from them. May the Almighty God bless you all.

TABLE OF CONTENTS

LIST OF FIGURES

LIST OF TABLES

LIST OF PLATES

LIST OF APPENDICES

ABBREVIATIONS AND SYMBOLS

%	-----	Percentage
°C	-----	Degree Celcius
^{o}F	-----	Degree Fahrenheit
ABU	-----	Ahmadu Bello University
AC	-----	Alternating Current
AISI	-----	American Iron and Steel Institute
ANSI	------	American National Standards Institute
AWS	------	American Welding Society
AMP	-----	Ampere
ANOVA	-----	Analysis of Variance
ASS	-----	Austenitic Stainless Steel
ASTM	-----	America Society of Testing and Materials
BCC	-----	Body Centered Cubic
CERT	-----	Constant Extension Rate Tensile test
Cl^{-}	----	Chloride Ion
CL	-----	Confidence Limit
cm/min	-----	Centimeter Per Minute
Cr	-----	Chromium
CV	-----	Coefficient of Variance
DC	-----	Direct Current
DCEN	-----	Direct Current Electrode Negative
DCSP	-----	Direct Current Straight Polarity
DF	-----	Degree of Freedom
EDS	-----	Energy Dispersive Spectrometer
EAF	-----	Electric Arc Furnace

E-MEM	-----	Eagle's Minimum Essential Medium
EPR	-----	Electrochemical Potentiokinetic Reactivation
FZ	-----	Fusion Zone
FCC	-----	Face Centered Cubic
Fe-C	-----	Iron-Carbon
FCAW-G	-----	Gas-shielded flux cored arc welding
FCAW	-----	Flux-Cored Arc Welding Processes
FDE	-----	Factorial Design of Experiment
GMAW	-----	Gas Metal Arc Welding
g/cm^3	-----	Gram per Centimeter Cube
g/dm^3	-----	Grams per Decimeter Cube
GTAW	-----	Gas Tungsten Arc Welding
HAZ	-----	Heat Affected Zone
HCl	-----	Hydrochloric Acid
HRA	-----	Rockwell Hardness Number Scale A
HS	-----	High Sulfur
IGC	-----	Intergranular Corrosion
IGSCC	-----	Intergranular Stress Corrosion Cracking
LS	-----	Low Sulfur
LSD	-----	Least Significance Difference
MPa	-----	Mega Pascal
Mo	-----	Molybdenum
$MgCO_3$	-----	Magnesium Carbide
NaOH	-----	Sodium Hydroxide
NDT	-----	Non-Destructive Techniques
Ni	-----	Nitrogen

PAN	-----	Peugeot Automobile Nigeria Limited
PBS	-----	Phosphate Buffered Saline
RSM	-----	Response Surface Methodology
R^2_{Pred}	-------	Predicted Regression Correlation
R2	-----	Regression Correlation
R^2adj	-----	Adjusted Regression Correlation
SAW	-----	Submerged Arc Welding
SCC	-----	Stress Corrosion Cracking
SEM	-----	Scanning Electron Microscope
SME	-----	Small and Medium scale Enterprise
SMAW	-----	Shielded Metal Arc Welding
SS	-----	Stainless Steel
StdDev	-----	Standard Deviation
SWPSs	-----	Standard Welding Procedure Specifications
USA	-----	United State of America
WIG	-----	Wolfram Inert Gas
WL	-----	Weight Loss
WRC	------	Welding Research Council
Wt	-----	Weight
XPS	-----	X-Ray Photoelectron Spectroscopy
XRD	-----	X-Ray Diffraction
$^{-}$OH	-----	Hydroxyl ion

ABSTRACTS

The resistance and susceptibility of austenitic stainless steel (ASS) type 304, exposed to sodium hydroxide (NaOH) and hydrochloric acid (HCl) media (0.5M concentrations) at ambient temperatures was investigated using design expert software 6.0.6 and scanning electron microscope (SEM). The austenitic stainless steel flat bar of 3mm thickness was cut into length of 100mm; they were further cut into two equal parts with the two faces plain to have a 90° angle, leaving a root and face gap of 2mm. The flat bars were then joined together using gas metal arc welding (GMAW) process using stainless steel electrode wire of 0.9mm diameter (G 19.9 L). After welding, some specimens were immersed in the two media (sodium hydroxide and hydrochloric acid) for forty (40) days in an interval of eight (8) days and some samples served as standards for comparison and analysis. Tensile, Izod impact and hardness tests were carried out. The results of the studies show that welding parameters and corrosion really affect the mechanical properties of the alloy, the control strength (without welding) was 225MN/m^2 while that of the welded without immersion (C_4) was 133MN/m^2. The control impact energy (without welding) was 11.5J, while that of the welded without immersion (C_3) was 21.7J. Also, the welded control sample without immersion (C_3) for hardness tests were FZ = 30.2HRA and HAZ = 35.1HRA. The design expert was used to determine the surface responses and interactions between the parameters while SEM was used to examine the test specimen's surface morphology after immersion in the corrosive media. It was found that increase in welding current and speed at constant voltage gave the optimum performance of the ASS weldment in NaOH and HCl environments obtained at speed of 30mm/sec to 40mm/sec and current of 100A to 110A. This shows a corresponding minimal material deterioration. Surface corrosion deposit composition was analyzed with the SEM paired with energy dispersive spectrometer (EDS). Mechanical destructive tests (hardness, impact and tensile tests) were also used to examine the materials optimum performance in sodium hydroxide and hydrochloric acid media and it was found that hardness, impact and tensile strength increased with increasing weld parameters. It is concluded from the research that relatively high speed and current at a constant voltage gives a satisfactory weldment with a better integrity. This research work showed the observed susceptibility of ASS type 304 to stress corrosion cracking and the aggressiveness of chloride ion (Cl^-) in the corrosive medium.

CHAPTER ONE

1.0 INTRODUCTION

1.1 Background

The importance of austenitic stainless steel (ASS) in industrial applications and development cannot be over-emphasized. Its excellent properties which range from high tensile strength, good impact strength, corrosion and wear resistances have found various applications in many engineering industries today. In addition, ASS sheets have gained wide acceptance in the fabrication of components, requiring high temperature resistance and corrosion resistance such as metal bellows used in expansion joints in aircraft, aerospace and petroleum industries. This material is used in almost all environments that require an optimization of these properties, some of which are low and high pressure boilers and vessels, fossil-fired power plant, flue gas desulphurization equipment, evaporator tubing, super heater reheating tubing and steam heaters and pipes to mention but a few (Streicher, 1977; Munoz et al., 2004;Galal et al., 2005 and Kondapalli et al., 2013).

The austenitic stainless steel has been dominating the manufacturing and metallurgical field since the time of its first commercial production of stainless steels. Superior properties combined with the comparable ease of production and fabrications due to their excellent weldability, make this steel a most favoured one (Sathiya et al., 2012).

Austenitic stainless steels have many advantages from a metallurgical point of view. They can be made soft enough (i.e., with a yield strength of about 200 MPa) to be easily formed by the same tools that work with carbon steel, but they can also be made

incredibly strong by cold work, up to yield strengths of over 2000 MPa (290 ksi)(www.asminternational.org). Their austenitic (face centered cubic-fcc) structure is very tough and ductile. They also do not lose their strength at elevated temperatures as rapidly as ferritic (body centered cubic-bcc) iron base alloys. The least corrosion-resistant versions can withstand the normal corrosive attack of the everyday environment that people experience, while the most corrosion-resistant grades can even withstand boiling seawater (www.asminternational.org). This steel (ASS), has a nickel content of at least 7%, which makes the steel structure fully austenitic and gives it ductility, a large scale of service temperature, non-magnetic properties and good weldability (Suresh et al., 2011).

Austenitic stainless steels are among the most widely used types of stainless steel. The most commonly used grades are the American Iron and Steel Institute (AISI) 300 series of alloys (Sedriks, 1996). Starting from the basic 304 alloy (Fe-19Cr-10Ni), Mo is added to improve resistance to pitting (2-3 wt. % in the case of type 316 and 3-4 wt. % in type 317). Sensitization due to Chromium depletion during welding and other heat treatments, and the possible resultant intergranular corrosion, can be avoided through the use of low-carbon grades (304L, 316L, 317L, in which C is limited to 0.03 wt. % max.). The addition of Cr also imparts greater oxidation resistance, whilst Ni improves the ductility and workability of the material at room temperature (Fraser, 2009).

Austenitic stainless steels offer excellent resistance to corrosion. These high chromium steels are ductile and strong. They are non-magnetic and can be readily formed and welded. Higher strengths can be obtained by cold working, although this makes the alloy slightly magnetic and may reduce its corrosion resistance(www.asminternational.org).

Because of its inherent corrosion resistance, austenitic stainless steels, known as 300 series (AISI standard), have become cost-effective, staple materials for long-term applications in many industrial sectors including gas, petroleum, petrochemicals, fertilizers, food processing, and pulp industries as well as power generating plants. They have found also widespread use for the manufacturing of chemical installations including stationary pressure tanks and tanks for transport of liquid and compressed gases, pipelines of high diameter in hydraulic power plants, for manufacturing of ships, for transport of chemicals and installations of drilling rigs, etc (Abdel-Monem, 2012).

As the name implies the microstructure of austenitic stainless steel consists entirely of fine grains of austenite in the wrought condition. When subjected to welding, however, a secondary ferrite phase may be formed on the austenite grain boundaries, in the heat affected zone and in the weld metal. The extent of the formation of this secondary phase may depend on the composition of the steel or filler material and the heat input during welding (www.boc.com.au).

Generally, when metals are exposed to an environment containing water molecules, they can give up electron, becoming themselves positively charged ions. The corrosion process (anodic reaction) of the metal dissolving as ions generates some electrons that are consumed by a secondary process (cathodic reaction); these two processes have to balance their charges (www.stoprust.com).

In another development, welding parameters are developed to achieve a specific weld quality and production output. However, a change in any parameter will have an effect on the final weld quality, so the welding variables normally are written down or stored in the welding equipment memory. Therefore, to determine the welding parameters, the

national and international welding standards and also welding experience in application are taken into consideration for gas metal arc welding method (Ugur et al., 2011).

Generally, duplex stainless steels have a mixture of austenitic and ferritic grains in their microstructure; addition of 5% Nickel to ferritic stainless steel gives a duplex stainless steel, and addition of 8% Nickel to ferritic stainless steel gives a fully austenitic stainless steel(www.keytometals.com).

1.2 Statement of the Problem

Many research findings have proved that improper techniques employed in welding austenitic stainless steels may lead to serious consequences of the welded structures (Avery, 1963; Parijslaan, 2002). Failure as a result of poor mechanical properties and poor corrosion resistance have also found their places in annals of times, from household equipment to industrial structures such as railways, road bridges, storage tanks and ocean liners. One of such failures is the corrosion cracking of a grade 304 stainless steel pipe improperly seam welded and meant for the conveying of glucose solution in Illinois USA (James, 2000). The Point Pleasant Bridge Disaster in Ohio in USA was traced to stress corrosion cracking initiated during welding (Chamberlain and Trethewey, 1988). Many other failures have proved to be welding prone or propagated.

However, a vast majority of repairs of failed components in industries are carried out using one of the welding processes and the success depends on many factors such as weldability of the material, type of damage, availability of suitable welding technique, possibility of carrying out pre- heating or post-weld heat treatment and post repair inspection by non-destructive techniques (NDT).

But with all the aforementioned favourable properties of ASS, they still fail mostly at weld points which can be as a result of the welding process, process variables used and the welding environmental conditions. Hence, it is therefore pertinent to investigate the influence of some welding parameters on the mechanical and corrosion behavior of austenitic stainless steel in hydrochloric acid (HCl) and sodium hydroxide (NaOH) environments.

1.3 Present Research

Arc welding is a type of welding that uses a welding power supply to create an electric arc between an electrode and the base material to melt the metals at the welding point. They can use either direct (DC) or alternating (AC) current, and consumable or non-consumable electrodes. The process of arc welding is widely used because of its low capital and running costs(http://www.jansinc.com/welding.html). In this research, the effects of Gas Metal Arc Welding (GMAW) parameters on the mechanical and corrosion behaviour of austenitic stainless steel in some environments (HCl and NaOH) were investigated.

1.4 Aim and Objectives

The aim of this research is to investigate the effects of Gas Metal Arc Welding parameters on the mechanical and corrosion behaviour of austenitic stainless steel in hydrochloric acid and sodium hydroxide media. The specific objectives are:

1. to study the effects of GMAW parameters on the mechanical behaviour of austenitic stainless steels.
2. to determine the effects of GMAW parameters on the corrosion behaviour of austenitic stainless steel in acidic ax= b ccfzfcmnd basic media.

3. to determine the optimum GMAW parameters of austenitic stainless steel in acidic and basic media.
4. to use factorial design (Design-Expert 6.0.6 software) to determine the responses of the corrosion effects on the austenitic stainless steel.
5. to evaluate corrosion susceptibility of austenitic stainless steel in the different media mentioned above.

1.5Significance of the Study

Essentially, gas metal arc welding is one of the most widely used among the various arc welding processes today. There has been considerable interest in the investigation of the effects of various welding parameters on the mechanical and corrosion behaviour of weldments in different environments. During welding process, the fusion and heat affected zone (HAZ) normally undergo metallurgical transformations due to the weld heat, thus consequently affecting the mechanical properties of the materials leading to varying mechanical and microstructural properties of the material (Adebayo and Odepidan, 2002). Welding of austenitic stainless steels with high demand of sound mechanical properties require a high degree of control of welding parameters, consumable and thermo mechanical condition with regard to their effect on mechanical and metallurgical properties.

1.6 Scope of the Research

This research work is restricted to the effects of gas metal arc welding parameters on mechanical and corrosion behaviour of austenitic stainless steel plates when immersed in HCl and NaOH media. The study only covered the following areas:

1. The use of destructive mechanical testing machines to determine the respective mechanical properties of the samples.
2. The use of scanning electron microscope (SEM) to determine the surface morphology of the ASS before and after immersion in the corrosive media.
3. The use of gas metal arc welding process in the welding operation.
4. The use of grinding and polishing machines to grind and polish the samples before and after welding.
5. The use of Design-Expert 6.0.6 software to determine theeffect(s) and interactions between the parameters.
6. The use of digital weight balance to determine the weight loss of the samples after immersion in the corrosive environments (hydrochloric acid and sodium hydroxide).

CHAPTER TWO

2.0 LITERATURE REVIEW

2.1 Introduction to Stainless Steel

Generally, different types of steels are produced according to the properties required for their application, and various grading systems are used to distinguish steels based on the properties. According to the American Iron and Steel Institutes (AISI), steels can be broadly categorized into four groups based on their chemical compositions (www.metals.about.com, 2013);

1. Carbon Steels
2. Alloy Steels
3. Stainless Steels
4. Tool Steels

In 1913, stainless steel was accidentally discovered by an English Metallurgist named Harry Brearly, while working at Firth Brown's research laboratory. He made the discovery that adding chromium to low carbon steels produced a corrosion resistance metal called stainless steel (www.bssa.org.uk/about_stainless_steel.php?id=31).

Stainless steels are generally defined as an iron alloy containing a minimum of 10.5 wt% of chromium. The properties of stainless steels are primarily determined by the presence of this chromium. Apart from carbon and chromium content, modern stainless steels may also contain other important elements such as nickel, niobium, molybdenum, titanium, copper, manganese, silicon, nitrogen, phosphorus and sulfur. This level of chromium is the minimum level to ensure formation of a stable layer of protective chromium rich oxide on the surface. When exposed to corrosive environments, the chromium in the steel combines with oxygen in the atmosphere to form a thin layer of chromium-containing oxide known as passive film. If the metal is cut or

scratched and the passive film is disrupted, more oxide will quickly form and cover the exposed surface protecting it from oxidation corrosion (Jonathan and Gordon, 1999).

2.2 Stainless Steels Classification

Generally, stainless steels are commonly divided into six groups, depending on the specific amounts of alloying elements, which control the microstructure of the alloy.They are identified as ferritic, austenitic, martensitic, duplex, precipitation hardening and super alloys stainless steels (www.sppusa.com).

2.2.1 Ferritic stainless steels

Ferritic stainless steels have a "body-centered-cubic" (BCC) crystal structure, which is the same as pure iron at room temperature.

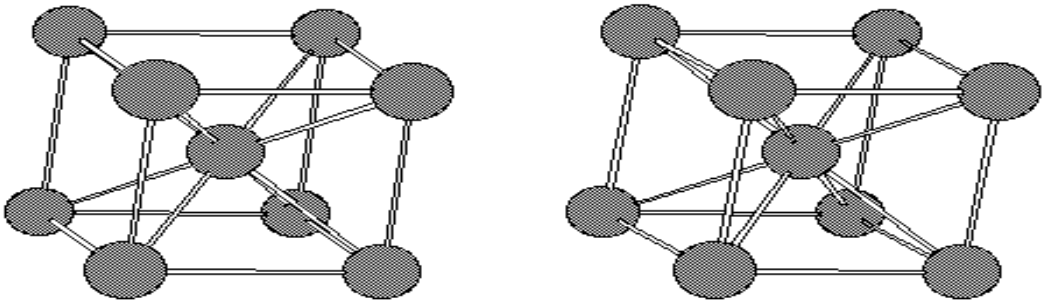

Figure 2.1: Ferritic stainless steel structures (www.bssa.org.uk/topics.php?article=20)

Ferritic stainless steels are a nickel free alternative suitable for various applications ranging from rough industrial applications of grade 403 to 421 having corrosion resistance comparable to 401/404 type materials. The absence of nickel helps to keep the pricing stable and makes ferritic grades more attractive and cost optimized choice. Furthermore, the chromium content can be optimized taking into account a very wide range of applications: it contain 10.5 to 30% Cr, up to

0.20% C and sometimes ferrite promoters Al, Nb (Cb), Ti and Mo.They are ferritic at all temperatures, do not transform to austenite and therefore, are not hardenable by heat treatment. This group includes the more common types 405, 409, 430, 442 and 446. (Damian and Armao, 2003). They are very successfully used in important applications, such as washing-machine drums and exhaust systems, they actually have much broader application potential, in numerous fields. They can be formed into more complex shapes and joined using most conventional joining methods, including welding. In material selection decisions, these grades are often weighed against 304 austenitic grades (Charles et al., 2007).

However, they have slightly higher yield strength and much lower strain hardening than ASS. Since ferritic steels have body centered cubic crystal, they are less ductile than austenitic steel, and are not hardenable by heat treatment like martensitic steels (www.business dictionary.com). This grade of stainless steel represent about 25% of the total production of stainless steel and due to welding problems and low toughness properties compared to austenitic grade, they are restricted to thinner gauges even if they are often the cost saving grade (Tanimu, 2013).

2.2.2 Martensitic stainless steels

Martensitic stainless steels are essentially alloys of iron and chromium that has a body centered tetragonal structure in heat treated conditions. The compositions of these alloys are specifically formulated to render them amenable to quench and temper heat treatment, in order to produce high level of strength and hardness (Jonathan and Gordon, 1999).

They are ferromagnetic, hardenable by heat treating, and generally resistant to corrosion only in relatively mild environments. Chromium content is generally in the range of 10.5 to 18%, and

carbon content can exceed 1.2%. The most commonly used alloy within the martensitic stainless steel family is type 410, which contains approximately 12 wt% Cr and 0.1 wt% C to provide strength. Martensitic stainless steel is very strong steel that does not achieve high levels of strain. It is commonly classified as a 400 series alloy in American Iron and Steel Institute (AISI) classification(Crawford, 2011).

The 400 series is a mixture of martensitic and ferritic stainless steels. These steels contain Carbon and Chromium as their main alloying elements, as well as manganese and small amounts of other alloying elements such as nickel, niobium and titanium. Their corrosion resistance and toughness are inferior to those of austenitic stainless steels but they are stronger (Crawford, 2011).

2.2.3 Austenitic stainless steels

Austenitic stainless steels are the most weldable of the stainless steels and can be divided rather loosely into three groups: common chromium-nickel (300 series), manganese chromium- nickel-nitrogen (200 series) and specialty alloys. Austenitic is the most popular stainless steel group and is used for numerous industrial and consumer applications, such as in chemical plants, power plants, food processing and dairy equipment. Austenitic stainless steels have a face-centered cubic (FCC) structure that is maintained over a wide range of temperatures. Though generally very weldable, some grades can be prone to sensitization of the weld heat-affected zone and weld metal hot cracking (www.aws.org, 2013).

Austenitic stainless steels in general contain 16% to 26% chromium, up to 8% to 10% nickel and have very low carbon content. Some of these steels are alloyed with little amount of molybdenum, columbium and titanium (Jonathan and Gordon, 1999).

As shown in figure 2.2, in the ferritic stainless steel, the iron and chromium atoms are arranged on the corners of a cube and in the center of that cube. In the austenitic stainless steels the atoms, based iron, chromium and nickel, are arranged on the corners of the cube and in the center of each of the faces of the cube(www.totalmateria.com).

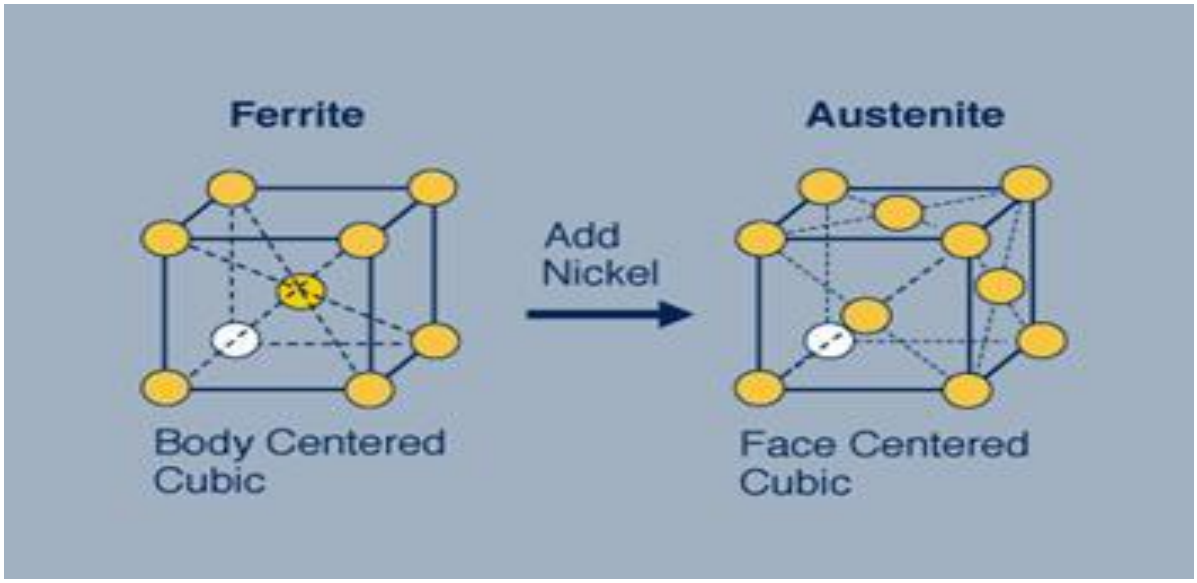

Figure 2.2: Formation of austenitic stainless steel(www.totalmateria.com).

2.2.4 Duplex stainless steels

Duplex stainless steel is two phased alloys based on the iron-chromium- nickel system. These alloys usually comprise equal proportions of the body centered cubic (BCC) ferrite and face centered cubic (FCC) austenite phase in their microstructure and generally have low carbon content as well as molybdenum, nitrogen, tungsten, and copper. Typical chromium contents range from 20% to 30% by weight, nickel ranges from 5% to 10% by weight (Tanimu, 2013).

Duplex stainless steel offers excellent resistant to corrosion and very high mechanical strength. The high corrosion resistance of duplex stainless steel ensures significantly more uptime than

carbon steels and conventional stainless steels, while the mechanical strength allows for lighter constructions, more compact system design and less welding (Sandvik, 2013).

Primarily used in chemical plants and piping applications, the duplex stainless steels are developing rapidly today and have a microstructure of approximately equal amounts of the body centered cubic (BCC) ferrite and face centered cubic (FCC) austenite. They generally have low carbon content as well as additions of molybdenum, nitrogen, tungsten and copper (www.aws.org, 2013).

Essentially, the ratio of ferrite to austenite in duplex stainless steels depends mainly on the chemical composition. The presence of ferrite and austenite provide better intergranular corrosion (IGC) resistance. Duplex stainless steels are in most cases, tougher than ferritic stainless steels. Strengths of duplex stainless steels can in some cases be double than that for austenitic stainless steels. Whilst duplex stainless steels are considered resistant to stress corrosion cracking, they are not as resistant to this form of attack as ferritic stainless steels. However, the corrosion resistance of the least resistant duplex stainless steels is greater than that for the most commonly used grades of stainless steels i.e. 304 and 316. Duplex stainless steels are also magnetic, a property that can be used to easily differentiate them from common austenitic grades of stainless. (www.azom.com/article.aspx?ArticleID=2870).

2.2.5 Precipitation hardening stainless steels

Precipitation-hardening stainless steels are chromium-nickel stainless, which contain alloying additions such as aluminum, copper, niobium, molybdenum or titanium that allow them to be hardened by a solution and aging heat treatment. Precipitation hardening stainless steels contain

between 11% to 18% chromium, 3% to 27% nickel, and 0.05% to 0.15% carbon. They generally have more corrosion resistance than the martensitic or austenitic matrix. These alloys are commonly categorized into three distinct types, namely; martensitic, semi austenitic and austenitic (Tanimu, 2013).

Precipitation hardening (commonly called age-hardening) occurs when, two phases precipitate from a supersaturated solid solution. For example:

Precipitation: Solid A→ Solid A' + Solid B ----------(2.1)

The primary requirement of an alloy for precipitation hardening is that the solubility of B in A decreases with decreasing temperature, so that a supersaturated solid solution forms on rapid cooling(Chris and Alan, 2007).

2.2.6 Super alloy stainless steels

Superalloy is an alloy consisting of three or more elements that is very expensive and designed to perform at elevated temperatures. Superalloys are used when grade 316 or 317 alloys are inadequate to withstand attack. They contain very large amounts of nickel and/or chrome and molybdenum. They are usually much more expensive than the usual 300 series alloys and can be more difficult to find. These alloys include Alloy 20 and Hastelloy (www.sppusa.com).

2.3 Microstructure of Stainless Steels

The mechanical properties of materials predominantly depend on the microstructure in stainless steel, it will depends on the phase transformation characteristic (Balmforth and Lippold, 2000). At high temperature, austenite is formed, which is a face centered cubic crystal structure which dissolves 2% C and is soft and ductile. Under equilibrium cooling condition, it transforms to

ferrite and pearlite for the hypo-eutectoid steels or cementite and pearlite for hyper-eutectoid steels.

Ferrite, which has a body centered cubic crystal structure that can hold 0.025%C and is also soft and ductile but not as the austenite (Pascoe, 1982). Martensite is formed if the cooling rate is high, that suppresses the transformation of austenite to pearlite. This phase is hard, brittle, highly stressed internally and has a needle-like appearance under microscope (Dauda, 2008).

During solidification, duplex stainless steels first solidify as ferrite. As the temperature decreases, austenite develops. For duplex stainless steel, a structure of austenite islands in a ferrite matrix can be observed. The microstructure in duplex stainless steel is usually composed of approximately equal amounts of austenite and ferrite. The austenite ratio can be increased to about 55% to 60% in order to improve the toughness properties and maintain a sufficient ratio in the heat affected zone (Charles, 1997).

2.3.1 Physical properties of stainless steels

The average physical properties of each of the main group of stainless steels are listed in the table 2.1 below. This includes elastic modulus, density, coefficient of thermal expansion, thermal conductivity, specific heat, electrical resistivity, magnetic permeability and melting range.

Table 2.1 Physical Properties of Some Stainless Steels.

Property	**Austenitic Grades**	**Ferritic Grades**	**Martensitic Grades**	**Precipitating Hardening Grades**
Elastic Modulus;10^6 GPa(psi)	195(28.3)	200(29.0)	200(29.0)	200(29.0)
Density; g/cm^3(Ib/in^3)	8(0.29)	7.8(0.28)	7.8(0.28)	7.8(0.28)
Coeff. Of Therm. Expansion; μm/m^{o}C($\mu in/in^o$F)	16.6(9.2)	10.4(5.8)	10.3(5.7)	10.8(6.0)
Thermal conductivity; W/mK (Btu/hrft.^{o}F)	15.7(9.1)	25.1(14.5)	24.2(14.0)	22.3(12.9)
Specific heat; J/kg^o(Btu/Ib.^{o}F)	500(0.12)	460(0.11)	460(0.11)	460(0.11)
Electrical resistivity; μcm	74	61	61	80
Magnetic permeability	1.02	600-1100	700-1000	95
Melting Range ^{o}C(^{o}F)	1375-1450 (2500-2650)	1425-1530 (2600-2790)	1425-1530 (2600-2790)	1400-1440 (2560-2625)

(Source:www.weldingengineering.com).

2.3.2 Mechanical properties of stainless steels

Essentially, metals can be broken, bent, twisted, dented, scratched and otherwise damaged. With such widely varying properties, it becomes a problem to express in few words exactly what type of service a piece of metal can withstand without having the knowledge of its mechanical properties. The mechanical properties of stainless steels are those associated with the ability of the metal to resist mechanical forces and loads. These mechanical properties include strength, stiffness, elasticity, plasticity, ductility, toughness, resilience, brittleness, malleability, creep and hardness. These properties are directly linked to the carbon and nitrogen contents and microstructure (www.arcelormittalstainless.com).

Generally, the austenitic stainless steels have higher tensile strength and elongation than the ferritic stainless steels but lower yield strengths. Reduction in area is about the same for both groups. Essentially, ferritic stainless steels have lower elongation at fracture and strain hardening properties than ASS. As for plain carbon steels, ferritic stainless steels in the annealed state present a yield point followed by stress drop on the stress strain curves.Duplex stainless steels constitute an important stainless steel group which has found increasing use in recent years in engineering structures exposed to aggressive environments due to their excellent mechanical properties. This alloy displays properties characteristics of both austenitic and ferritic stainless steels. These combined properties can mean some compromise when compared with pure austenitic and pure ferritic stainless steels (www.arcelormittalstainless.com).

The yield strength of duplex stainless steel is 2-3 times higher than that of 18Cr-10Ni austenitic stainless steels, the ferrites usually contribute to the high strength, but the strength in duplex stainless steel is higher than for pure ferritic stainless steels (Bennefois et al., 1991). This can be explained by small grain size in duplex stainless steels (Vannevik et al., 1996), caused by the mutual hindering of the growth of ferrite and austenite grains (Atamert and King, 1993), implying higher strength for the two phase structures than its constitutes.

2.3.3 Corrosion resistance of stainless steel

Stainless steels are corrosion resistant due to the formation of an invincible 2-4mm thick, passive film that is established in oxidizing environments when the steel contains at least 12% chromium. This film has the ability to be rebuilt by oxidation of the underlying metal when it has been damaged. There are, however, environments in which permanent breakdown of the passive layer occur either uniformly or locally, causing corrosion of the unprotected surface. Different media

can cause different types of corrosion attack, which may vary in nature and appearance. Uniform corrosion or general corrosion occurs with an even corrosion rate over the whole surface that is exposed to the corrosive medium (often for the steel an aggressive acid e.g. hydrochloric acid or hydrofluoric acid). The corrosion rate is generally expressed as the material loss in mm/year and can thus be used as an estimation of the lifetime (Tanimu, 2013).

Pitting corrosion is a localized form of corrosion by which cavities or "holes" are produced in the material. Pitting is considered to be more dangerous than uniform corrosion damage because it is more difficult to detect, predict and design against (www.nace.org/Pitting-Corrosion).Pitting corrosion most often occurs where chloride ions cause a local breakdown of the passive layer. The presence of halides, such as chloride in natural or acidic solutions increases the corrosiveness of both organic and inorganic acids. The solution becomes more aggressive at high chloride concentrations, low pH and high temperatures, but also small amounts of chlorides, 250 ppm may affect the pitting corrosion of stainless steel in domestic water heaters (Caes-Ove and Sven-Aven, 1995). The pits often appear to be smaller at the surface, but may have larger cross-section areas deeper inside the metal, (as shown in figure 2.3 below). The pitting corrosion is often more deleterious than uniform corrosion due to the rapid propagation rate and it is not possible to circumvent the problem by dimensioning with thicker gauges as for uniform corrosion.

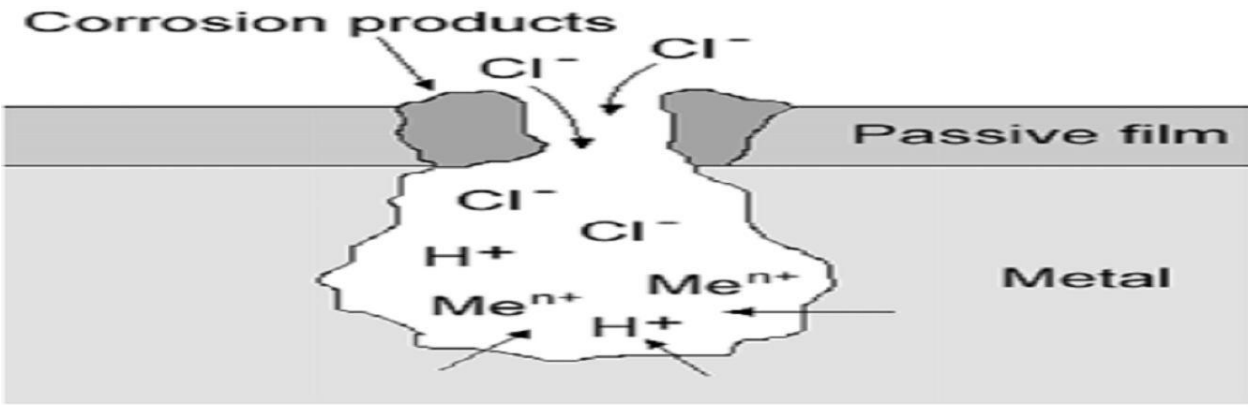

Figure 2.3: Principal cross-section of a corrosion pit (Charles, 1991)

When choosing a stainless steel for a certain application, it is important to consider all factors that can affect the corrosion resistance such as the environment, concentrations, pH, impurity content and the service temperature. Other factors that can have an effect on the performance of the product are weld defect, the presence of oxide from welding or heat treatment, contamination of the steel surface by particles of non-alloyed steel, microbial activity, the presence of crevices and chlorination of water. More information about the corrosion performance of different stainless steels and the ability to withstand certain environments, concentrations, pH, e.t.c. can be found in the Outokumpu Corrosion Handbook (Sridhar and Kolts, 1987).

2.4 Welding and Characteristics of Welding Process

Joining has increasingly been used in the material technology because materials having different mechanical and microstructural properties need to be efficiently and effectively joined so as to increase its performance. Therefore, joining process involves bringing together of two or more separate parts into permanent or temporary union in order to act as one member (Ibhadode, 2001). In other word, welding is a process of joining two or more pieces of the same or dissimilar metals to achieve complete coalescence. This is the only method of developing a monolithic structure and it is often accomplished by the use of heat and or pressure, with or without filler metal. The

most common welding processes are (Tanimu, 2013; www.zhweijun.wordpress.com andwww.substech.com);

1. **Arc welding**: This obtains heat from an electric arc and maintains it between two electrodes or between an electrode and the work piece.

Advantages of Arc Welding

1. Versatility - readily applied to a variety of applications and a wide choice of electrodes
2. Relative simplicity and portability of equipment
3. Low cost
4. Adaptable to confined spaces and remote locations
5. Suitable for out-of-position welding

Disadvantages of Arc Welding

1. Not as productive as continuous wire processes
2. Likely to be more costly to deposit a given quantity of metal
3. Frequent stop/starts to change electrode
4. Relatively high metal wastage (electrode stubs)
5. Current limits are lower than for continuous or automatic processes

2. **Resistance welding:** This obtains the heat needed for welding from the resistance of the work piece to the electric current. Resistance welding has different types of welding, for example resistance spot welding, resistance seam welding and projection welding. For the resistance welding are used widely, the resistance welding process which use the application of electric current and mechanical pressure to create a weld are mastered by welder or other people.

Advantages of Resistance Welding:

1. High speed welding
2. Easily automated
3. Suitable for high rate production
4. Economical

Disadvantages of Resistance Welding:

1. Initial equipment costs
2. Lower tensile and fatigue strengths
3. Lap joints add weight and material

3. **Oxy-fuel welding**: Here, the heat is generated through the combustion of a fuel gas and oxygen to produce the heat required for joining.

Advantages of Oxy-fuel Welding:

1. Low capital cost
2. No electrical requirement
3. Consumable costs low
4. Can be used to cut thick sections e.t.c

Disadvantages of Oxy-fuel Welding

1. Primarily limited to mild and low alloy steel
2. Less suitable for stainless steels and aluminum
3. Wide HAZ
4. Quality influenced by parameters and torch nozzle and plate surface condition

4. **Solid State Welding** is a welding process, in which two work pieces are joined under a pressure providing an intimate contact between them and at a temperature essentially below the melting point of the parent material. Bonding of the materials is a result of diffusion of their interface atoms.

Advantages of Solid State Welding:

1. Weld (bonding) is free from microstructure defects (pores, non-metallic inclusions, segregation of alloying elements)
2. Mechanical properties of the weld are similar to those of the parent metals
3. No consumable materials (filler material, fluxes, shielding gases) are required
4. Dissimilar metals may be joined (steel - aluminum alloy steel - copper alloy).

Disadvantages of Solid State Welding:

1. Thorough surface preparation is required (degreasing, oxides removal, brushing/sanding)
2. Expensive equipment.

5. **Thermit Welding** is a welding process utilizing heat generated by exothermic chemical reaction between the components of the thermit. The molten metal, produced by the reaction, acts as a filler material joining the work pieces after Solidification Thermit Welding is mainly used for joining steel parts, therefore common thermit is composed from iron oxide (78%) and aluminum powder (22%).

Advantages of Solid State Welding:

1. For welding new necks to rolling mill roll with pinions
2. Used for welding large broken crankshafts
3. Used for building up damaged wobblers

4. For welding busted frames of machines.

Disadvantages of Thermit Welding

1. Low deposition rate with operating factor
2. It cannot weld low melting point
3. Extremely high level of fume
4. It has slag inclusion

6. **Laser Welding (LW)** is a welding process, in which heat is generated by a high energy laser beam targeted on the work piece. The laser beam heats and melts the work pieces edges, forming a joint. Energy of narrow laser beam is highly concentrated: 10^8 10^{11} W/in^2 (10^8-10^{10} W/cm^2), therefore diminutive weld pool forms very fast (for about 10^{-6} sec.). Solidification of the weld pool surrounded by the cold metal is as fast as melting. Since the time when the molten metal is in contact with the atmosphere is short, no contamination occurs and therefore no shields (neutral gas, flux) are required. The joint in Laser Welding (Laser Beam Welding) is formed either as a sequence of overlapped spot welds or as a continuous weld. Laser Welding is used in electronics, communication and aerospace industry, for manufacture of medical and scientific instruments, for joining miniature-components.

Advantages of Laser Welding:

1. Easily automated process;
2. Controllable process parameters;
3. Very narrow weld may be obtained;
4. High quality of the weld structure;
5. Very small heat affected zone;

6. Dissimilar materials may be welded;
7. Very small delicate work pieces may be welded;
8. Vacuum is not required;
9. Low distortion of work piece.

Disadvantages of Laser Welding:

1. Low welding speed;
2. High cost equipment;
3. Weld depth is limited.

7. **Electron Beam Welding** is a welding process utilizing a heat generated by a beam of high energy electrons. The electrons strike the work piece and their kinetic energy converts into thermal energy heating the metal so that the edges of work piece are fused and joined together forming a weld after Solidification. The process is carried out in a vacuum chamber at a pressure of about $2*10^{-7}$ to $2*10^{-6}$ psi (0.00013 to 0.0013 Pa). Such high vacuum is required in order to prevent loss of the electrons energy in collisions with air molecules.

   The electrons are emitted by a cathode (electron gun). Due to a high voltage (about 150 kV) applied between the cathode and the anode the electrons are accelerated up to 30% - 60% of the speed of light. Kinetic energy of the electrons becomes sufficient for melting the targeted weld. Some of the electrons energy transforms into X-ray irradiation. Electrons accelerated by electric field are then focused into a thin beam in the focusing coil. Deflection coil moves the electron beam along the weld. Electron Beam is capable to weld work pieces with thickness from 0.0004" (0.01 mm) up to 6" (150 mm) of steel and

up to 20" (500 mm) of aluminum. Electron Beam Welding may be used for joining any metals including metals, which are hardly weldable by other welding methods: refractory metals (tungsten, molybdenum, niobium) and chemically active metals (titanium, zirconium, beryllium). Electron Beam Welding is also able to join dissimilar metals.

Advantages of Electron Beam Welding:

1. It produces a weld of superb quality, with extremely deep penetration, while at the same time minimizing overall heat input
2. Can even weld extremely thin materials with ease
3. It can also weld thicker sections in a single pass.
4. It can be possible to achieve a nearly 0% reject rate

Disadvantages of Electron Beam Welding:

1. It is by far the most costly welding process
2. Requires a vacuum chamber containing a hard vacuum, only small to medium size items can be welded.
3. The process is time consuming.
4. The equipment is complex and there are quite a few process variables involved.

Generally, all welding processes must meet the following conditions(Tanimu, 2013);

1. Supply of energy to the joint interfaces to either make it plastic or molten.
2. Control of weld metallurgy and
3. Avoidance of atmospheric contamination and its effects and the mechanism for the removal of these contaminants.

2.5 Welding Methods for Austenitic Stainless Steels

The welding parameters used in different welding processes are in general the same for ASS's as well as for other stainless steels (Ibhadode, 2001);

1. **Shielded *metal arc welding*** (SMAW) is mainly used for filler passes. Owing to its low sensitivity to strong winds, SMAW is very suitable for welding on site. Repair welding is often done with this method because of its flexibility.
2. **Tungsten inert gas welding** (TIG) is particularly suitable for welding thin-wall materials. The method gives a very pure weld deposit of high quality.
3. **Plasma arc welding** (PAW) is also a suitable method for ASS's. It is mainly used by manufacturers of e.g. welded tubes and tube parts. If annealing cannot be made after welding, addition of nitrogen to the shielding or plasma gas is recommended, about 5% N_2 in the plasma gas or 10% N_2 in the shielding gas.
4. **Submerged arc welding** (SAW). The method is mainly used for thick sections of sheet metal. It is one of the oldest automatic welding used for providing high quality weld.
5. **Metal inert gas welding** (MIG) is suitable for light to medium steel fabrication work when high productivity is desired.
6. **Flux cored arc welding** (FCAW) is like MIG welding: a method which is used when a high productivity is desired.
7. **Laser and electron beam (EB) welding.** These processes are used without the addition of filler metal.
8. **Spot and Seam welding.** These methods are being used on ASS's. In order to improvethe austenite reformation in spot welding, the electrodes canbe kept in position after welding for a short-time resistance heating.

2.6 Welding Processes

2.6.1 Gas tungsten arc welding process

By definition, Gas Tungsten Arc Welding Process **(**GTAW) is a very precise arc welding process that uses a non-consumable tungsten electrode (www.toolingu.com/definition). In the GTAW process, also known as the Tungsten Inert Gas (TIG) or Wolfram Inert Gas (WIG) process, the energy necessary for melting the metal is supplied by an arc struck and maintained by tungsten or tungsten alloy electrode and the work piece, under an inert or slightly reducing atmosphere. Stainless steels are always welded in the DCEN (Direct Current Electrode Negative) or DCSP (Direct Current Straight Polarity) mode. In these conditions, it is the workpiece that is struck by the electrons, enhancing penetration, while the electrode, which is generally made from thoriated tungsten (2%ThO_2), undergoes very little wear. If filler is employed, it is in form of either bare rods or coiled wire for automatic welding. The inert gas flows which protects the arc zone from ambient air, enables a very stable arc to be maintained. Depending on the base material, shielding gas consists mainly of mixtures of argon (Ar), helium (He) and hydrogen (H_2). The common workpiece thickness ranges from 0.5mm to 3.5/4.0mm. (Pierre, 2007).

Advantages of Gas Tungsten-Arc Welding are (www.techtrain123.com);

1. Highly concentrated arc: This permits pinpoint control of heat allowing a narrow heat affected zone.
2. The shielding gas serves only to blanket the weld and exclude the active properties in the surrounding air.
3. No flux or slag: There is no requirement for flux with this process; therefore, there is no slag to obscure the operator's vision of the puddle.
4. No smoke or fumes: The process itself does not produce smoke or injurious fumes.
5. No sparks or spatter: In the GTAW process there is no transfer of metal across the arc.

2.6.2 Gas metal arc welding

Gas Metal Arc Welding (GMAW), by definition, is an arc welding process which produces the coalescence of metals by heating them with an arc between a continuously fed filler metal electrode and the workpiece. The process uses shielding from an externally supplied gas to protect the molten weld pool. The application of GMAW generally requires DC+ (reverse) polarity to the electrode (www.lincolnelectric.com).

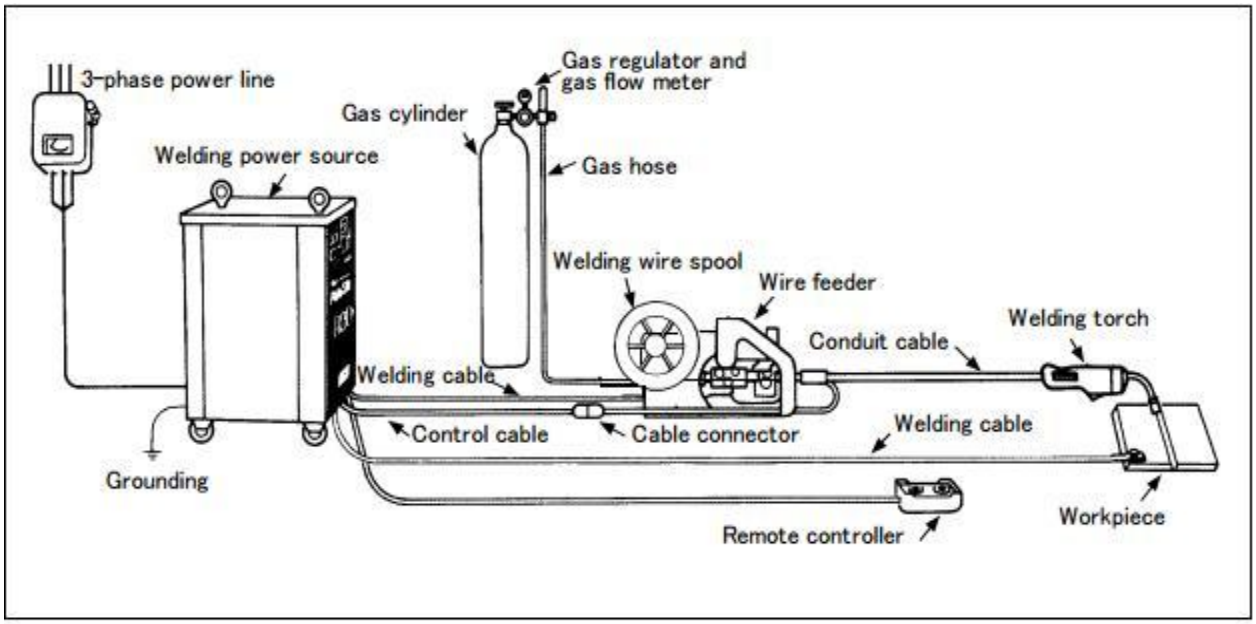

Figure 2.4: A typical arrangement of gas metal arc welding process. (Source: Kobe, 1995)

The advantages of this process are (www.lincolnelectric.com);

1. The ability to join a wide range of material types and thicknesses.
2. Simple equipment components are readily available and affordable.
3. GMAW has higher electrode efficiencies, usually between 93% and 98%, when compared to other welding processes.

4. Higher welder efficiencies and operator factor, when compared to other open arc welding processes.
5. GMAW is easily adapted for high-speed robotic, hard automation and semiautomatic welding applications.
6. All-position welding capability.
7. Excellent weld bead appearance.
8. Lower hydrogen weld deposit - generally less than 5 mL/100 g of weld metal.
9. Lower heat input when compared to other welding processes.
10. A minimum of weld spatter and slag makes weld clean up fast and easy.
11. Less welding fumes when compared to SMAW (Shielded Metal Arc Welding) and FCAW (Flux-Cored Arc Welding) processes.

The mechanism of metal transfer in the arc is an important process parameter, three principles being distinguished are (Pierre, 2007);

1. The short circuiting or dip transfer mode, in which the metal melts to form large droplets whose diameter is often greater than that of the wire. As the droplets forms at the end of the electrode, it makes contact with the weld pool and creates a short circuit, with a sudden increase in current. The surface tension causes a pinching effect which separates the droplet from the electrode. The frequency of this phenomenon is of the order of 20 to 100Hz, corresponding to cycle times between 0.01 and 0.05 seconds.

2. The spray transfer of mode, involving current densities above a certain transition level, of order of $200A/mm^2$. The electrode melts to give a stream of fine droplets. As the current densities increases further, the electrode tip becomes conical and the stream of even finer droplets is released axially.

3. The global transfer or gravity transfer mode; as in the previous case the melting occurs in the form of large droplets, which break away when their mass is sufficient to overcome surface tension forces and due to the greater arc length, fall freely before coming in contact with the weld pool.

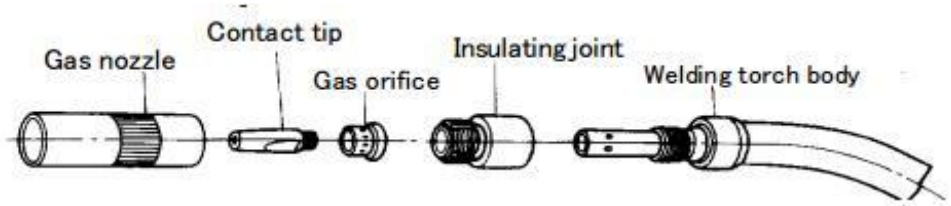

Figure 2.5: Arrangement of a contact tip in an air-cooled GMAW torch (Source: Kobe, 1995)

Essentially, GMAW requires shielding gas to prevent oxidation in the welding arc. Argon with 2% oxygen (O_2) gives a stable arc and is suitable for most applications. Argon with 3% carbon dioxide (CO_2) gives about the same result. The welding speed and penetration can sometimes be enhanced when helium (He) and hydrogen (H) are added to the argon + oxygen or argon + CO_2 shielding gas. Gases higher in CO_2 tend to produce significant carbon pick up by the weld pool together with chromium oxidation. It is for this reason that they are not recommended. The bead size and extend of penetration, will vary considerably with the workpiece grade, the type of joint, the transfer mode and the skill of the welder. For V joints and square butt joints welded in one run, the common workpiece thickness range is 1.0mm to 5.0mm (Pierre, 2007).

2.6.3 Shielded metal arc welding

Shielded metal arc welding (SMAW) method is a fusion welding process in which coalescence of the metals is achieved by the heat from an electric arc between an electrode and the work. This process is one of the most employed processes of fabricating metal components. It is fundamentally a fusion of two or more pieces of metals by the application of heat and sometimes

pressure. Thus welding involves a wide range of scientific variables such as time, temperature, electrode, power input and welding speed. In this method, welding parameters are the most important factors affecting the quality, productivity and cost of welding joint (Ugur et al., 2011).

The process remains widely used due to its great flexibility and simplicity of use.The welding quality of the shielded metal arc welding is determined by the welding parameters including the electrode diameter, welding current, welding speed, arc length, electrode advance angle, etc. In an effort to obtain high quality welds in shielded metal arc welding method, selection of ideal parameters should be performed according to engineering facts. Commonly, welding parameters are determined by trial and error, based on handbook values, and manufacturers' recommendations. On the other hand, this option may not yield optimal or in the vicinity of optimal welding performance (Afolabi, 2008).

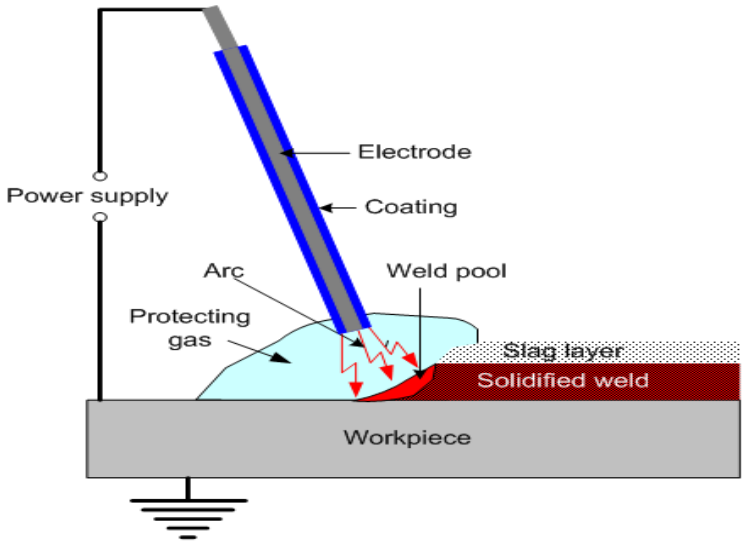

Figure 2.6: Schematic image of shielded metal arc welding (Ugur et al., 2011)

In shielded metal arc welding method, the electrodes are coated with a shielding flux of a suitable composition. The flux melts together with the electrode metallic core, forming a gas and a slag,

shielding the arc and the weld pool. The flux cleans the metal surface, supplies some alloying elements to the weld, protects the molten metal from oxidation and stabilizes the arc. The slag is removed after Solidification. Figure 2.6 shows a schematic image of shielded metal arc welding. As seen in figure 2.6, the process consists of electrode and its coating, arc formation, protecting gas, weld pool and solidified weld.

The common workpiece thickness range is (Pierre, 2007);

1. 1.0mm to 2.5mm (for single run processes)
2. 3.0mm to 10.0mm (for a multiple pass technique).

2.6.4 Selecting shielding gas for welding of stainless steels

At high temperature, all metals commonly used for fabrication will oxidize in the atmosphere. Essentially, all welding process provides shielding from the atmosphere by some method. When welding steels, the intension is to exclude oxygen, nitrogen, and moisture from the area about the molten puddle. In the oxy-fuel process, the weld pool is shield from the atmosphere by the combustion by- product of carbon monoxide (CO) and carbon dioxide (CO_2). In stick welding also known as SMAW, the CO and CO_2 are also the shielding gases. Submerged-arc welding shields the puddle by a different method. As the puddle progresses, the intense heat melts the flux in the joint area; this form a slag that covers the weld and excludes the atmosphere. GMAW and GTAW are both gas shielded processes in which the shielding gas is provided from an outside source. No fluxing agents are included in the filler metal of solid wire. The choice of shielding gas has a significant influence on the following factors (Pierre, 2007):

1. Shielding efficiency (controlled shielding gas),
2. Metallurgical and mechanical properties (loss of alloying elements and pick up of atmospheric gases),

3. Surface appearance (oxidation and spatter),
4. Arc stability and ignition,
5. Metal transfer,
6. Environment (emission of fumes and gases),
7. Corrosion resistance (loss of alloying elements, pick up of atmospheric gases and surface oxidation) and
8. Weld geometry (bead and penetration profiles).

Essentially, the basic gas for MIG welding is inert – argon (Ar) or helium (He), or a mixture of both. However, small additions of oxygen (O_2) or carbon dioxide (CO_2) can further stabilize the arc, improve the fluidity and also improve the quality of the weld (www.smt.sandvik.com).

2.7 Welding Parameters

Control of the operating variables in GMAW is essential if high production rates and the welds of good quality are to be obtained. Producing a weld bead that is the right size, shape and depth involves many variables. Some of the variables affecting weld quality in arc welding are classified into the following groups (Tewari et al.,2010; Bernard and Jack, 1999; Afolabi, 2008; Ugur et al., 2011;Cornu, 1988):

2.7.1 Welding current

Welding current is the most influential variable in arc welding process which controls the electrode burn off rate, the depth of fusion and geometry of the weldments. The welding current corresponds to the amount of heat generated during welding, and it depends on the material to be welded, material thickness, welding speed, and shielding gas.

2.7.2 Welding speed

Speed of welding is defined as the rate of travel of the electrode along the seam or the rate of the travel of the work under the electrode along the seam. On the other hand, it can also be defined as the speed of travel of the torch over the part or the part under the torch, is dependent on the flow rate of the material to be welded and the material thickness.

2.7.3 Welding voltage

This is the electrical potential difference between the tip of the welding wire and the surface of the molten weld pool. It determines the shape of the fusion zone and weld reinforcement. High welding voltage produces wider, flatter and less deeply penetrating welds than low welding voltages. Depth of penetration is maximum at optimum arc voltage.

2.7.4 Electrode size

Electrode size affects the weld bead shape and the depth of penetration at fixed current. Electrode size also influences the deposition rate. At any given current, a small diameter electrode will have a higher current density and a higher deposition rate than a larger electrode. However, a larger diameter electrode can carry more current than a smaller electrode, and produce a higher deposition rate at higher amperage. For the same values of current, arc voltage and welding speed, an increase in electrode diameter results in a slight increase in the spread of the bead.

2.7.5 Electrode work angle

The electrode may be held perpendicular to the workpiece or, tilted forward or backward with respect to the weld pool. As the arc stream tends to align itself along the axis of the electrode, the weld pool shape is different in each case, and so is the shape of the weld bead. It is observed that

in forehand welding, molten metal flows under the arc, the depth of penetration and reinforcement are reduced while the width of the weld increases, whereas in backhand welding the pressure of the arc scoops the molten metal from beneath the arc, the depth of penetration and height of reinforcement increases while the width of the weld is reduced.

2.7.6 Polarity

The amount of heat generated at the electrode and work piece, deposition rate, bead geometry and mechanical properties are affected by polarity. The change in polarity from DCEP to DCEN changes the amount of heat generated at electrode and the work piece and, hence the metal depositing rate, weld bead geometry and mechanical properties of the weld metal.

2.7.7 Electrode stick-out and melting rate

The distance between the current pick-up tip and the arc root, called electrode stick out, has a considerable effect on the weld bead geometry. Normally the distance between the contact tip and the work is 25-40 mm. The increase in melting rate of the electrode as a result of increase in electrode stick-out is proportionate to the product of current density and stick-out.

2.8Metallurgical Aspects of Welding

2.8.1. Welding metallurgy

Since most welding operations are carried out where one or more materials are repaired or joined together with a filler material at a high temperature, the metallurgy of all these materials and the temperature changes that they undergo are very important. To weld austenitic stainless steel, it is therefore important to understand how austenitic stainless steels transform at different cooling rates, and to know the effect of peak temperature in the heat affected zone (HAZ).

A study of the microstructure of all steels usually starts with the metastable iron-carbon (Fe-C) binary phase diagram (Figure 2.7). It provides an invaluable foundation on which to build knowledge of both carbon steels and alloy steels**,** as well as a number of various heat treatments.

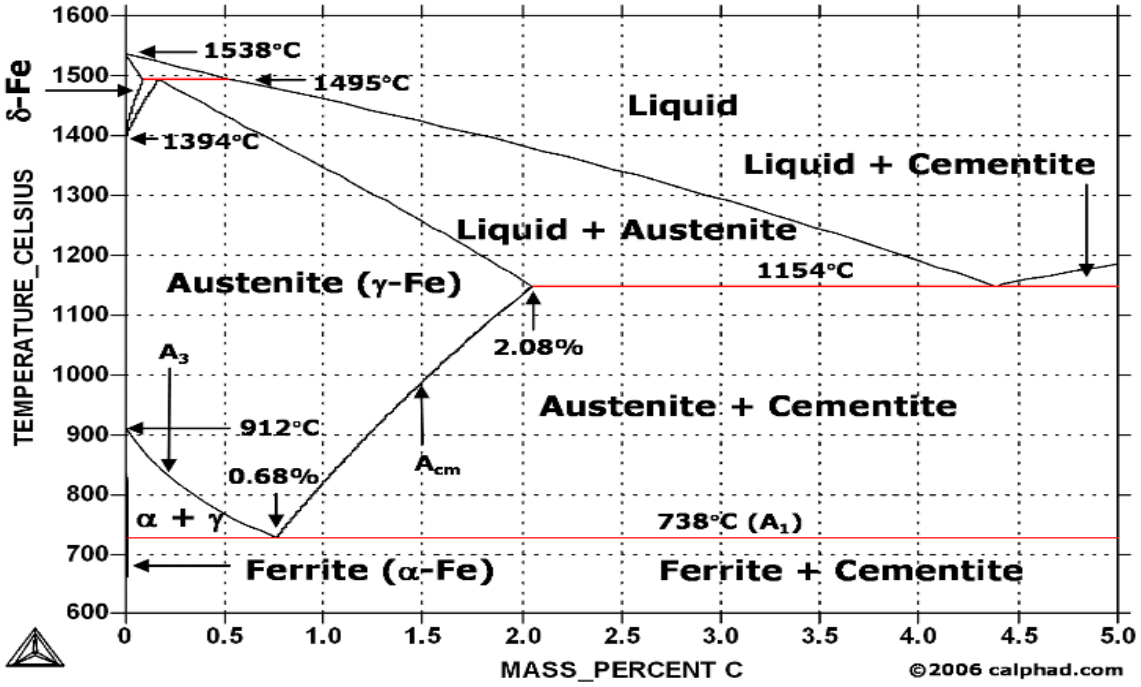

Figure 2.7:Metastable iron-carbon (Fe-C) phase diagram (www.calphad.com)

At the low-carbon end of the Metastable Fe-C phase diagram, ferrite (alpha-iron) is distinguished, which can at most dissolve 0.028 wt. % C at 738 °C, and austenite (gamma-iron), which can dissolve 2.08 wt. % C at 1154 °C. The much larger phase field of gamma-iron (austenite) compared with that of alpha-iron (ferrite) indicates clearly the considerably greater solubility of carbon in gamma-iron (austenite), the maximum value being 2.08 wt. % at 1154 °C. The hardening of carbon steels, as well as many alloy steels, is based on this difference in the solubility of carbon in alpha-iron (ferrite) and gamma-iron (austenite).

The vast majority of steels rely on just two allotropes of iron: (1) alpha-iron, which is body-centered cubic (BCC) ferrite, and (2) gamma-iron, which is face-centered cubic (FCC) austenite. At ambient pressure, BCC ferrite is stable from all temperatures up to 912 °C (the A_3 point), when it transforms into FCC austenite. It reverts to ferrite at 1394 °C (the A_4 point). This high-temperature ferrite is labeled delta-iron, even though its crystal structure is identical to that of alpha-ferrite. The delta-ferrite remains stable until it melts at 1538 ^{o}C.The steel portion of the Fe-C phase diagram covers the range between 0 and 2.08 wt. % C. The cast iron portion of the Fe-C phase diagram covers the range between 2.08 and 6.67 wt. % C. The steel portion of the metastable Fe-C phase diagram can be subdivided into three regions: hypo eutectoid (0 < wt. % C < 0.68 wt. %), eutectoid (C = 0.68 wt. %), and hyper eutectoid (0.68 < wt% C < 2.08 wt %). A very important phase change in the metastable Fe-C phase diagram occurs at 0.68 wt. % C. The transformation is eutectoid, and its product is called pearlite (ferrite + cementite) (www.calphad.com).

2.8.2 Heat affected zone

The heat-affected zone (HAZ) is the area of base metal, which has had its microstructure and properties altered by welding or heat intensive cutting operations. The heat from the welding process and subsequent re-cooling causes this change from the weld interface to the termination of the sensitizing temperature in the base metal. The extent and magnitude of property change depends primarily on the base metal, the weld filler metal, and the amount and concentration of heat input by the welding process. The time-temperature transformation of the metal's microstructure leaves a signature that is visible to the human eye. It can be seen by looking at a cut and polished weld specimen under a microscope. This visible change in microstructure is the

Heat Affected Zone and its geometry is the direct consequence of the weld's heating profile (Paul, 2006).

2.8.3 Weld fusion zone

It is the area between the two pieces of metal being joined or it refers technically to the area of coalescence produced by the welding process. This is actually produced by melting of a part of base metal in addition to the electrode/filler materials used or in another word, it is the admixture of the base metal and if used, the deposited metal (Dauda, 2008). Since a weld metal is similar to a casting, it will exhibit segregation of alloying elements. However, the primary solidification phase with duplex steels is normally ferrite, and this causes minimum segregation of chromium and molybdenum during solidification. Moreover, diffusion rates are high at temperatures just below the melting point, and homogenization of alloy elements in the ferrite can take place (Gooch, 1996).

2.9 Welding Procedure

The American Welding Society, acting under American National Standard Institute (ANSI) rules for consensus standards, publishes AWS Standard Welding Procedure Specifications (SWPSs) which are initiated by the Welding Procedures Committee of the Welding Research Council (WRC). In initiating SWPSs for experience in welded construction of the combination of basic materials, welding processes and welding filler metals covered by the scope of each SWPS (www.aws.org/standards).

However careful consideration should be given to the ranges specified to ensure they are achievable, as the ranges given by welding procedure standards do not always represent good

welding practice. For example welding positions permitted by the welding procedure standard may not be achievable or practical for certain welding processes or consumables (www.gowelding.com).

Typical items that should be recorded on SWPS common to all processes.

1. Procedure number
2. Process type
3. Consumable Size, Type and full Codification.
4. Consumable Baking Requirement if applicable
5. Parent material grade and spec.
6. Thickness range.
7. Plate or Pipe, Diameter range
8. Welding Position
9. Joint Fit Up, Preparation, Cleaning, Dimensions etc.
10. Backing Strip, Back Gouging information.
11. Pre-Heat (Min Temp and Method)
12. Interpass If Required (Maximum Temperature recorded)
13. Post Weld Heat Treatment. If Required (Time and Temperature)
14. Welding Technique (weaving, maximum run width etc.)
15. Arc Energy Limits should be stated if impact tests are required or if the material being welded is sensitive to heat input.

The question often arises whether an austenitic stainless steel should be preheated for welding. In general, preheating is not helpful because no structural changes, such as martensite formation,

occur in the weld or the heat-affected-zones. In some cases, preheating could be harmful in causing increased carbide precipitation, or greater warpage (www.nickelinstitute.org).

2.10 Weldability

Essentially, weldability, also known as joinability of a material refers to its ability to be welded. Many metals and thermoplastics can be welded, but some are easier to weld than others. A material's weldability is used to determine the welding process and to compare the final weld quality to other materials (Ibhadode, 2001).

Weldability means the relative ease of producing a defect-free weld with adequate mechanical properties and corrosion resistance. The principal defects of interest are hot cracks (fusion zone or heat affected zone hot cracking) and cold cracks (hydrogen assisted cracking). Most stainless steels are considered to have good weldability and may be welded by several welding processes including the arc welding processes, resistance welding, electron and laser beam welding, friction welding and brazing. For any of these processes, joint surfaces and any filler metal must be clean. The coefficient of thermal expansion for the austenitic types is 50% greater than that of carbon steel and this must be considered to minimize distortion. The low thermal and electrical conductivity of austenitic stainless steel is generally helpful in welding. Less welding heat is required to make a weld because the heat is not conducted away from a joint as rapidly as in carbon steel. In resistance welding, lower current can be used because resistivity is higher (Damian and Armao, 2003).

2.11 Filler Metal

Filler metal selection is critical to maintaining the mechanical and corrosion properties of the weld and HAZ. Filler metals that have a modified chemistry compared to the base metal are generally accepted. This filler metal chemistry is modified to provide comparable mechanical properties and better corrosion resistance and to allow for the loss of particular elements in the arc (Taylor, 1994). To accomplish the above goals, filler metals should be higher in nickel and contain nitrogen.

2.12 Heat Input

Generally, in arc welding, energy is transferred from the welding electrode to the base metal by an electric arc. When the welder starts the arc, both the base metal and the filler metal are melted to create the weld. This melting is possible because a sufficient amount of power (energy transferred per unit time) and energy density is supplied to the electrode. Heat input is a relative measure of the energy transferred per unit length of weld. It is an important characteristic because, like preheat and interpass temperature, it influences the cooling rate, which may affect the mechanical properties and metallurgical structure of the weld and the HAZ (see Figure 2.8). Heat input is typically calculated as the ratio of the power (i.e., voltage x current) to the velocity of the heat source (i.e., the arc) this is mathematically given as follows (Scott, 1999):

$$H = \frac{60EI}{1000S} \quad \text{.....(1)}$$

Where,

H = heat input (kJ/in or kJ/mm)

E = arc voltage (volts)

I = current (amps)

S = travel speed (in/min or mm/min)

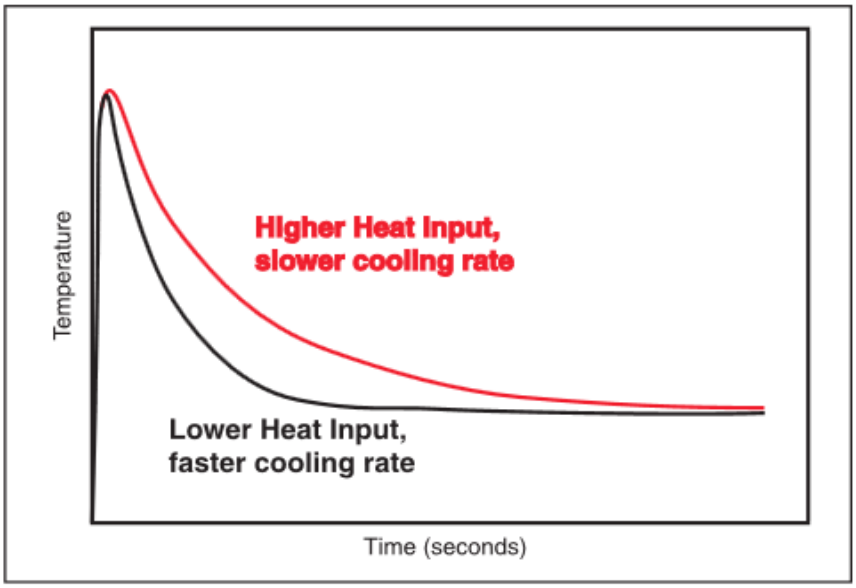

Figure 2.8: Heat input influence on cooling rate (Scott, 1999)

In austenitic stainless steel, heat input is very important because this energy input controls the overall cooling for adequate austenite formation in the welds. Too low heat input will result in excessive ferrite thus reducing toughness, corrosion resistance and increase materials susceptibility to hydrogen embrittlement. Conversely, too high heat input would result in a slow cooling rate; which may cause formation of secondary phases like alpha phase, thus reducing toughness and corrosion resistance (Tanimu, 2013).

2.13 Preheat and Multi-Pass

Preheating involves heating the base metal to a specific desired temperature, called the preheattemperature, prior to welding. There are five primary reasons to utilize preheat (Duane, 2003);

1. It slows the cooling rate in the weld metal and base metal, producing a more ductile metallurgical structure with greater resistance to cracking;

2. The slower cooling rate provides an opportunity for hydrogen that may be present to diffuse out harmlessly, reducing the potential for cracking;
3. It reduces the shrinkage stresses in the weld and adjacent base metal, which is especially important in highly restrained joints;
4. It raises some steels above the temperature at which brittle fracture might occur in fabrication; and
5. It can help to ensure specific mechanical properties, such as weld metal notch toughness and ductility.

No preheat at all is required when welding austenitic stainless steels. Essentially, interpass temperature in a multiple-pass weld is the temperature of the weld between weld passes. Limit of a maximum of 150^{o}C(302^{o}F) interpass temperature applies to all austenitic stainless steel welding to reduce susceptibility to sensitization during welding and also prevent hot cracking (www.eng-tips.com).

2.14 Factorial Design

Factorial experiments permits to evaluate the combined effect of two or more experiments variables when evaluated simultaneously. Information obtained from factorial experiments is more complete than those obtained from a series of single factor experiments, in the sense that factorial experiments permit the evaluation of interaction effects. An interaction effect is an effect attributable to the combination of variables above and beyond that which can be predicted from the variables considered separately (Manoj et al., 2010).

2.14.1. Factorial design of experiment in process optimization

The conventional method of studying a process by changing one variable at a time and keeping the other variables at a constant level does not depict the combined effects of all the factors involved in the optimization of a process. Moreover, the univariate method is time-consuming and also requires a large number of experiments to determine optimum levels, which may or may not be reliable. This limitations of the conventional method can be eliminated by simultaneously varying all the parameters affecting the process by using statistical factorial experimental design such as the response surface methodology (RSM) (Elibol, 2002). RSM, initially described by Box and Wilson (1951), is an experimental approach to identify the optimum conditions for a multivariate system.

2.15 Review of Related Works

Tanimu, (2013) investigated the effects of welding and heat treatment on mechanical properties of duplex stainless steel using GMAW and SMAW processes. He found out that welding and heat treatment really affected the mechanical properties of the alloy, having the control strength as 811.47MN/m^2 while that of GMAW and SMAW ranged from 177.07 to 257.32MN/m^2 and 452.23 to 678.98MN/m^2 respectively. He also found that the control impact energy was 162.70J, while that of the GMAW and SMAW range from 38.64 J to 56.20J. He equally noted that SMAW gave better results close to the one used as control than the GMAW process and heat treatment improved the mechanical properties of the alloy after welding.

Almubarak, et al (2013) study the effect of high nitrogen content on corrosion behavior of austenitic stainless steels in seawater under severe conditions such as tensile stresses and existence of sensitization in the structure. A constant tensile stress has been applied to sensitized specimens types 304, 316L, 304LN, 304NH, and 316NH stainless steels. Microstructure

investigation revealed various degrees of stress corrosion cracking. SCC was severe in type 304, moderate in types 316L and 304LN, and very slight in types 304NH and 316NH. The electrochemical polarization curves showed an obvious second current peak for the sensitized alloys which indicated the existence of second phase in the structure and the presence of intergranular stress corrosion cracking. Electrochemical potentiokinetic reactivation (EPR) test provided a rapid and efficient nondestructive testing method for showing passivity, degree of sensitization and determining IGSCC for stainless steels in seawater. A significant conclusion was obtained that austenitic stainless steels of high nitrogen content corrode at a much slower rate increase pitting resistance and offer an excellent resistance to SCC in seawater.

Iliyasu, et al (2012) investigated the susceptibility and resistance of type 304 austenitic stainless steel exposed to sulphuric acids (0.3M to 1M concentration) at ambient temperatures and at higher temperatures. Weight loss method was used to examine the corrosion rate of the steel after immersion in the corrosive media. The Constant Extension Rate Tensile Test (CERT) was also performed with a tensometer to determine the susceptibility of the steel to stress corrosion cracking in the corrosive media. The susceptibility of type 304 austenitic stainless steel to stress corrosion cracking in the corrosive media and its high corrosion of below 0.1mm/yr was also observed.

Loto, et al (2012) investigated the resistance and susceptibility of austenitic stainless steel, Type 304, exposed to strong tetraoxosulphate (VI) acids (2 and 5 M concentrations) contaminated with sodium chloride at ambient temperatures by gravimetric and metallographic/scanning electron microscopy surface characterization methods. Scanning electron microscope (SEM) was used to examine and characterize the test specimen's surface morphology after immersion in the corrosive

media. Surface corrosion deposit composition was analyzed with the SEM paired with energy dispersive spectrometer (EDS). The severe general and pitting corrosion and the resistance of the steel to corrosion at different concentrations of the acid chloride media was also observed. The results obtained showed the weak corrosion resistance/appreciable corrosion susceptibility of the stainless steel alloy to the test environments.

Majumder, (2011) investigated the effect of welding input parameters with respect to the amount of heat input in the weld metals. The welding trials were carried out using mild steel plate with different bevel angles. The polynomial regression equations were used to develop the mathematical relation between the input and output parameters effects. Finally the prediction equations were validated with the experimental result.

Abdel-Monem, et al (2011) investigated the Effect of Laser Beam Welding Parameters on Microstructure and Properties of Duplex Stainless Steel. The results achieved disclosed that welding parameters play an important role in obtaining satisfactory properties of welded joint. High laser power and/or high welding speed together with adjusting laser spot at specimen surface have produced welded joints with a remarkable decrease in fusion zone size and an acceptable weld profile with higher weld dept/width ratio. Besides, acceptable mechanical and corrosion properties were obtained.

Mehmet, et al (2011) conducted a study to determine the optimum welding parameters in connecting high alloyed X53CrMnNiN219 and X45CrSi93 steels by friction welding. He found out that the material loss increased with increase in friction and rotating pressure.

Mohd, et al (2011) investigated the effect of arc voltage and current on mechanical and microstructure properties of 5083-aluminium alloy joints used in marine applications. They found out that the different welding voltages and current settings remarkably affect the 5083-aluminium alloy joints.

Albrimi, et al (2011) investigated the electrochemical behaviour of AISI 316 austenitic stainless steel (SS) in de-aerated hydrochloric and sulphuric acid solutions using the open-circuit potential, cyclic voltammetric and chronoamperometric techniques. Enhanced corrosion of steel samples occurred with bigger HCl concentrations, as the potential range of passivity was shortened and both the pitting and the protection potentials became less noble. Conversely, the SS electrodes exhibited a greater corrosion resistance in solutions containing sulphuric acid of the same concentration. The aggressive effect of chloride ions towards steel corrosion was also investigated through controlled additions of NaCl to both electrolytic media and the analysis of the corresponding effects on the shape of the voltammetric curves. Chronoamperometric measurements run by setting different potential values to steel electrodes allowed the determination of the induction time for pit initiation, and the rates of pit nucleation and pit growth.

Dı´az-Cedre, et al (2010) has studied the influence of the shielding atmosphere characteristics and the effect of the welding current. The experiment was carried out using factorial design methods. Based on the experimental results, the regression equations were developed considering the O_2/CO_2 ratio and the welding current as the independent variables.

Afolabi, et al (2009) investigated the corrosion behavior of austenitic and duplex stainless steels in various concentrations of lithium, bromide solution by using the conventional weight loss measurement method. The results obtained show that corrosion of these steels occurred due to the aggressive bromide ion in the medium. Duplex stainless steel shows a greater resistance to corrosion than austenitic stainless steel in the medium. This was attributed to equal volume proportion of ferrite and austenite in the structure of duplex stainless steel coupled with higher content of chromium in its composition. Both steels produced electrochemical noise at increased concentrations of lithium bromide due to continuous film breakdown and repair caused by reduction in medium concentration by the alkaline corrosion product while surface passivity observed in duplex stainless steel is attributed to film stability on this steel.

Aleksandra and Marjetka (2009) studied the evolution of the passive film formed on duplex stainless steel 2205 and AISI 316L stainless steel in artificial saliva and a simulated physiological solution using cyclic voltammetry and potentiodynamic measurements. The extent of the passive range slightly decreased with the increasing chloride concentration from artificial saliva to the simulated physiological solution. The formation of pits during the potentiostatic conditions was studied using atomic force microscopy and the results showed an increasing growth of pits for the AISI 316L compared to duplex stainless steel 2205 and, furthermore, a decreased corrosion resistance of both materials in the simulated physiological solution compared to the artificial saliva.

Afolabi, (2008) investigated the effect of electric arc welding parameters (power input, weld geometry, welding speed, and post-weld heat treatment) on the corrosion behaviour of austenitic stainless steel in chloride medium. He used electrode potential measurement coupled with zinc

rod reference electrode to evaluate the corrosion behaviour of the samples. He found that the 3.6kW power input produces the highest resistance weld corrosion while chamfered face edge preparation is the best corrosion resistant sample in chloride medium. The post-weld heat treatment proved that the best heat treatment temperature occurred at range between 700^{o}C and 800^{o}C while the medium speed welded ASS sample proved to be the best compared with the fast-speed and low-speed weld. The results also showed that the best electrode for welding stainless steel is a stainless steel-cored electrode.

Habsah, et al (2008) investigated the effect of temperature on corrosion behavior of AISI 304 stainless steel in the presence of magnesium carbide ($MgCO_3$) salt at 900^{o}C, 950^{o}C and 1000^{o}C for 24-120 h. The results indicated that the initial carbonate coating caused acceleration in oxidation, resulting in the formation of scales, followed by the decreased in oxidation rate due to evaluation of CO/CO_2 gas. The mass change of metal increased as the temperature and time exposure increased. The morphological structure of deposits were analysed by using a scanning electron microscope (SEM).

Luo, et al (2007) investigated the general corrosion behavior of austenitic and ferritic steels (316L, 304, N controlled 304L, and 410) in supercritical water. After exposure to deaerated supercritical water at 480 ºC/25 MPa for up to 500 h, the four steels studied were characterized using gravimetry, scanning electron microscopy/energy dispersive X-ray spectroscopy (SEM/EDS), X-ray photoelectron spectroscopy (XPS), and X-ray diffraction (XRD). The results show that the 316L steel with a higher Cr and Ni content has the best corrosion-resistance performance among the steels tested. In addition to the oxide layer mixed with Fe_3O_4 and

$(Fe,Cr)_3O_4$ that formed on all the samples, a Fe_3O_4 loose outer layer was observed on the 410 steel.

Daisuke, et al (2002) evaluated the corrosion resistance of the nickel-free high nitrogen austenitic stainless steel without manganese, Fe-23Cr-2Mo-1.5N (mass %) (HNS) as biomaterials, by the polarization test in various electrolytes: 0.9%NaCl solution (saline), phosphate buffered saline (PBS). Hanks' solution (Hanks)n and eagle's minimum essential medium (E-MEM). Conventional austenitic stainless steel, 316L, was also polarized for comparison. The both alloys were spontaneously passivated in all electrolytes. The HNS did not show pitting corrosion in the polarization range in all electrolytes although the 316L showed pitting corrosion. Passive current densities of the HNS in all electrolytes were lower than those of 316L. Therefore; the HNS shows higher passivity and resistance to pitting corrosion than 316L. The passive current density in Hanks of HNS was lower than that in saline, indicating that the protectiveness of surface oxide film increased with the existence of inorganic ions such as phosphate and calcium ions. On the other hand, the passive current density in E-MEM was higher than that in Hanks, but was lower than that in saline.

White, et al (1996) investigated the effects of Gas-shielded flux cored arc welding (FCAW-G) parameters and atmospheric exposure on diffusible hydrogen content of the weld deposit. The study showed that, hydrogen content of FCAW-G welds increase with increasing current and decreasing tube-to-work distance. At shorter tube-to-work distance and higher currents, there is less time for resistive heating to evaporate hydrogen-containing residuals from the wire surface. Also, at higher current, it is believed that the metal drops achieve smaller diameters, which increases the surface-area-to-volume ratio of the drop.

Shirali and Mills (1993) investigated the effect of various welding parameters on the penetration of GTA welds. Increases in welding speed were found to reduce penetration; however, increases in welding current were observed to increase the penetration in high sulfur (HS) casts and decrease penetration in low sulfur (LS) steels. Plots of penetration as a function of increasing linear energy (the heat supplied per unit length of weld) revealed a similar trend with increased penetration in HS casts, but the penetration in LS casts was unaffected by increases in linear energy. Their results support the Burgardt- Heiple proposition that changes in welding parameters on penetration can be explained in terms of their effect, sequentially, on the temperature gradient and the Marangoni forces operating in the weld pool. Increases in arc length were found to decrease weld penetration regardless of the sulfur concentration of the steel, and the effects of electrode geometry and welding position on weld penetration were also investigated.

Murugan, (1993) studied the development of the mathematical models using the five level factorial technique to predict the weld bead geometry for depositing 316L stainless steel onto structural steel IS 2062 in single wire surfacing using the SAW process. They investigated the following weld bead parameters (penetration, reinforcement, width and dilution) as affected by the following SAW process variables (open-circuit voltage, wire feed-rate, welding speed and nozzle-to-plate distance). It was shown that the developed models can be employed easily in automated or robotic welding, in the form of a program, for obtaining the desired high quality welds. The results demonstrated that the bead penetration is not affected significantly by the voltage and nozzle-to-plate distance and the width is not affected by the latter.

However, no research work has been specifically carried out on the effects of gas metal arc welding parameters on the mechanical and corrosion behaviour of austenitic stainless steel immersed in corrosive alkaline (NaOH) and acidic (HCl) media using design expert software. Therefore, this research will provide more detailed information on the behaviour of ASS in acidic and alkaline environments and the interactions of welding parameters using design expert software.

CHAPTER THREE

3.0 MATERIALS, EQUIPMENT AND METHOD

3.1 Introduction

This chapter described details of materials and the experimental procedure required to effectively carry out this research on the effects of arc welding parameters on mechanical and corrosion behavior of austenitic stainless steel in some selected environments.

3.2 Materials

Austenitic stainless steel was used for this research work which was sourced locally at Kakuri Market in Kaduna, and its chemical composition was determined.Other materials that were used are:

i. Stainless steel electrode wire of 0.9mm diameter (G 19.9 L),
ii. Acetone,
iii. Etching reagent,
iv. Distill water,
v. SiC abrasive paper grit 120, 340, 400, 600 and 800
vi. Hydrochloric acid (HCl) 0.5 Molar concentrationand
vii. Sodium hydroxide (NaOH) 0.5 Molar concentration.

3.3 Equipment

The main equipment for this research were as follows:

i. Gas metal arc welding machine: SAFMIG 300 BLX

ii. Digital weighing balance: Sartorius Analytical Weight Balance ED224S Max 220g, d=0, 1mg.

iii. Izod impact testing machine: MODEL; 6701, Capacity 120 FT.LB, Machine No; E51425/9

iv. Indentec universal hardness testing machine: MODEL; 8187.5 LKV (B), INDENTER; Diamond cone (120^{o}).Scale-A (Rockwell Hardness Testing Machine)

v. Grinding machine to grind the samples: MODEL: ML 300

vi. Polishing machine: Polimet polisher, Serial No. 281-GGG-V-897

vii. Tensile testing machine: Monsanto Tensometer, Type W" Serial No. 9875.

viii. Scanning Electron Microscope (SEM): Phenom ProX

ix. Milling machine: MOTEURS LEROY, DINMO 80^{o}, current 15.6A

x. Guillotine shear: EDWARDS, MODEL 3.25/300, Capacity 3070x3.25mm

3.4 Methodology

3.4.1 Pre-welding sample preparation

The procedure in carrying out the sample preparation was as follows:

i. The A 3mm diameter of austenitic stainless steel was cut into 144 equal parts (samples) of 50mm x 15mm x 3mm rectangular bars each for impact test, hardness test and for immersion in the two media. Also, 20 samples of ASS 120mm x 15mm x 3mm were prepared for tensile tests; the 144 samples (76 sets) were used for the welding while 4 samples were used as control.

ii. The samples to be welded were cut to produce a plain face sample for butt wedding, leaving a root opening of 2mm. The butt welding method was implemented as shown in the sample preparation below in figure 3.1

iii. Both welded and unwelded specimens were cleaned of dirt and oil using paper grit of 120, 340, 400, 600 and 800 and acetone respectively. And a grinding machine was used to grind their surfaces prior to and after welding in order to have smooth surfaces for further mechanical tests.

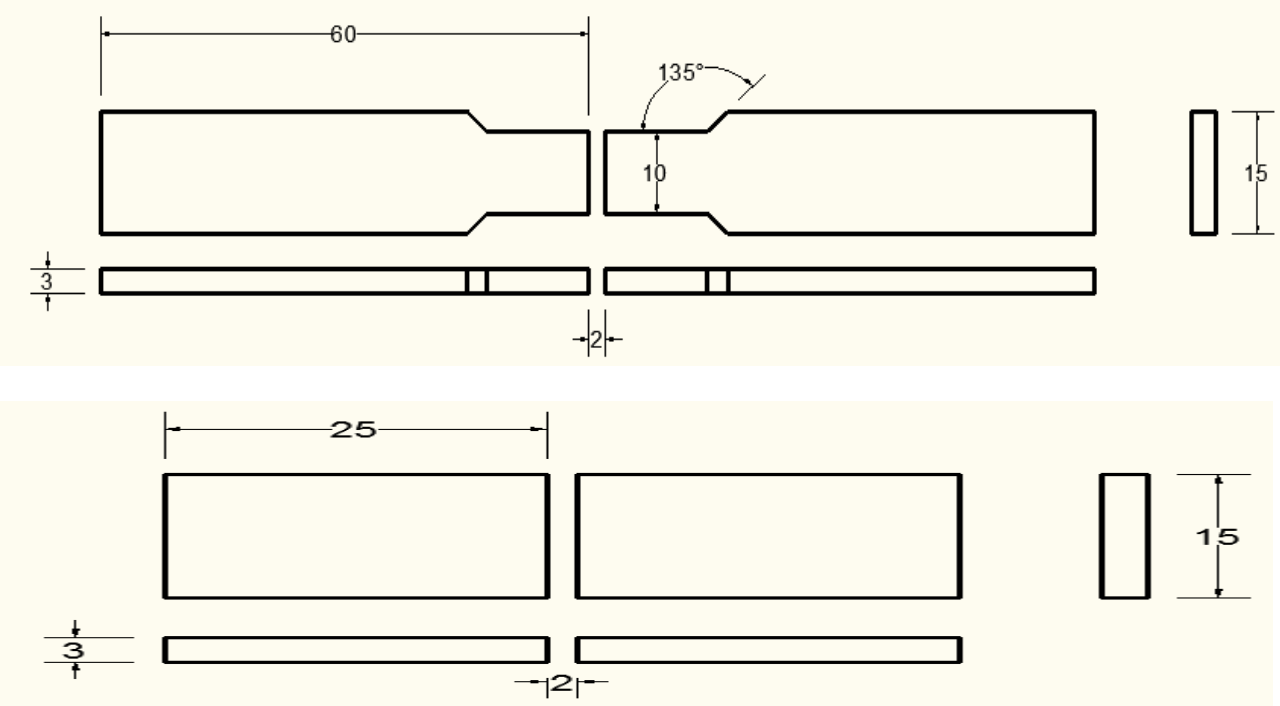

Figure 3.1: Standard Joint Preparations for plain face sample for welding.

3.4.2 Welding procedure

The gas metal arc welding machine was used to weld the 140 samples (70 sets) and the number of passes used was one on each of the specimen. The samples were welded at an angle of 30^{o} using argon gas as shielded gas. The welded samples were cooled in an ambient temperature. The welding process was carried out in Peugeot Automobile Nigeria Limited (PAN), Kaduna.

3.5 Welding Parameters Analysis

For this particular research, the specific welding parameters considered using Design-Expert Software 6.0.6. were;

3.5.1 The welding speed

The welding speed was set within the ranges of 20cm/min, 30cm/min and 40cm/min as low, centre and high levels respectively as shown in table 3.1 below.

3.5.2 The welding current

The number of levels of welding current needed depend greatly on the welding application and the associated welding speed. The current was appropriately set to standard to carry out the welding process. It was set at low, centre and high levels at 90 Amperes, 100 Amperes and 110 Amperes respectively as shown in table 3.1 below.

3.5.3 The welding voltage

This is the electrical potential difference between the tip of the welding wire and the surface of the molten weld pool. It determines the shape of the fusion zone and weld reinforcement. High welding voltage produces wider, flatter and less deeply penetrating welds than low welding voltages. Depth of penetration is maximum at optimum arc voltage. But the voltage here was kept constant at 230 volts during the welding operation.

3.5.4 Full factorial design of experiment for the welding parameters of ASS

Three factors which are important variables in welding of metals were selected to study the corrosion behaviour of ASS in hydrochloric acid and sodium hydroxide media. The variables were; Speed (S), Current (I) and constant Voltage (E) which are represented as A, B and C respectively. The corrosion behaviour was investigated by varying only two factors at two levels

(2^2), high (+1) and low (-1) with a centre point (0) in the experimental runs (Table 3.1 and 3.2). The interactions between these factors were studied and optimization was done using interaction plots, three dimensional plots and cube plots (Okibe, 2014). Design Expert software 6.0.6 was used to generate the experimental runs and for the statistical analysis of weight loss in milligram of the ASS in the two corrosive media (HCl and NaOH) in an interval of eight (8) for forty (40) days.

Table 3.1: Factors and levels used for the welding parameters;

Welding parameters	**Symbol**	**Unit**	**Factor Levels**		
			Low (-)	**Centre (0)**	**High (+)**
Speed	S	cm/min	20	30	40
Voltage	E	Volts	230	230	230
Current	I	Amp	90	100	110

Table 3.2: Design matrix for welding parameters of ASS in HCl and NaOH media

Std	**Run**	**A: Speed (cm/min)**	**B: Current (Amp)**	**C:Voltage (volts)**
1	1	20	90	230
3	2	20	110	230
5	3	30100	230	
4	4	40110	230	
2	5	4090	230	
6	6	30100	230	

3.5.5 Preparation of stock solution

The preparation of the stock solution is in accordance to (Ojokuku, 2001);

i. Preparation of 0.5M of sodium hydroxide (NaOH)

Molar mass of NaOH = 23+16 +1 = 40g

But 1 mol dm^3 contains 40g of NaOH

0.5mol dm^3 contains Xg solution.

∴ Xg = 40.00× 0.5/1

= <u>20.00 g/ dm^3</u>

ii. Preparation of 0.5M of hydrochloric (HCl) acid.

Standard concentrated HCl acid has a density of 1.18g/cm^3 and a percentage purity of 36%. It has a molar mass of 35.5g. To obtain the molarity of the concentrated HCl acid, the following relation was used:

$$Molarity = \frac{Concentration}{Molar\ Mass} \quad \text{----------3.1}$$

But;Concentration = standard volume x density x percentage purity.

Therefore, for 1 litre (1000cm^3) of standard HCl acid,

Concentration = 1000cm^3 x 1.18g/cm^3 x 36 %

Hence, the molarity is given by:Molarity = (1000 x 1.18 x 36)/ 35.5 = 11.97M

From the relation by (Calister, 2007)

$C_1V_1 = C_2V_2$……..3.2

Where: C= Concentration of the acid and

V = Volume of the acid

500$cm^3$of 0.5M HCl acid is required. Hence,

$$11.97 \times V_1 = 0.5 \times 500$$

$V_1 = (0.5 \times 500)/ 11.97 = 20.89\ cm^3$

Therefore, 20.89cm^3 of HCl from Standard Winchester bottle was dissolved in 500cm^3 of distilled water to obtain the desired concentration. This is in accordance with (Aluko, 2014).

3.5.6 Weight loss measurement

The samples of austenitic stainless steel was cut into pieces and polished with silicon carbide papers of grit size 120. The initially weighed samples were immersed in 1dm^3 of volumetric flask containing solution each of 20.00g/ $dm^3$and 20.89 $cm^3$of NaOH and HCl respectively for 40 days. The test specimens were taken out of the corrosive media (each) after every 8 days, wash with distilled water and acetone, air dried and re-weighed according to Yawas (2005).

The weight loss of the austenitic stainless steel samples were assessed using the digital weighing balance of 0.0001g sensitivity.The specimens were weighed after every 8 days and it continued for 40 days.

3.6 Mechanical (Destructive) Test Procedure

3.6.1 Tensile test

Tensile test is one of the most widely used of the mechanical test, here the ASS of 3mm thickness was cut into 120mmand a width of 15mm from a flat bar and was machined on a milling machine into a standardized shape of the sample with a central reduced section for tensile test . A flat bar of ASS undergoing machining on a milling machine is shown in Plate Id. Figure 3.2 presents standard samples for tensile test.

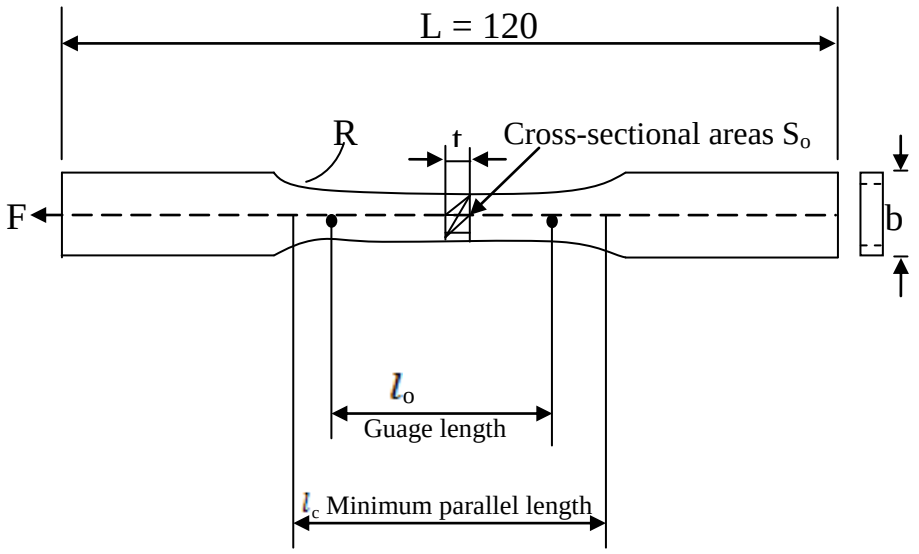

a

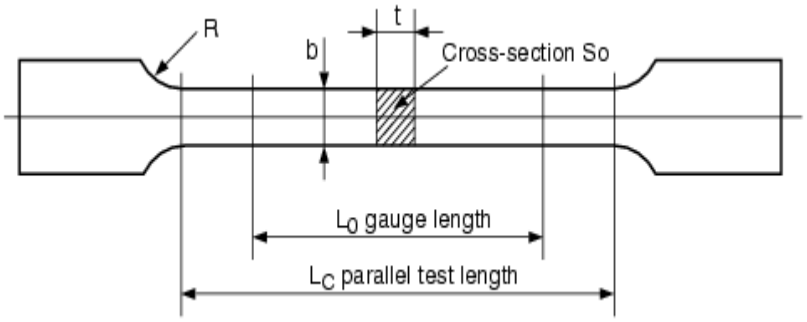

b

Figure 3.2: Dimensions of sample for tensile test

The samples were subjected to tensile tests in accordance with ASTM E8 Standard Method. These tests were carried out using the Monsanto Tensometer, Type "W" with a capacity of 20kN. Twenty (20) samples were prepared and subjected to tensile test. Before the test was carried out, each of the samples was cut at the centre and chamfered on a milling machine. GMAW process was used to weld the specimen at the point of cut. Five of the prepared samples were welded but not immersed, twelve samples were welded and immersed in the two media (NaOH and HCl) while one sample was not welded and not immersed (as control). Thereafter all the specimens

were subjected to tensile test. Monsanto Tensometer was used to perform the test. Here the specimen was gripped in between the chucks of the Tensometer, which can apply a measured load of up to 20kN to the specimen held between the chucks. The diameters of all the samples were noted and the autographic recording drum of the machine was covered with a graph sheet and the pointer set at zero before the commencement of the tests. The load was then applied by hand using the load handle until the specimen was pulled to fracture. The load is measured by the deflection of a spring, which in deflecting causes a mercury piston to displace mercury in to a small bore glass tube adjacent to a graduated scale. The load against extension graph was plotted and traced out on the graph, from the graph we obtained the maximum load, the breaking load and the strain of the specimen which is change in length/ gauge length and also the percentage elongation was determined. The experiment was carried out in Mechanical Engineering Department, Ahmadu Bello University, Zaria.

3.6.2 Impact test

The impact test continues to be used as an economical quality control method to determine the notch sensitivity and impact toughness of engineering materials (www.wmtr.com). The reliability of a material can be determined, by measuring its resistance to fracture, either ductile or brittle of fracture toughness (Ives, 2001). The impact tests was conducted in accordance with ASTM A370 "Standard Method and Definitions for Mechanical Testing of Steel Products". Thirty seven (37) samples of ASS sheet of 3mm thickness, width 15mm and length 50mm was used for impact test. These samples were cut into two halves and welded along the cut section using GMAW machine with stainless steel electrode core wire. V- notches of 0.3mm depth was made on the samples and were tested for toughness using the Izod impact testing machine and the results obtained were

recorded in joules. Plate I shows the Izod impact testing machine used for the impact test. The test was done in Mechanical Engineering Department, ABU Zaria

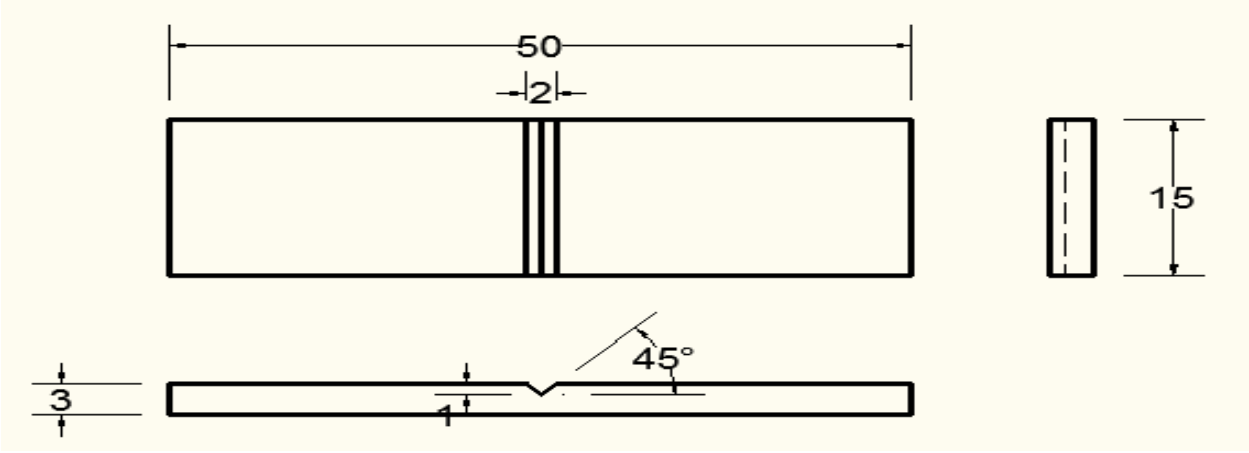

Figure 3.3: Sample for impact test with a notch of 0.3mm

Plate; I: Izod impact testing machine used for the impact test.

3.6.3 Hardness test

The hardness value of the samples of austenitic stainless steel was determined according to the American Society of Testing and Materials (ASTM E18-79) using Indentec Universal Hardness

Testing machine (Rockwell type) Model 8187.5 LKV (B) with diamond cone indenter 120^{o}, minor load of 10kgf, major load of 60kgf. Before the test, the mating surfaces of the indenter, plunger rod and the test samples were thoroughly cleaned by removing the dirt, scratches and oil. The hardness test was carried out in Metallurgical and Materials Engineering Department, Ahmadu Bello University, Zaria, Kaduna state.

Plate; II: Identec universal hardness testing machine type 8187.5 LKV model B (ABU, Zaria)

3.7 Metallography of Austenitic Stainless Steel

3.7.1. Scanning Electron Microscopy of austenitic stainless steel.

Microstructural analysis of the metal was carried out by the use of a scanning electron microscope (SEM) in order to expose and make visible the structural characteristics of the specimen. The welded and the unwelded austenitic stainless steels were viewed using Phenom ProX scanning electron microscope with a magnification of 5000x. The samples for investigation were prepared in accordance with the specifications of the machine (SEM). The setup was then loaded into the

column which is connected to the monitor in a closed loop for which control and feedback are actualized. A finely focused electron beam with voltage energy of 15kv was used across the surface of the welded sample (FZ and HAZ parts) and also with the unwelded sample. The magnification is computed by the ratio of the image width of the output medium divided by the field width of the scanned area. The tests were carried out at the Chemical Engineering Department, Ahmadu Bello University, Zaria, Kaduna State, Nigeria.

3.8 Labeling of Samples

The samples after preparation were conveniently labeled before the various tests were carried out on them. The labelling is given in table 3.3 below;

Table 3.3 sample labelling

Sample C	Control sample not welded and not immersed (As received)
Sample C_1	Sample welded with 20cm/min speed and 90A current at constant voltage of 230V
Sample C_2	Sample welded with 20cm/min speed and 110A current at constant voltage of 230V
Sample C_3	Sample welded with 30cm/min speed and 100A current at constant voltage of 230V
Sample C_4	Sample welded with 40cm/min speed and 110A current at constant voltage of 230V
Sample C_5	Sample welded with 40cm/min speed and 90A current at constant voltage of 230V

Note that during the course of this research,some sets of C_1- C_5 were used as control while other sets were immersed in the different media (hydrochloric acid and sodium hydroxide).

CHAPTER FOUR

4.0RESULTS

4.1 Introduction

This chapter presents the results of the factorial experimental design of the samples immersed in sodium hydroxide and hydrochloric acid media. Also, the mechanical tests conducted on the welded joints of all the samples as well as the microstructural analysis of the samples (control, weldments and heat affected zone) using scanning electron microscope.

4.2Chemical Composition of Research Material

Table 4.1: Chemical Composition of austeniticstainless steel.

Element	C	Si	Mn	P	S	Cr	Ni	Mo
% by wt	0.1220	0.5400	1.3600	0.0300	0.0190	20.1200	8.3400	0.1880
Element	Al	Cu	Co	Ti	Nb	V	W	Pb
% by wt	0.0095	0.2570	0.1060	0.0027	0.0360	0.0660	0.0350	0.0064
Element	B	Sn	As	Bi	Ca	Fe	Total	
% by wt	0.0014	0.0110	0.0210	<0.0015	>0.0024	68.7000	100	

4.3 Results of factorial design

Table 4.2 ANOVA for the factorial model for speed and current at a constant voltage for NaOH environment.

Source	Sum of Squares	DF	Mean Square	F Value	Prob>F	Remark
Model	$2.163X10^{-5}$	3	$7.209X10^{-6}$	50.44	0.0195	Significant
A	$5.063X10^{-6}$	1	$5.063X10^{-6}$	35.42	0.0271	Significant
B	$1.056X10^{-5}$	1	$1.056X10^{-5}$	73.91	0.0133	Significant
AB	$6.002X10^{-6}$	1	$6.002X10^{-6}$	42.00	0.0230	Significant
Residual	$2.858X10^{-7}$	2	$1.083X10^{-7}$			
Lack of Fit	$4.083X10^{-8}$	1	$4.083X10^{-8}$	0.17	0.7532	Not Significant
Pure Error	$2.450X10^{-7}$	1	$2.450X10^{-7}$			
Cor Total	$2.191X10^{-5}$	5				

Std. Dev. $3.780\ X10^{-4}$ R^2 0.9870

Mean $1.867\ X10^{-3}$ R^2_{Adj} 0.9674

C.V 20.25 R^2_{Pred} 0.8927

C.L 95% Adeq Precision 18.466

Where

C.V is theCoefficient of Variance

C.L is theConfidence Limit

Table 4.3 ANOVA for the factorial model for speed and current at a constant voltage for HCl environment**.**

Source	**Sum of Squares**	**DF**	**Mean Square**	**F Value**	**Prob>F**	**Remark**
Model	$1.011X10^{-3}$	3	$3.372X10^{-4}$	63.66	0.0155	Significant
A	$1.156X10^{-5}$	1	$1.156X10^{-5}$	2.18	0.2776	Not Significant
B	$3.497X10^{-4}$	1	$3.497X10^{-4}$	66.02	0.0148	Significant
AB	$6.502X10^{-4}$	1	$6.502X10^{-4}$	122.77	0.0080	Significant
Residual	$1.059\ X10^{-5}$	2	$5.297X10^{-6}$			
Lack of Fit	$4.813X10^{-6}$	1	$4.813X10^{-6}$	0.83	0.5291	Not Significant
Pure Error	$5.780X10^{-6}$	1	$5.780X10^{-6}$			
Cor Total	$1.022X10^{-3}$	5				

Std. Dev. $2.301\ X10^{-3}$ R^2 0.9896

Mean 7.6% R^2_{Adj} 0.9741

C.V 3.04 R^2_{Pred}0.7613

C.L 95% Adeq Precision 23.52

Table 4.4 Design matrix and responses of welding parameters of ASS in NaOH environment

Std	Run	A: Speed (cm/min)	B: Current (Amp)	C: Voltage (volts)	WL_8 (mg)	WL_{16} (mg)	WL_{24} (mg)	WL_{32} (mg)	WL_{40}
1	1	20	90	230	0.0024	0.0012	0.0024	0.0016	0.0035
3	2	20	110	230	0.0009	0.0004	0.0011	0.0012	0.0037
5	3	30	100	230	0.0020	0.0021	0.0018	0.0017	0.0028
4	4	40	110	230	0.0008	0.0002	0.0006	0.0004	0.0020
2	5	40	90	230	0.0016	0.0059	0.0053	0.0040	0.0094
6	6	30	100	230	0.0009	0.0014	0.0010	0.0024	0.0034

Table 4.5 Design matrix and responses of welding parameters of ASS in HCl environment

Std	Run	A:Speed (cm/min)	B:Current (Amp)	C:Voltage (volts)	WL_8 (mg)	WL_{16} (mg)	WL_{24} (mg)	WL_{32} (mg)	WL_{40}
1	1	20	90	230	0.0608	0.0699	0.0795	0.1103	0.1073
3	2	20	110	230	0.0708	0.0767	0.1047	0.1309	0.1880
5	3	30	100	230	0.0485	0.0752	0.0901	0.1005	0.0971
4	4	40	110	230	0.0470	0.0546	0.0970	0.0974	0.0759
2	5	40	90	230	0.0631	0.0988	0.1356	0.2151	0.3498
6	6	30	100	230	0.0480	0.0786	0.1412	0.1016	0.1181

4.3.1 Interactions between two welding variables

The response surface plots and the interactions between speed and current at constant voltage for ASS specimens immersed in NaOH and HCl acid for 8, 16, 24, 32 and 40 days are presented in figures 4.1 to 4.10

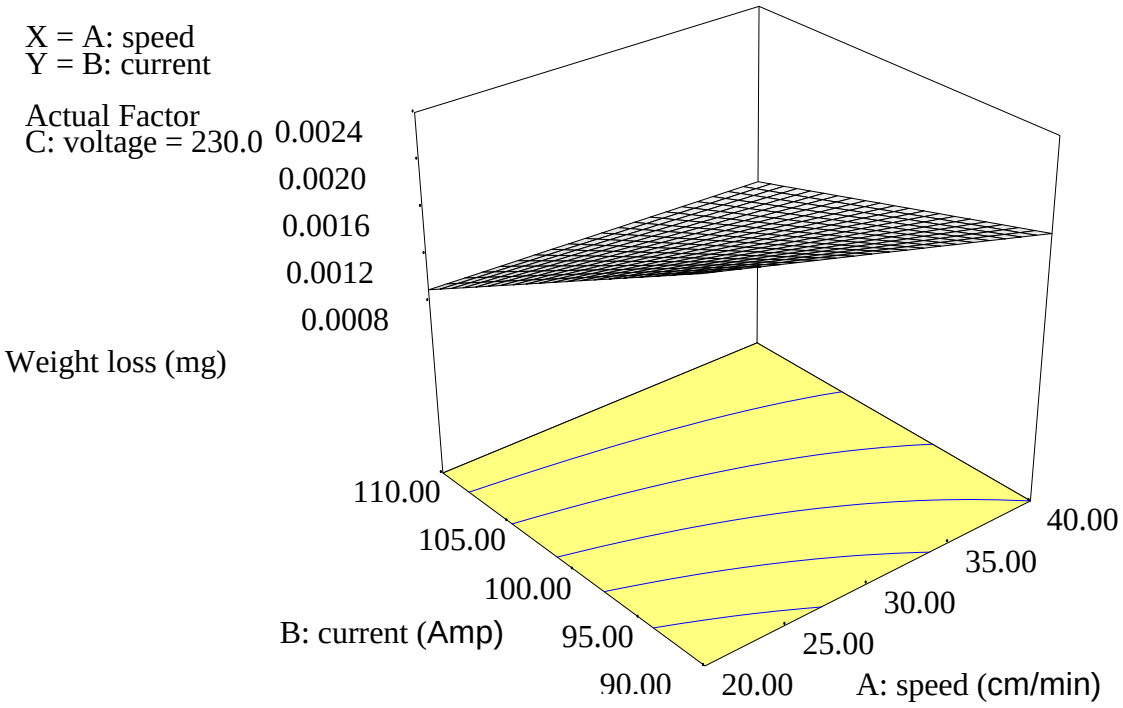

Figure 4.1: Response surface plot for ASS immersed in NaOH for 8 days

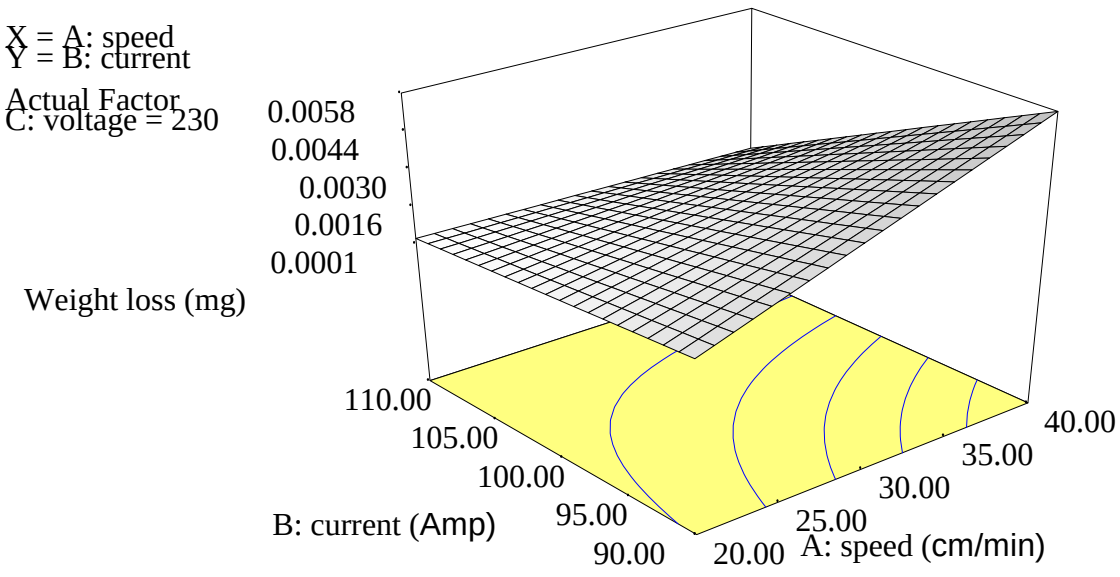

Figure 4.2: Response surface plot for ASS immersed in NaOH for16 days

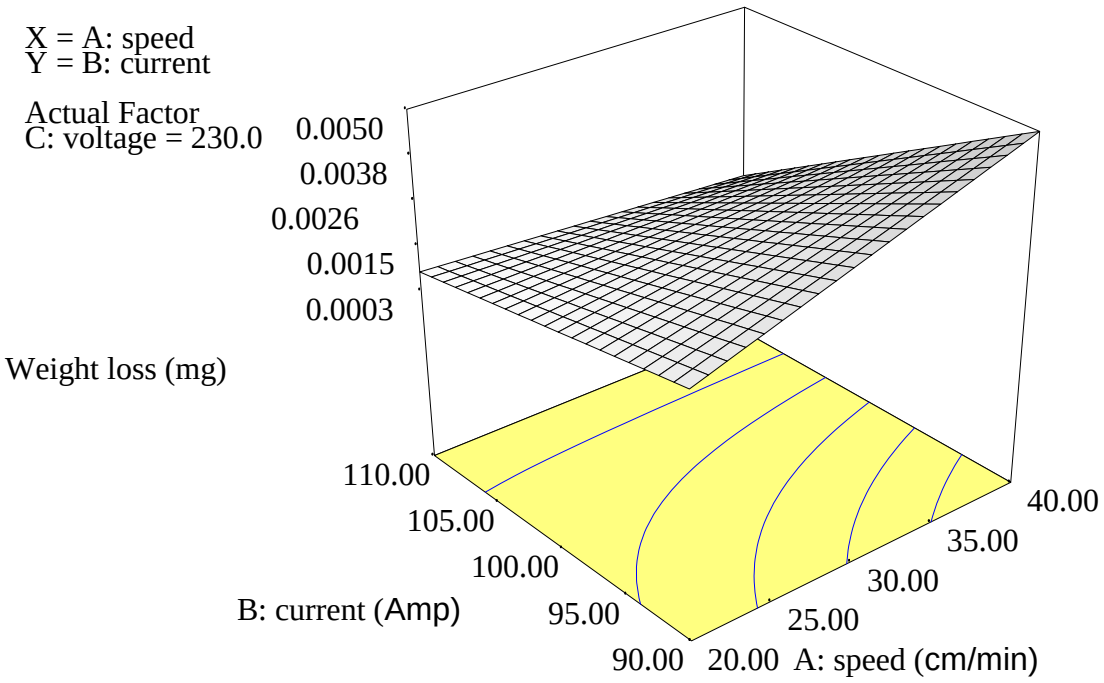

Figure 4.3: Response surface plot for ASS immersed in NaOH for 24 days

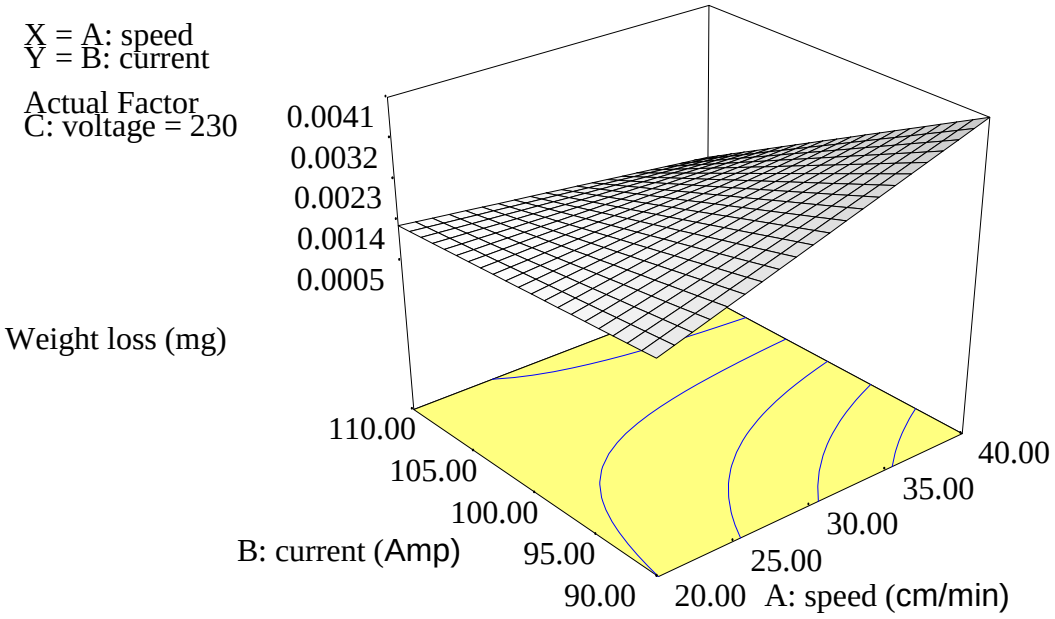

Figure 4.4: Response surface plot for ASS immersed in NaOH for 32 days

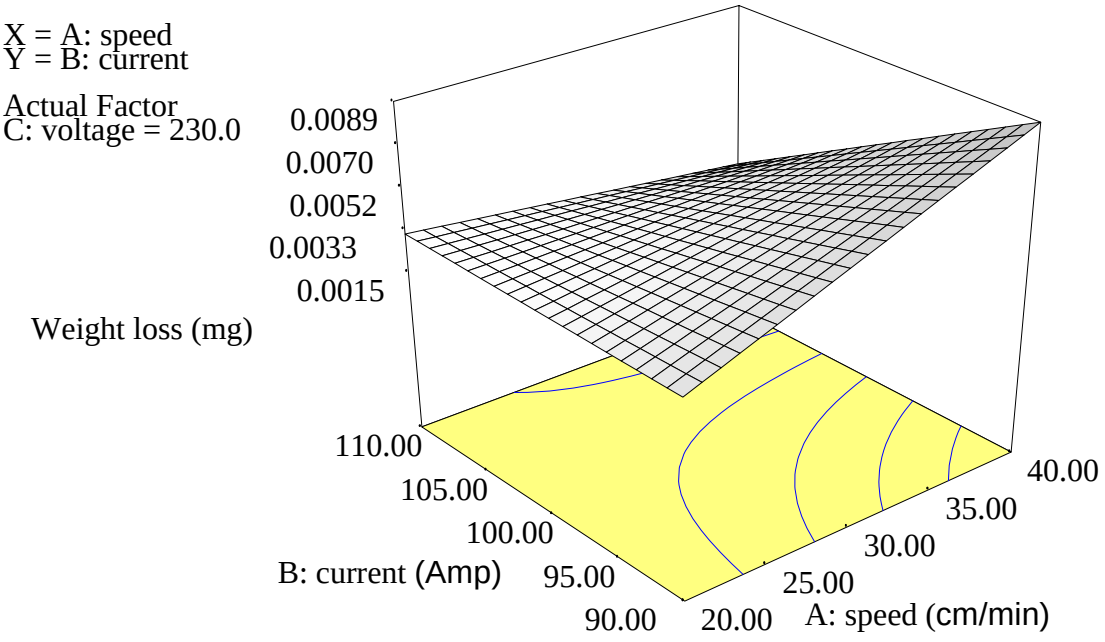

Figure 4.5: Response surface plot for ASS immersed in NaOH for 40 days.

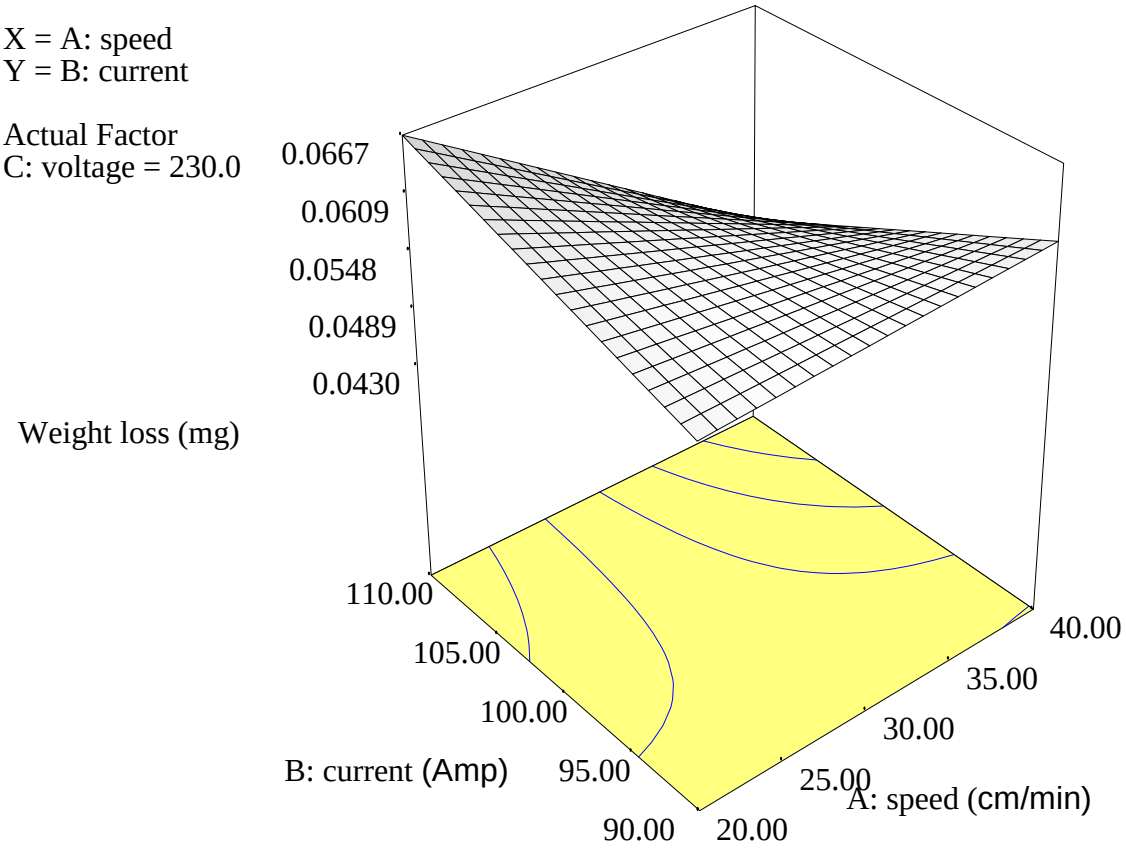

Figure 4.6: Response surface plot for ASS immersed in HCl for 8 days

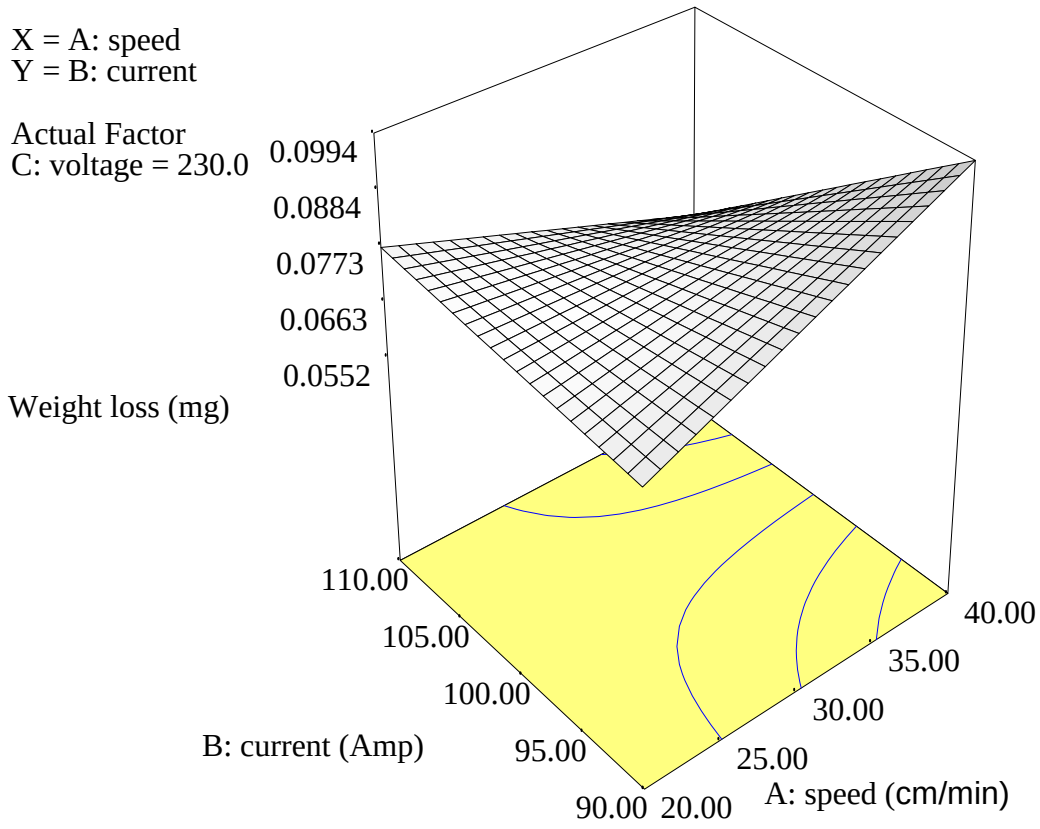

Figure 4.7: Response surface plot for ASS immersed in HCl for 16 days

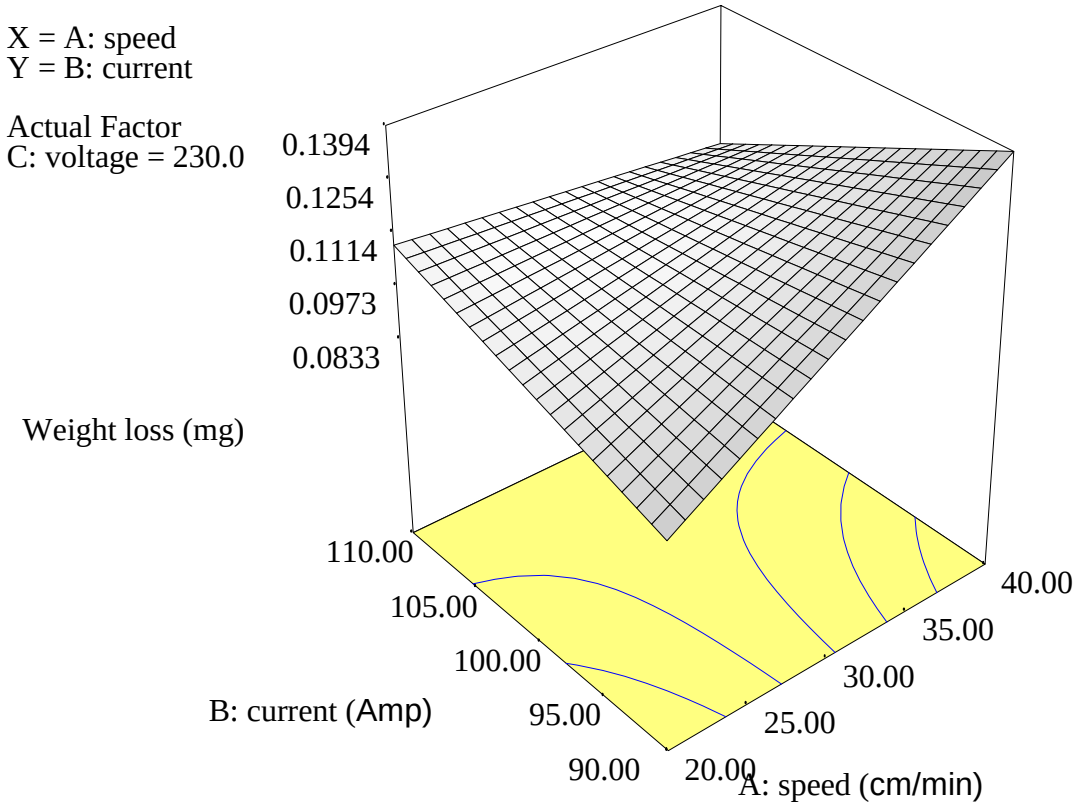

Figure 4.8: Response surface plot for ASS immersed in HCl for 24 days

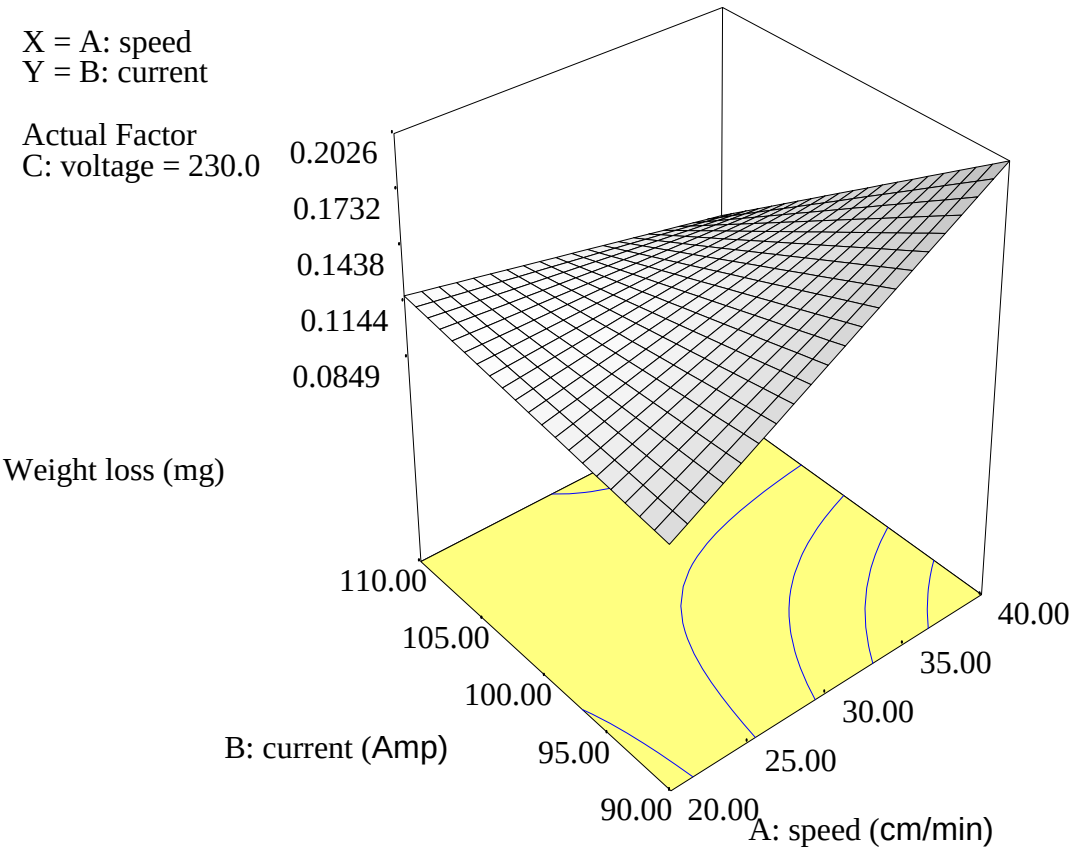

Figure 4.9: Response surface plot for ASS immersed in HCl for 32 days

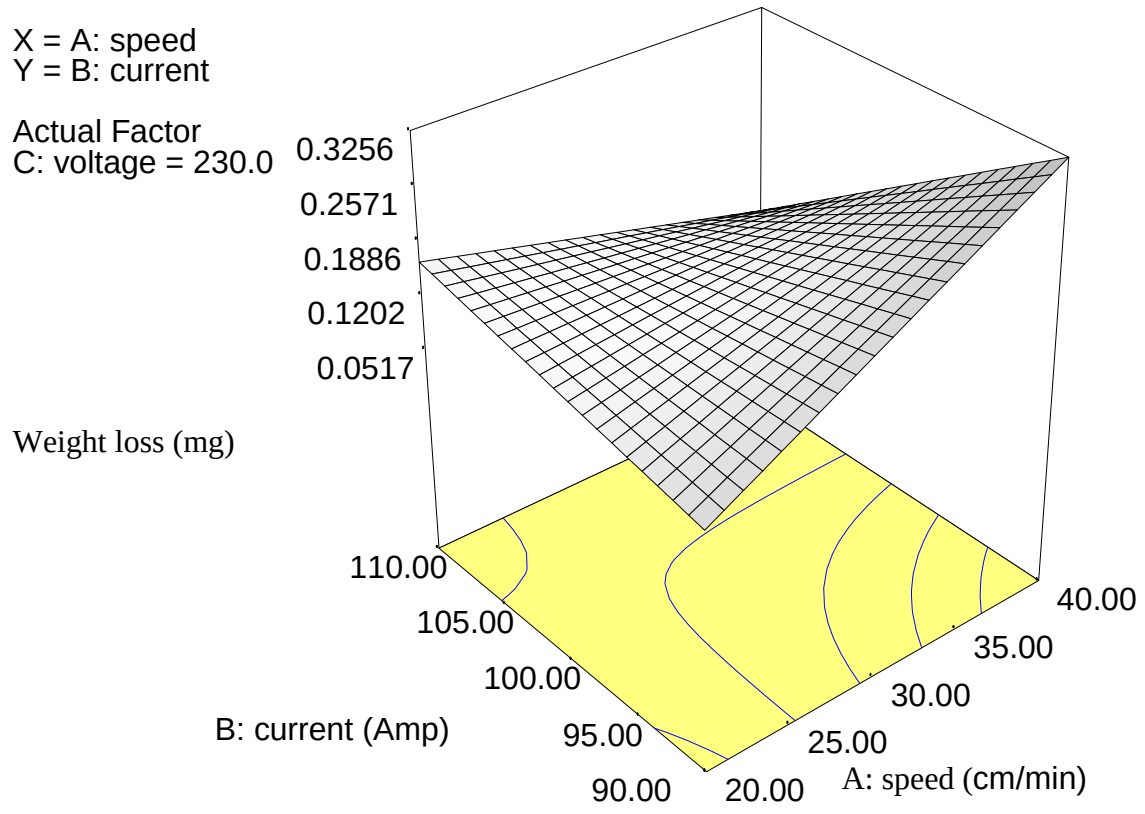

Figure 4.10: Response surface plot for ASS immersed in HCl for 40 days

4.3.2 Interaction between two welding variables and a constant

The interactions between speed and current at constant voltage for ASS specimens immersed in NaOH and HCl acid for 8, 16, 24, 32 and 40 days are presented in figures 4.11 to 4.20

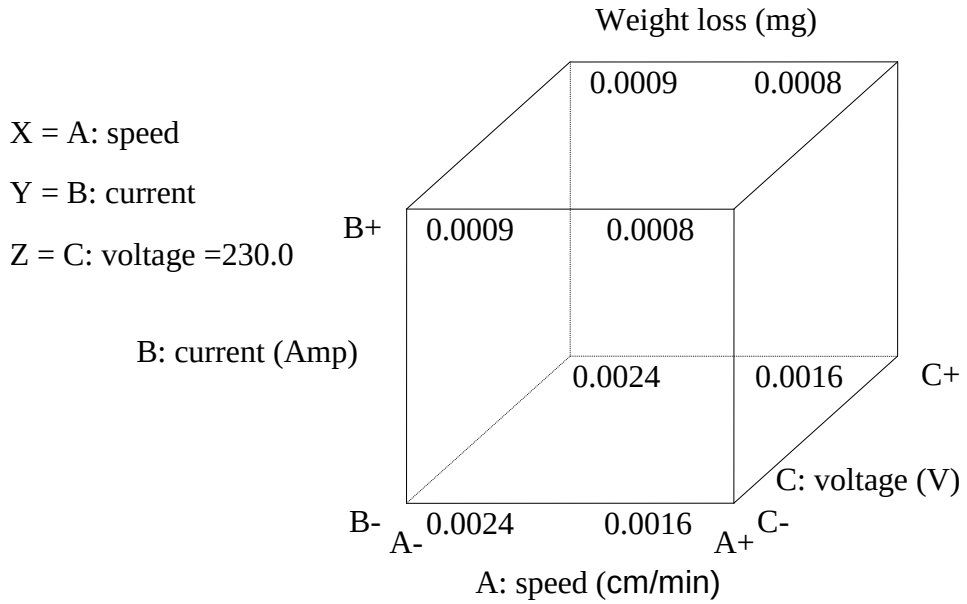

Figure 4.11: Cube plot for ASS immersed in NaOH for 8 days

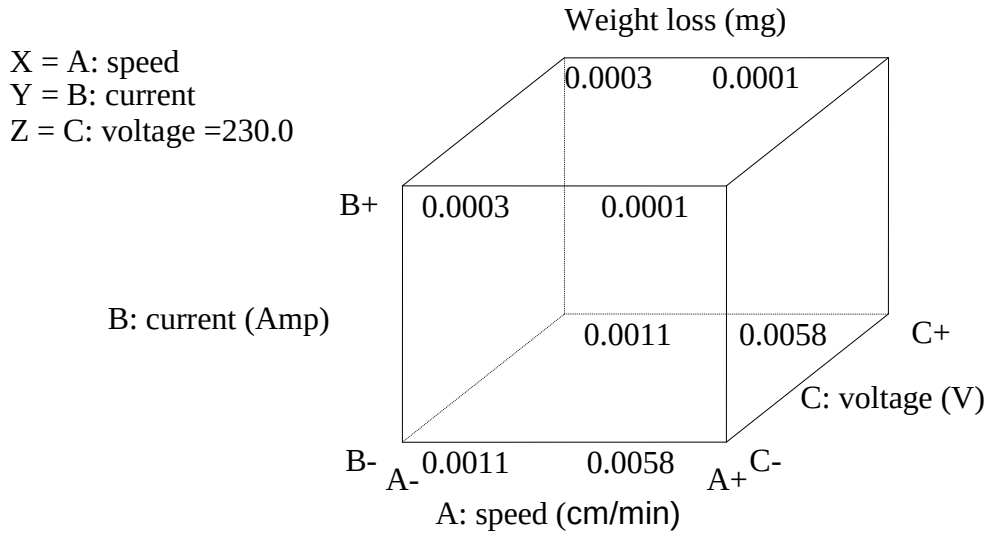

Figure 4.12: Cube plot for ASS immersed in NaOH for 16 days

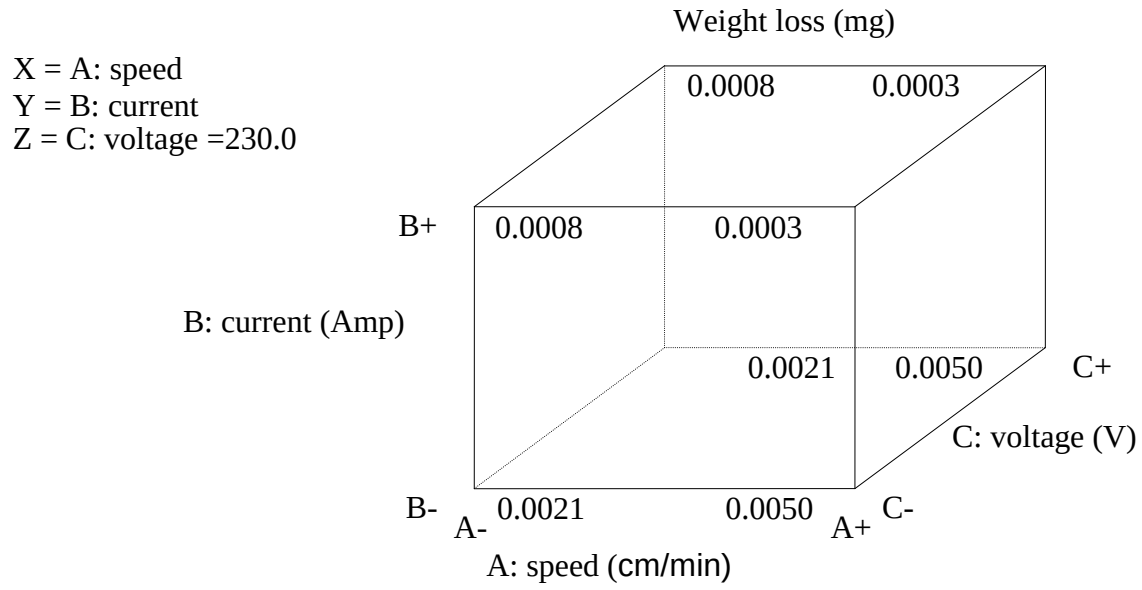

Figure 4.13: Cube plot for ASS immersed in NaOH for 24 days

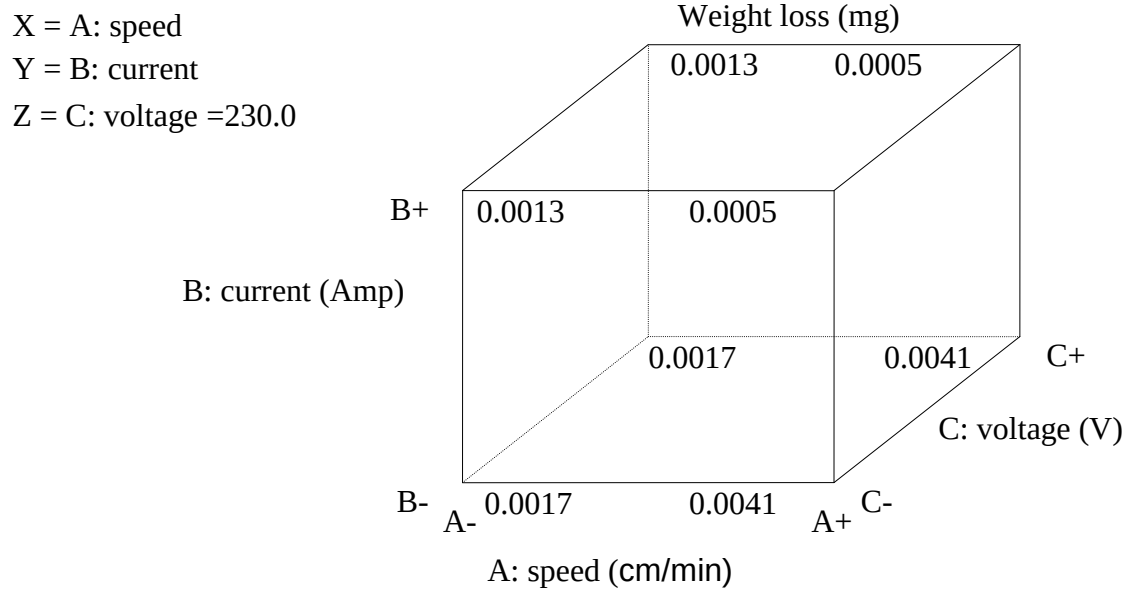

Figure 4.14: Cube plot for ASS immersed in NaOH for 32 days

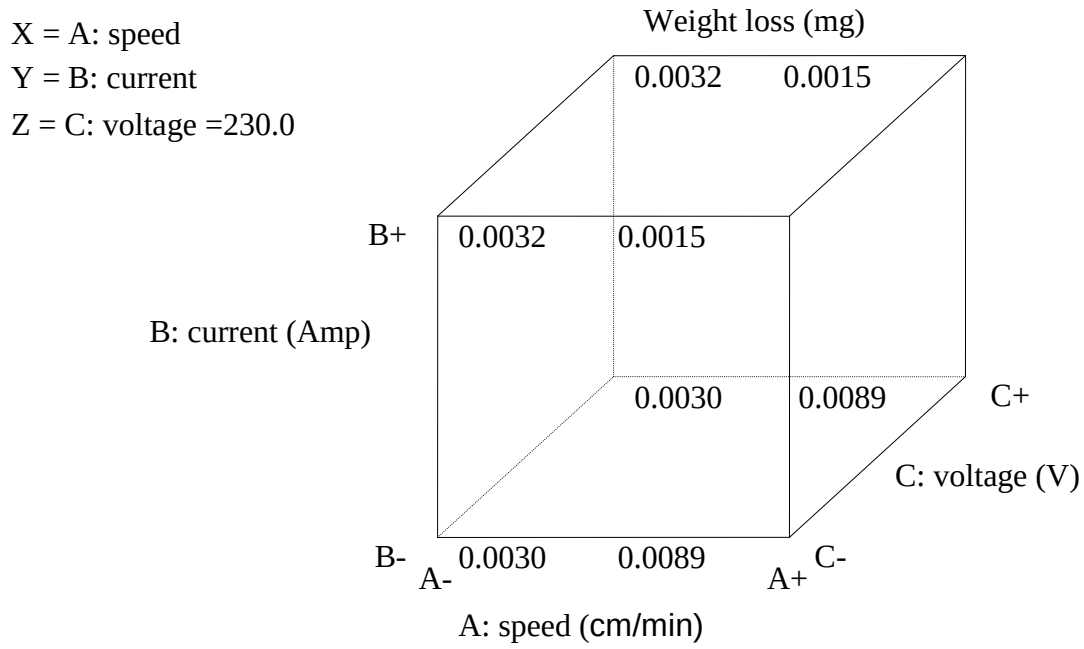

Figure 4.15: Cube plot for ASS immersed in NaOH for 40 days

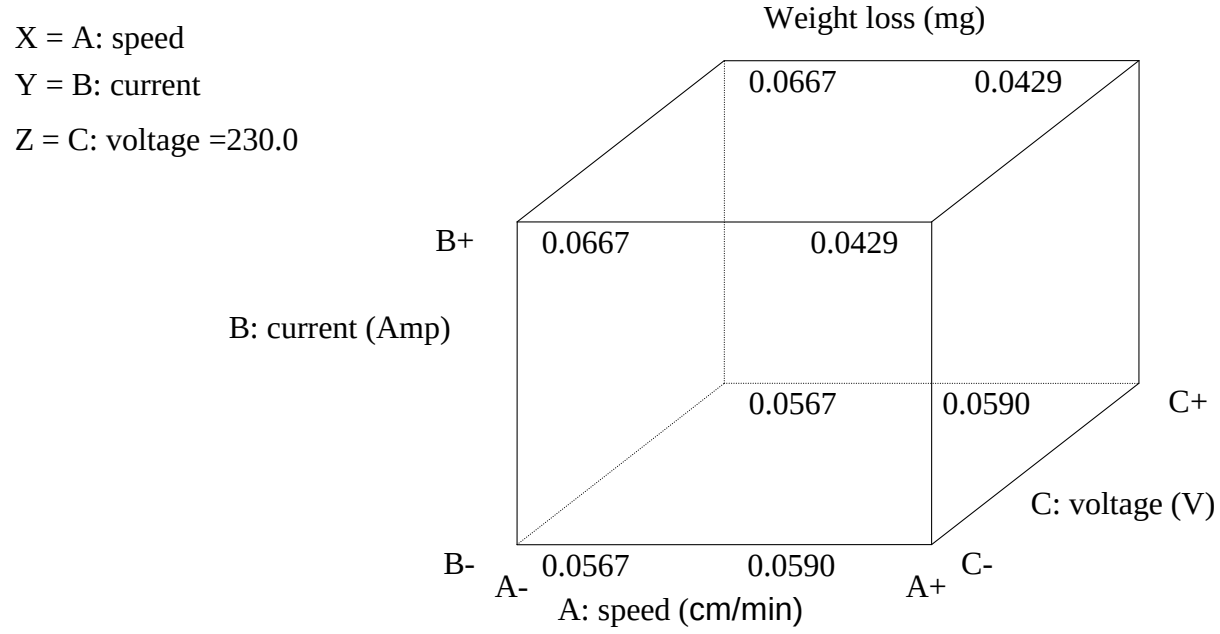

Figure 4.16: Cube plot for ASS immersed in HCl for 8 days

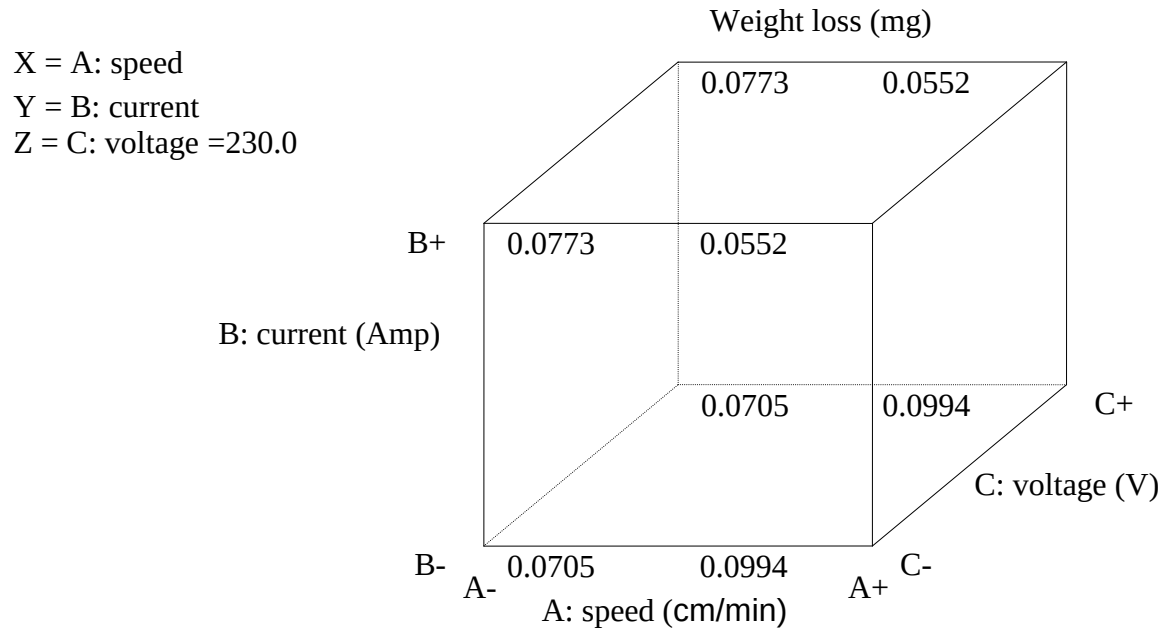

Figure 4.17: Cube plot for ASS immersed in HCl for 16 days

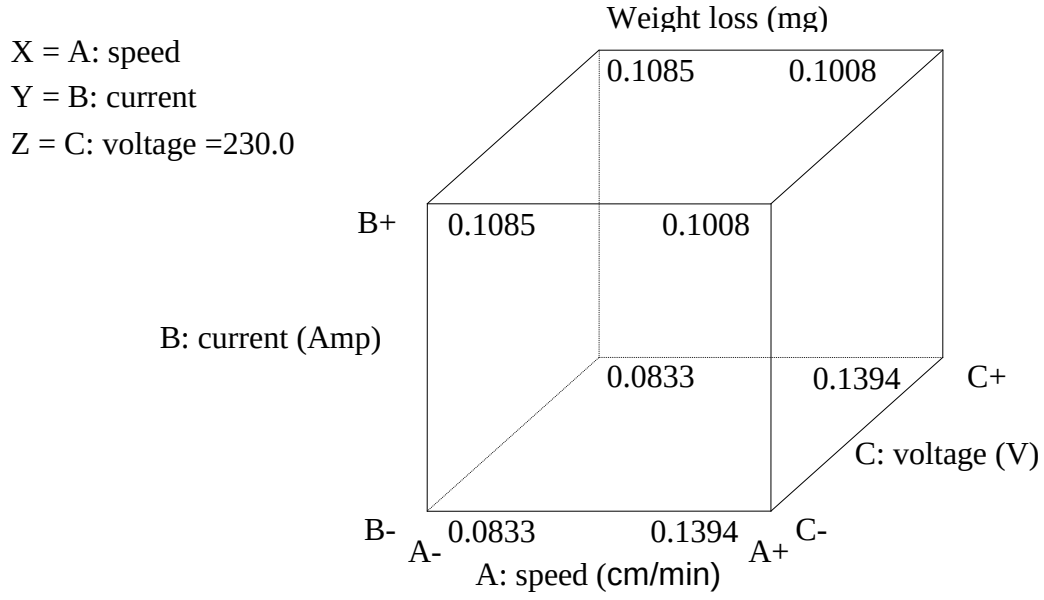

Figure 4.18: Cube plot for ASS immersed in HCl for 24 days and the interaction between speed, current and voltage.

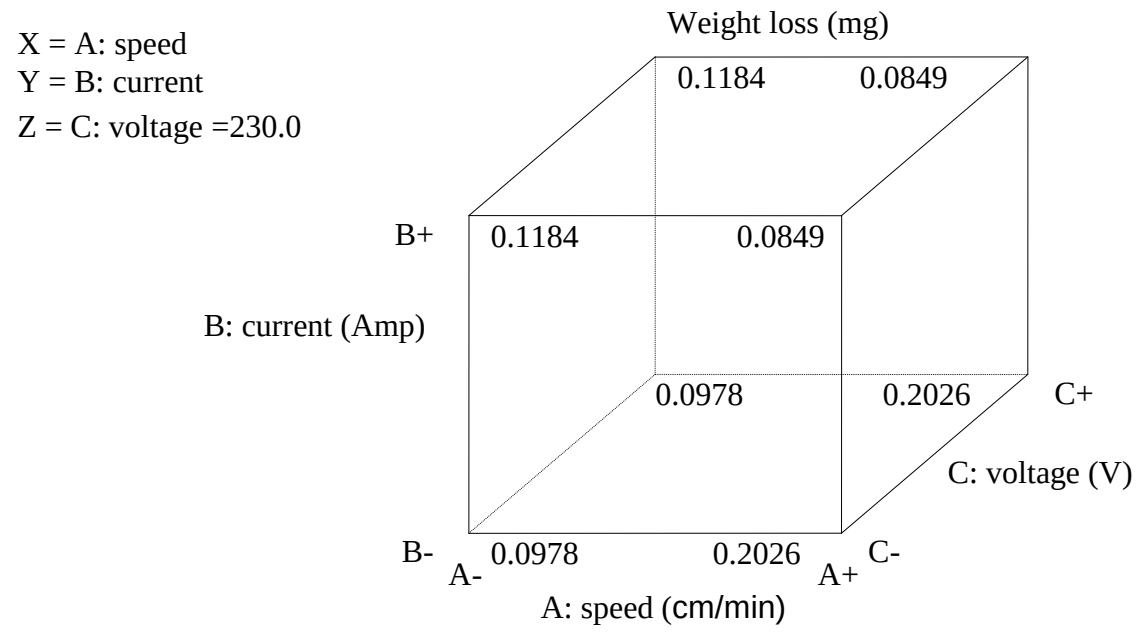

Figure 4.19: Cube plot for ASS immersed in HCl for 32 days

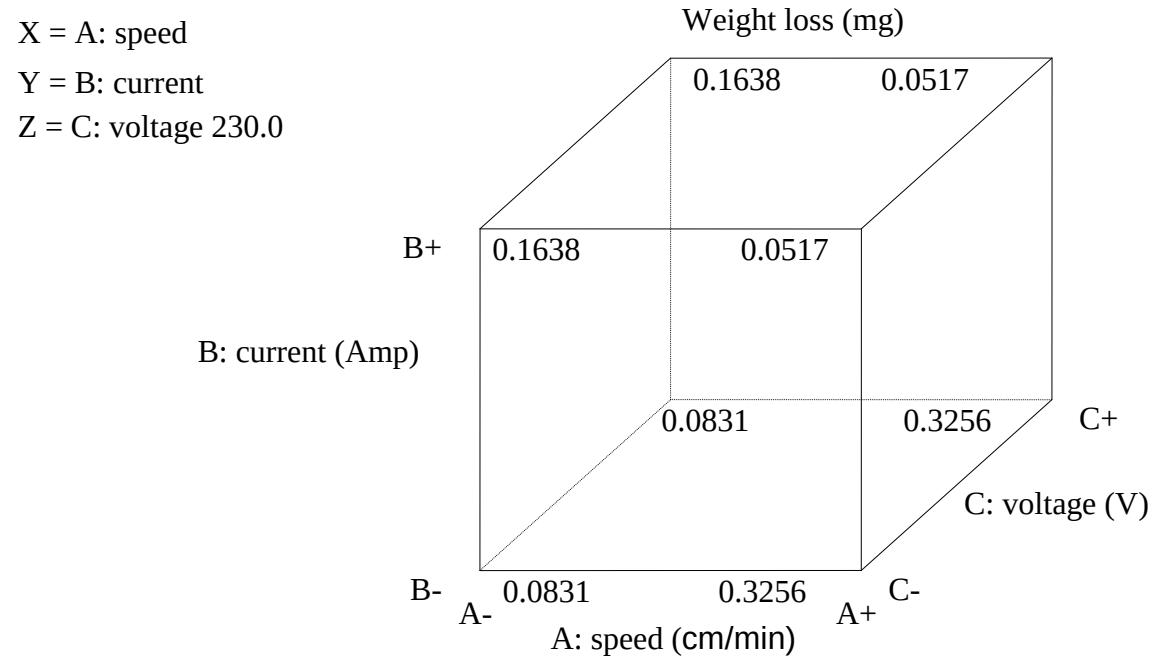

Figure 4.20: Cube plot for ASS immersed in HCl for 40 days

4.4 The Mechanical Properties of the Samples

4.4.1 Hardness values of the samples

The comparison of hardness value of ASS at a given parameter in NaOH with a control samples is given in figure 4.21 to 4.25

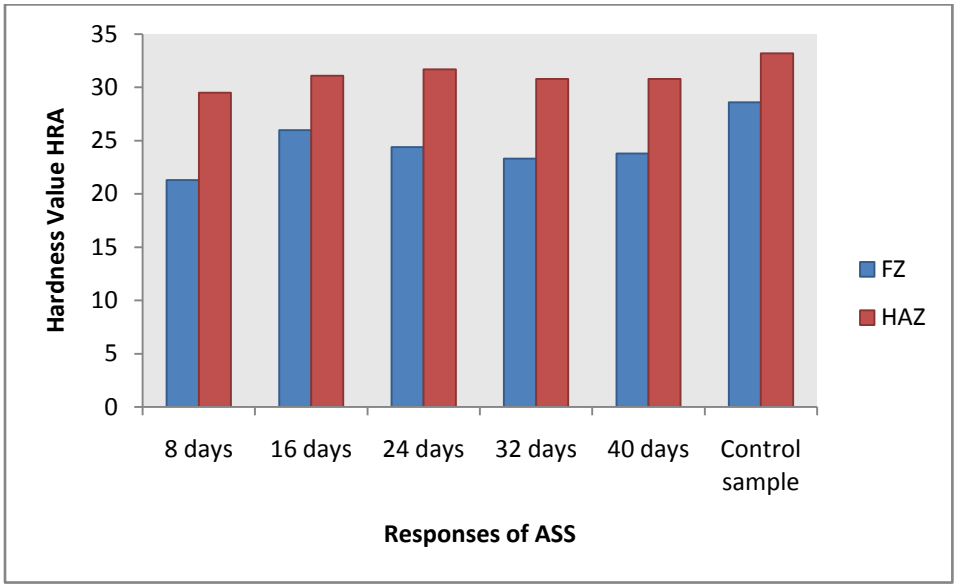

Figure 4.21: Comparison of hardness value of ASS at a given parameter (C1) in NaOH medium with a control sample.

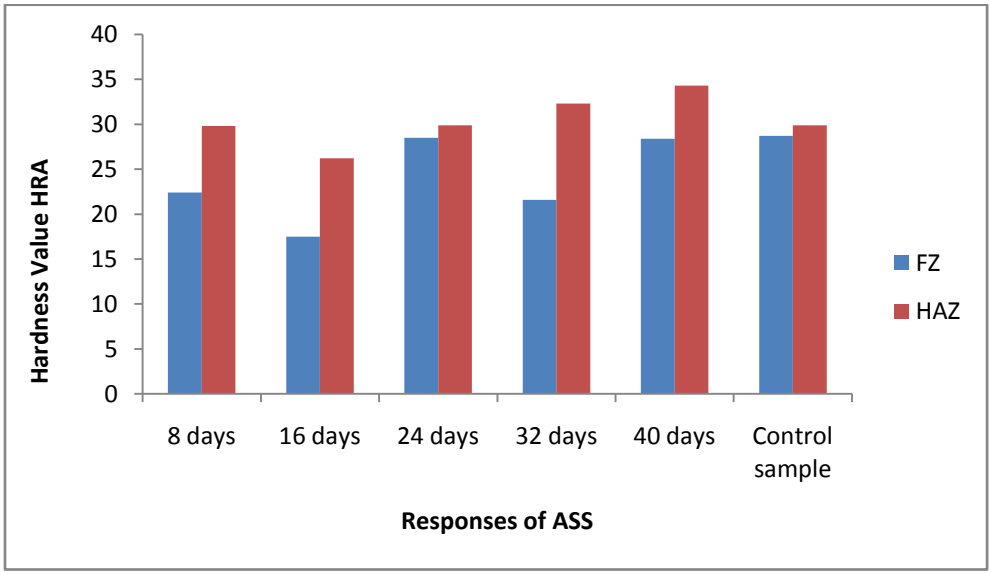

Figure 4.22: Comparison of hardness value of ASS at a given parameter (C_2) in NaOH medium with a control sample.

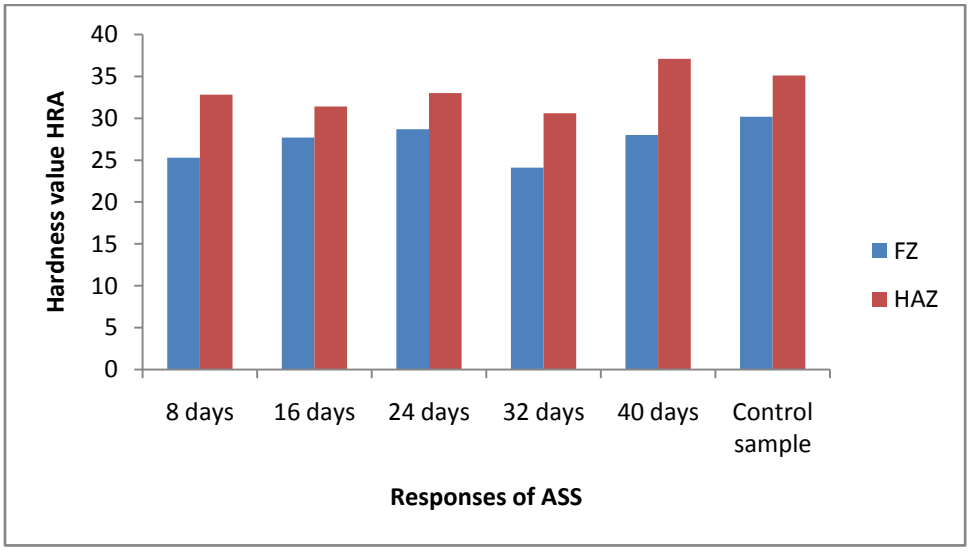

Figure 4.23: Comparison of hardness value of ASS at a given parameter (C_3) in NaOH medium with a control sample.

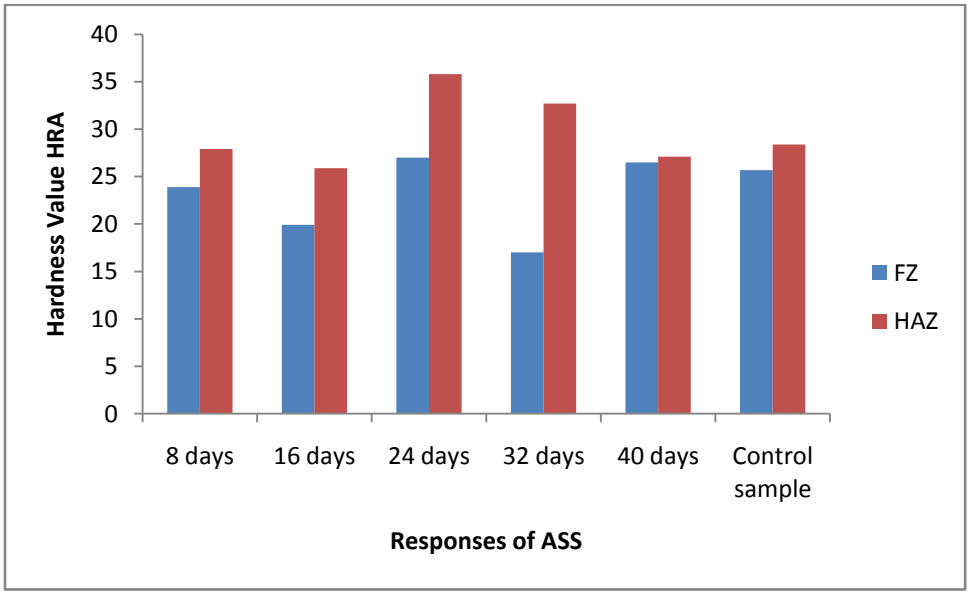

Figure 4.24: Comparison of hardness value of ASS at a given parameter (C_4) in NaOH medium with a control sample.

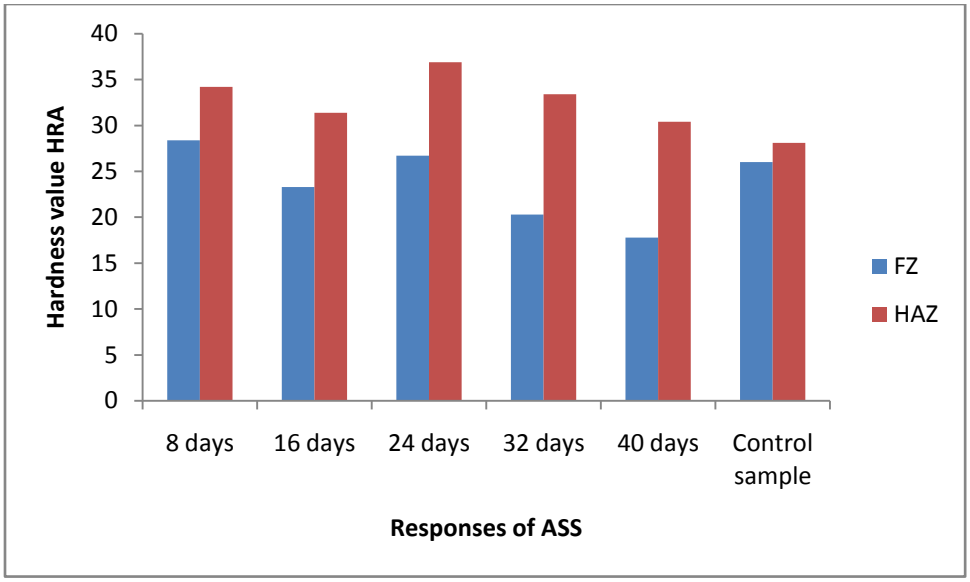

Figure 4.25: Comparison of hardness value of ASS at a given parameter (C_5) in NaOH medium with a control sample.

The comparison of hardness value of ASS at a given parameter in HCl with a control samples is given in figure 4.26 to 4.30

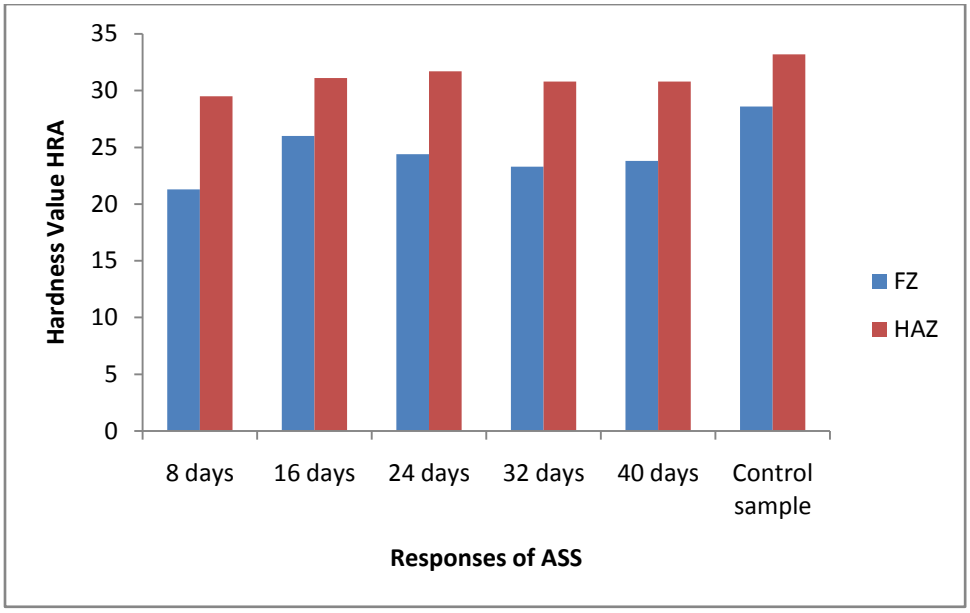

Figure 4.26: Comparison of hardness value of ASS at a given parameter (C_1) in HCl medium with a control sample.

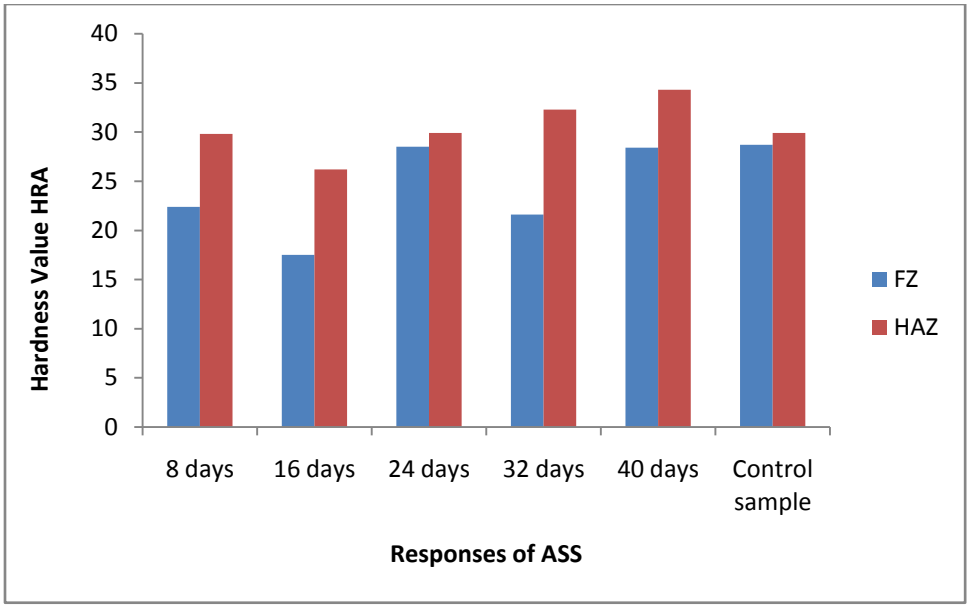

Figure 4.27: Comparison of hardness value of ASS at a given parameter (C_2) in HCl medium with a control sample.

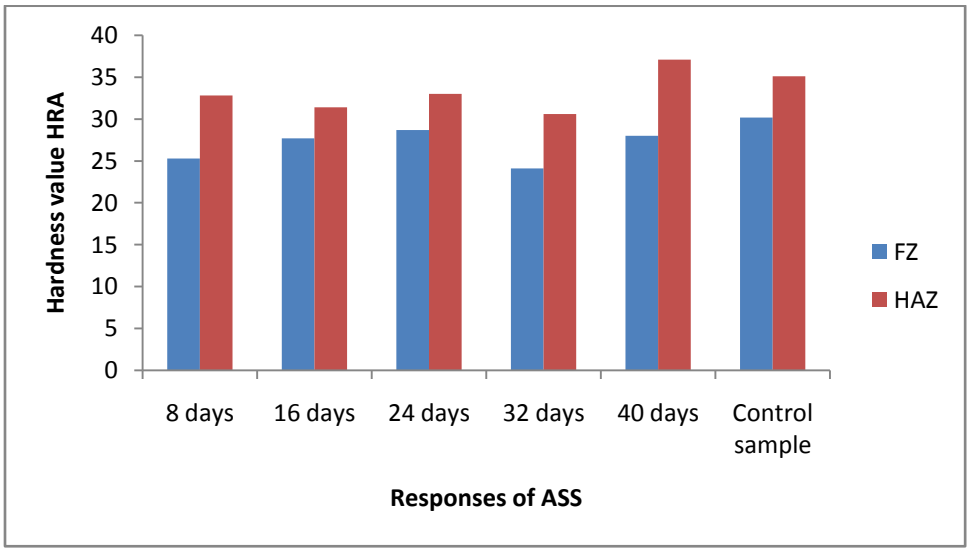

Figure 4.28: Comparison of hardness value of ASS at a given parameter (C_3) in HCl medium with a control sample.

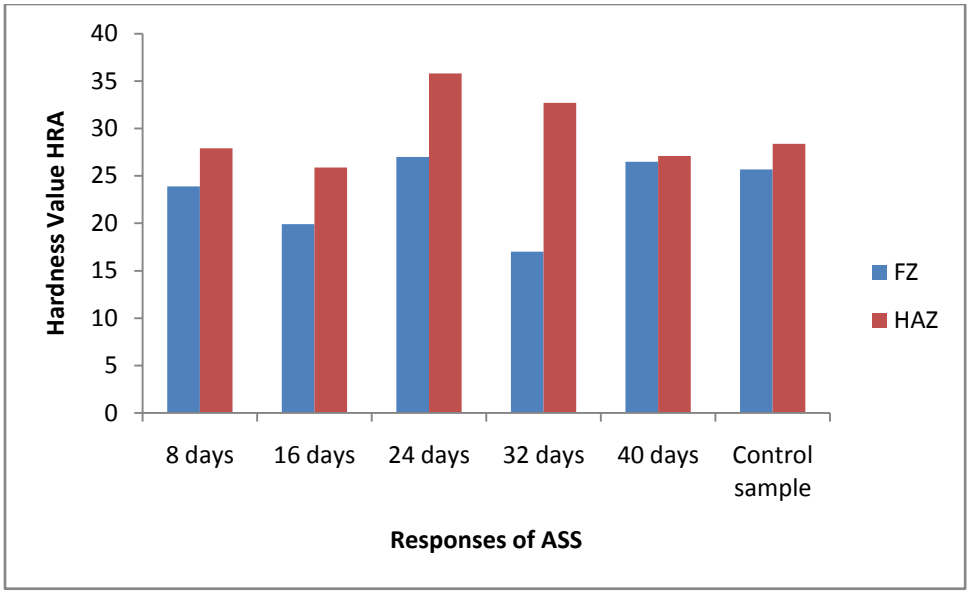

Figure 4.29: Comparison of hardness value of ASS at a given parameter (C_4) in HCl medium with a control sample.

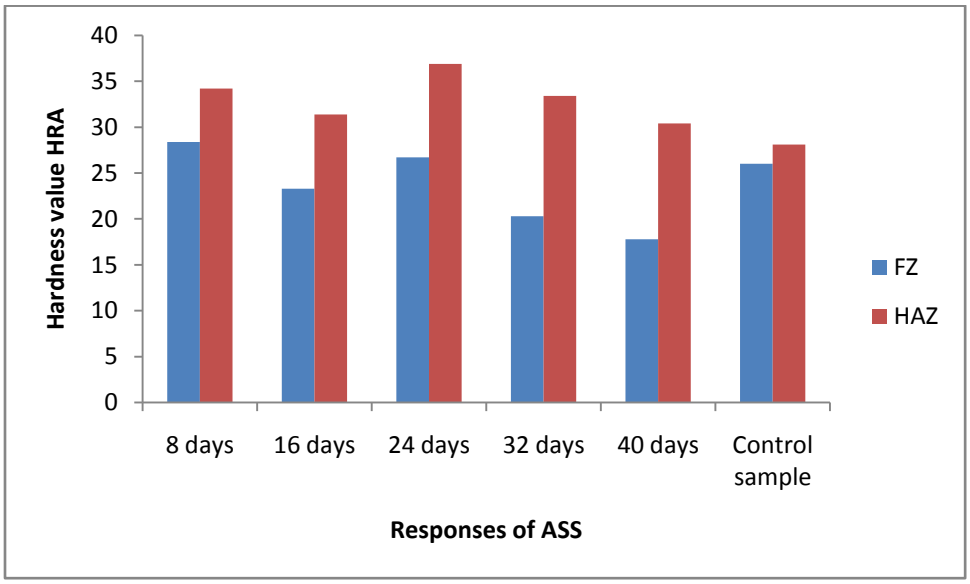

Figure 4.30: Comparison of hardness value of ASS at a given parameter (C_5) in HCl medium with a control sample.

4.4.2 Tensile properties of the samples

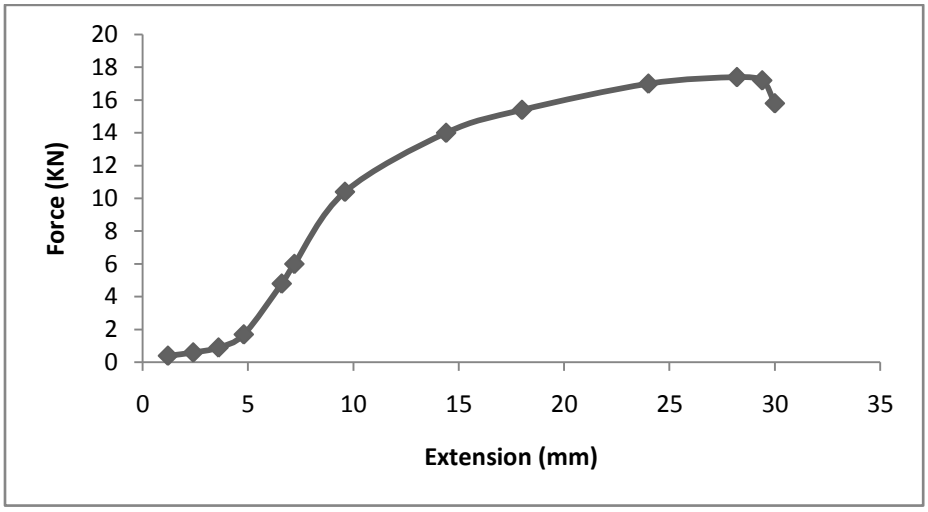

Figure4.31: Load-Extension Curveof tensile test on unwelded ASS (C).

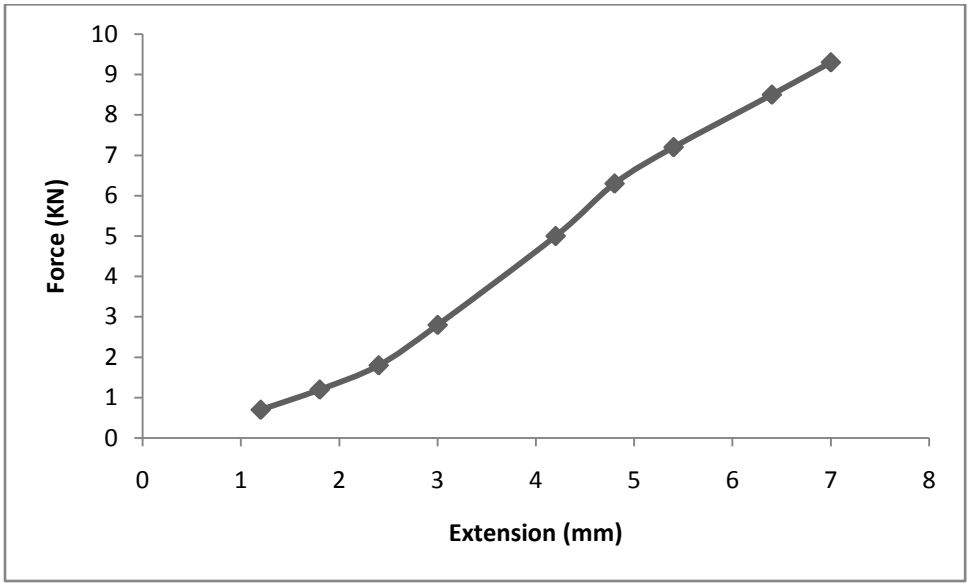

Figure4.32: Load-Extension plot of tensile test on welded ASS (C_1)

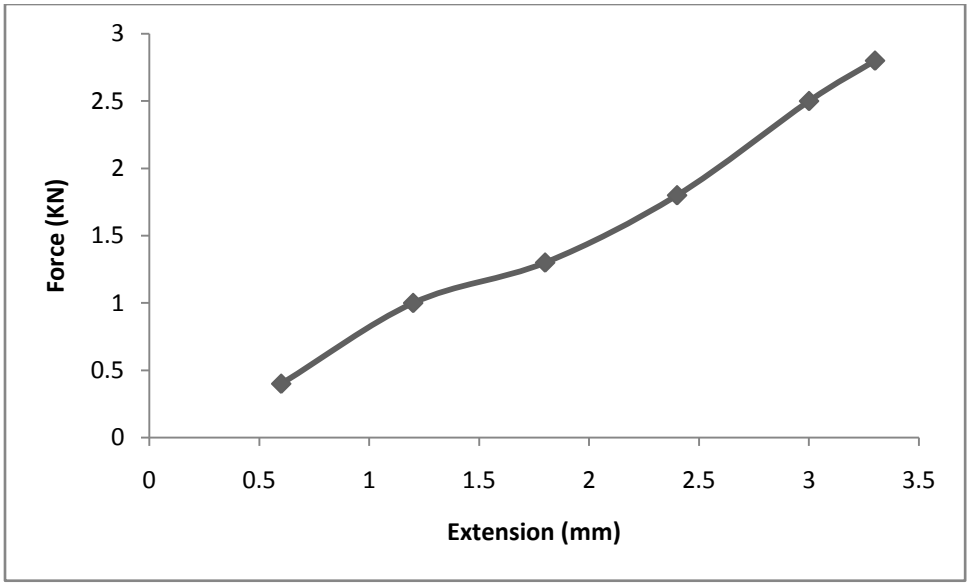

Figure4.33: Load-Extension of tensile test on welded ASS (C_2)

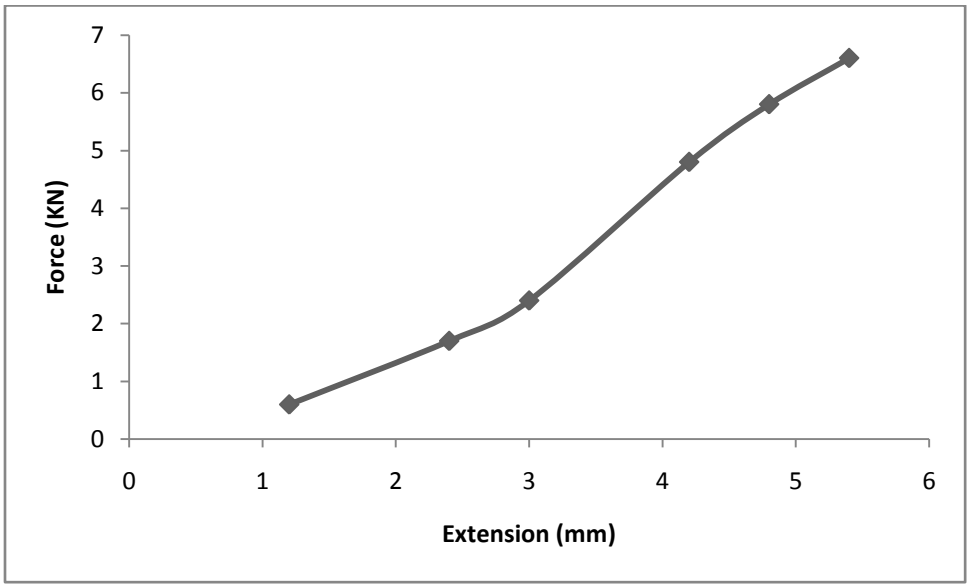

Figure4.34: Load-Extension of tensile test on welded ASS (C_3)

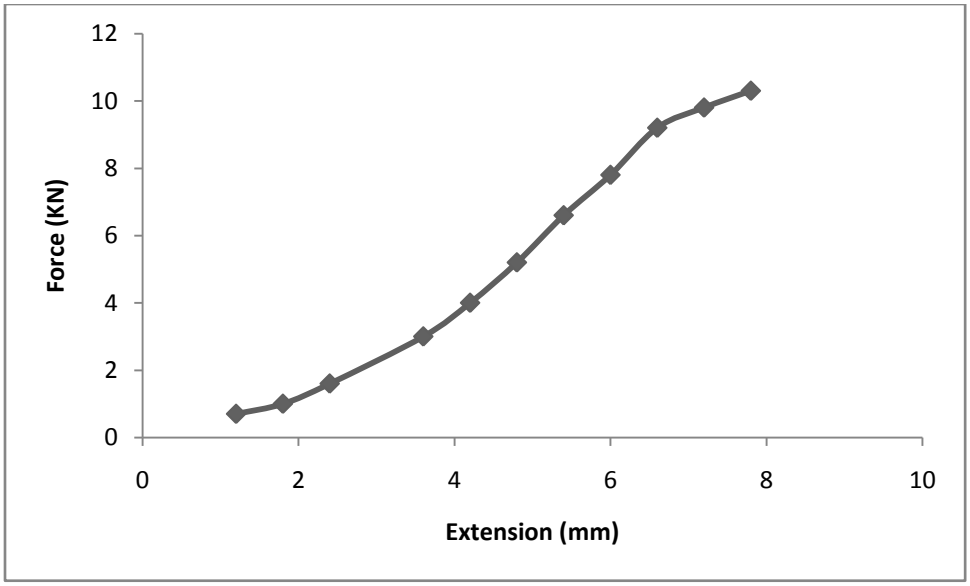

Figure4.35: Load-Extension of tensile test on welded ASS (C_4)

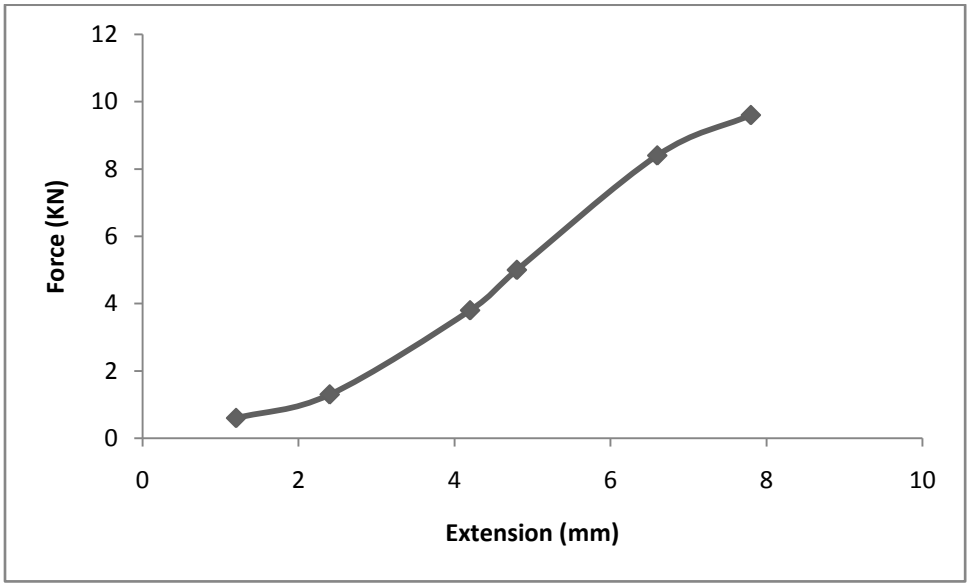

Figure b4.36: Load-Extension of tensile test on welded ASS (C_5)

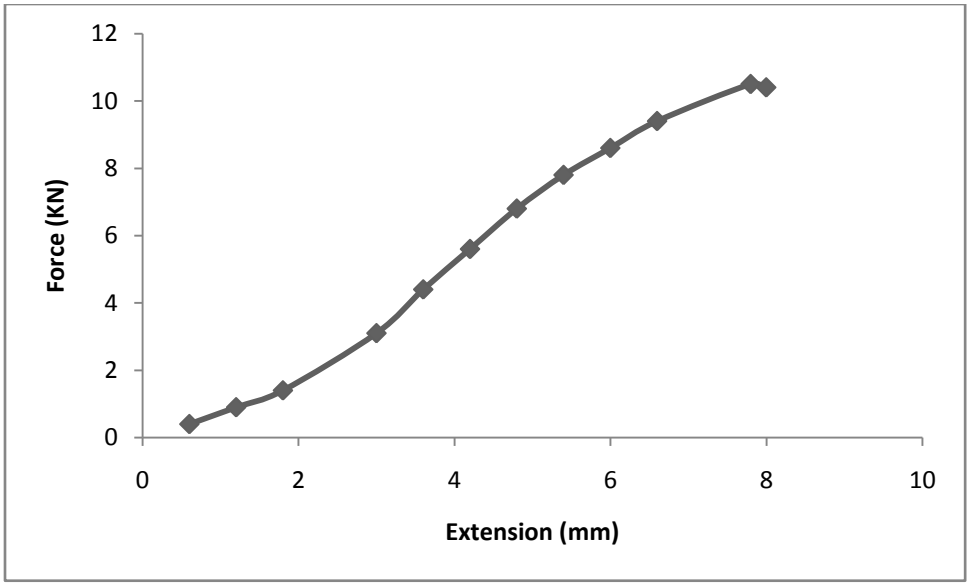

Figure 4.37: Load-Extension of tensile test on welded ASS (C_1) in HCl for 8 days.

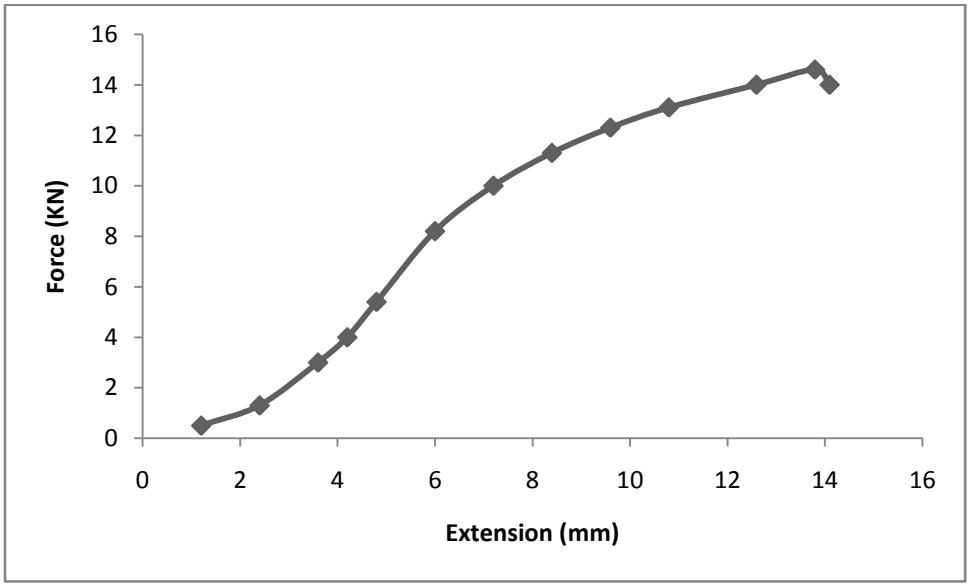

Figure 4.38: Load-Extension of tensile test on welded ASS (C_1) in NaOH for 8 days.

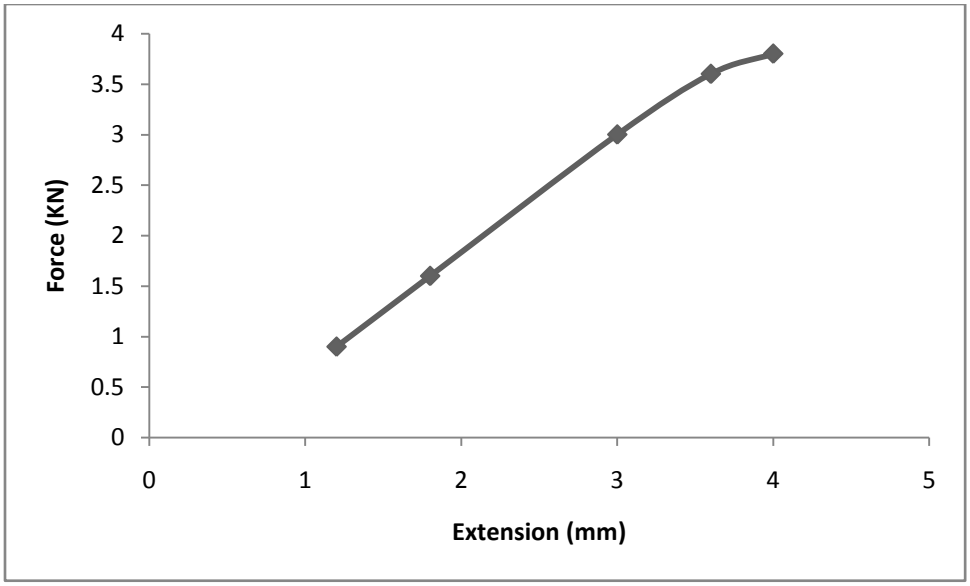

Figure 4.39: Load-Extension of tensile test on welded ASS (C_2) in HCl for 16 days

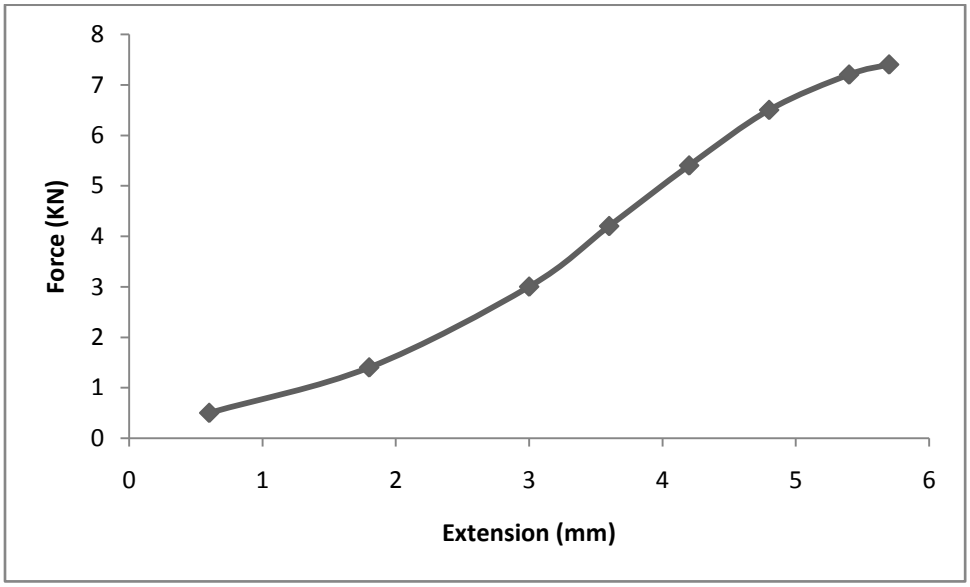

Figure 4.40: Load-Extension of tensile test on welded ASS (C_2) in NaOH for 16 days.

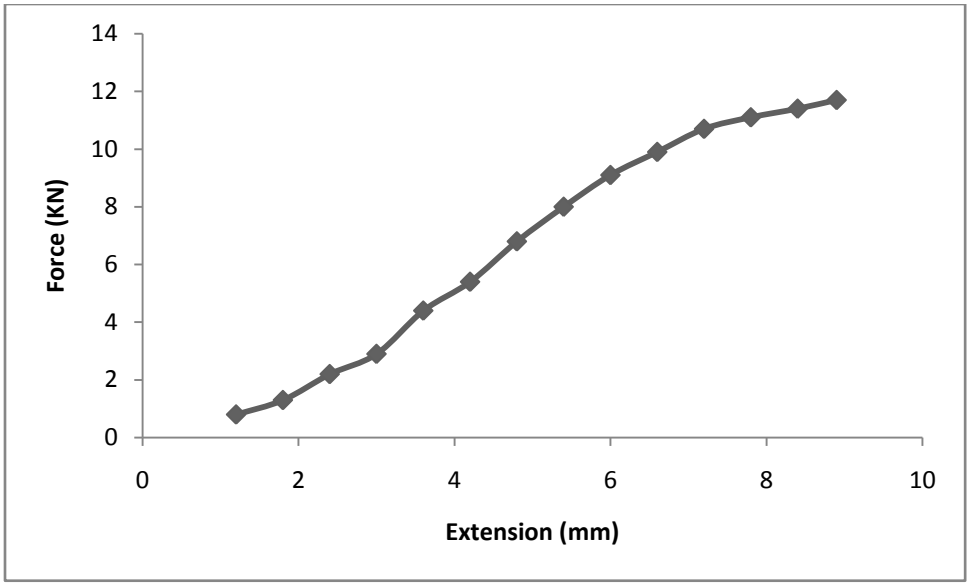

Figure 4.41: Load-Extension of tensile test on welded ASS (C_3) in HCl for 24 days.

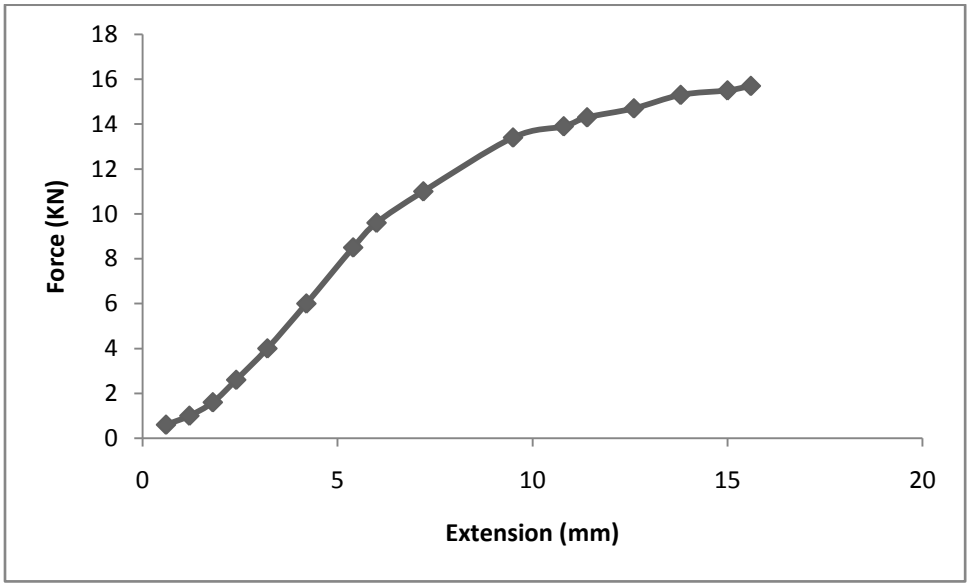

Figure 4.42: Load-Extension of tensile test on welded ASS (C_3) in NaOH for 24 days.

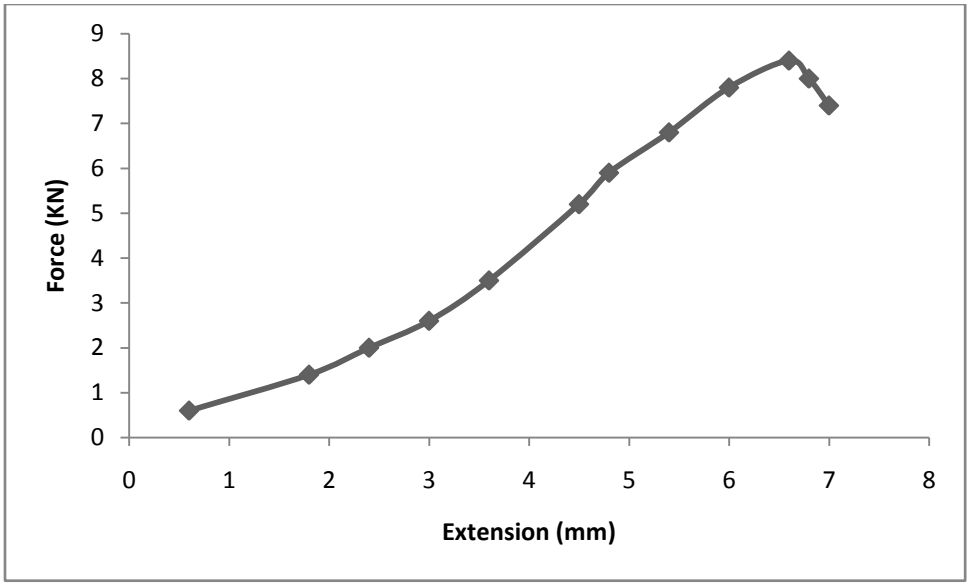

Figure 4.43: Load-Extension of tensile test on welded ASS (C_4) in HCl for 32 days.

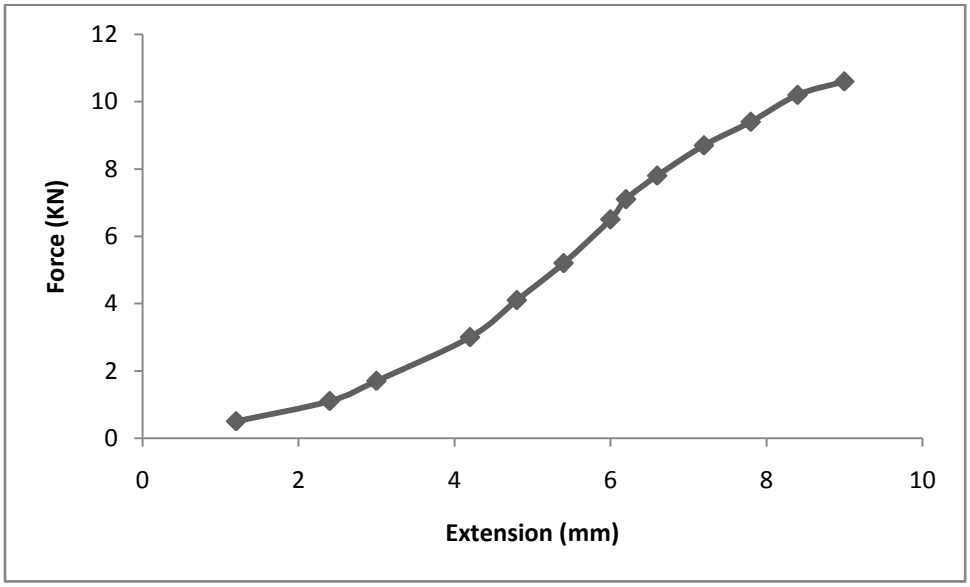

Figure 4.44: Load-Extension of tensile test on welded ASS (C_4) in NaOH for 32 days

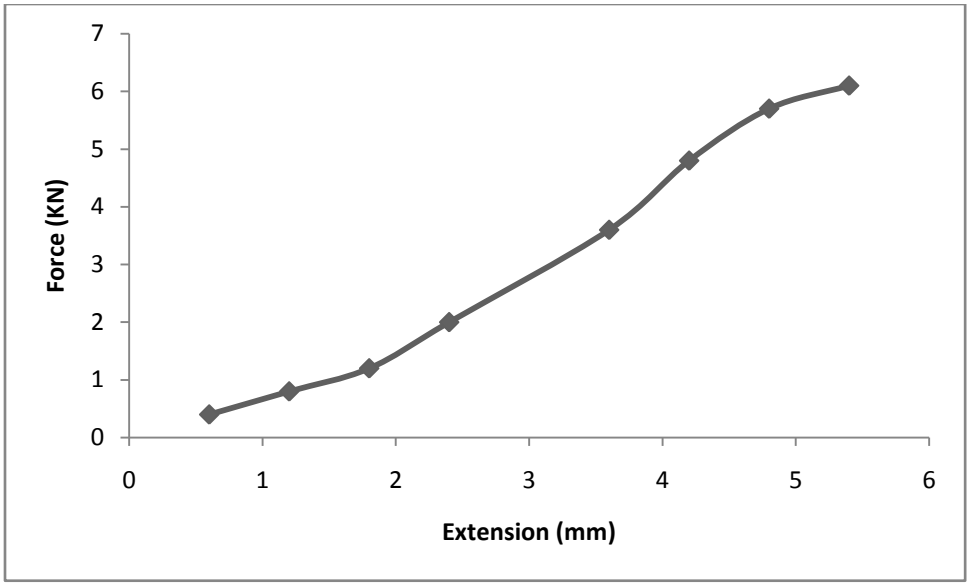

Figure 4.45: Load-Extension of tensile test on welded ASS (C_5) in HCl for 40 days.

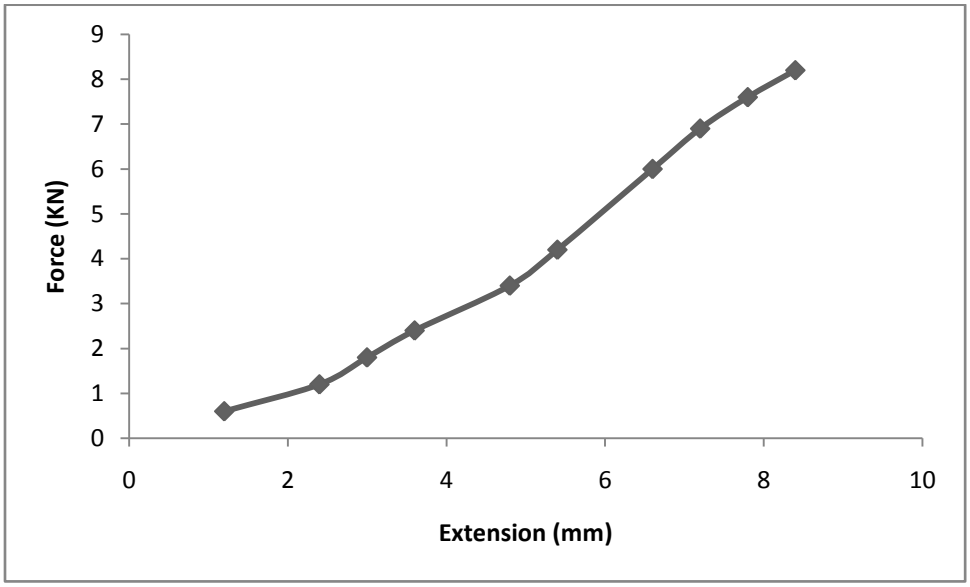

Figure 4.46: Load-Extension of tensile test on welded ASS (C_5) in NaOH for 40 days.

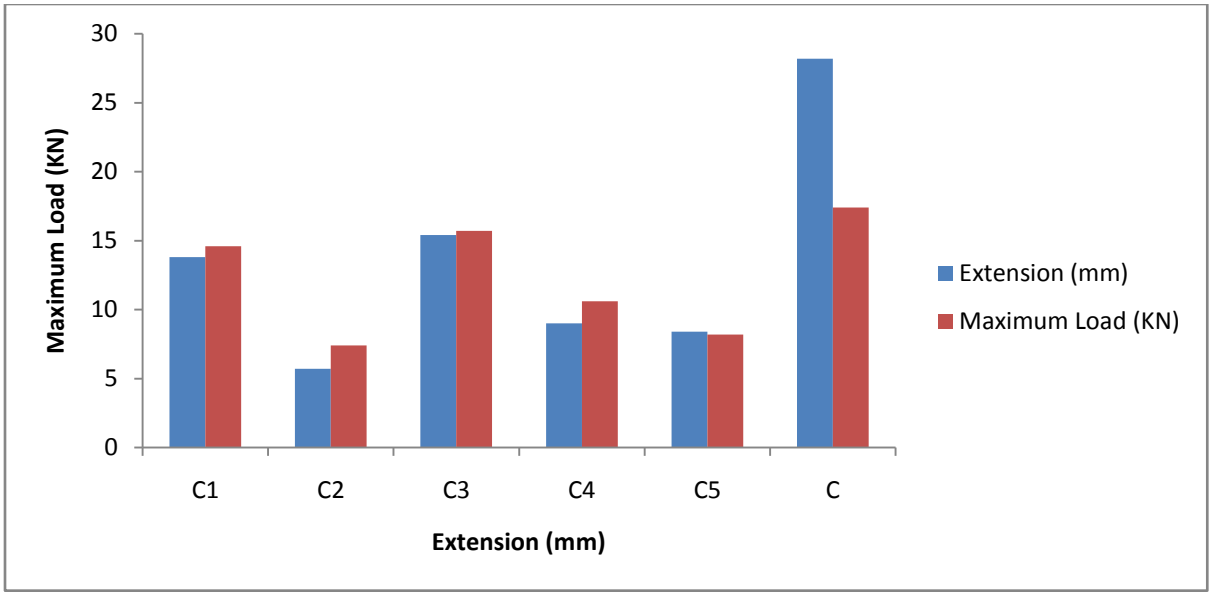

Figure 4.47: Load-Extension of tensile test on the samples of ASS immersed in NaOH medium.

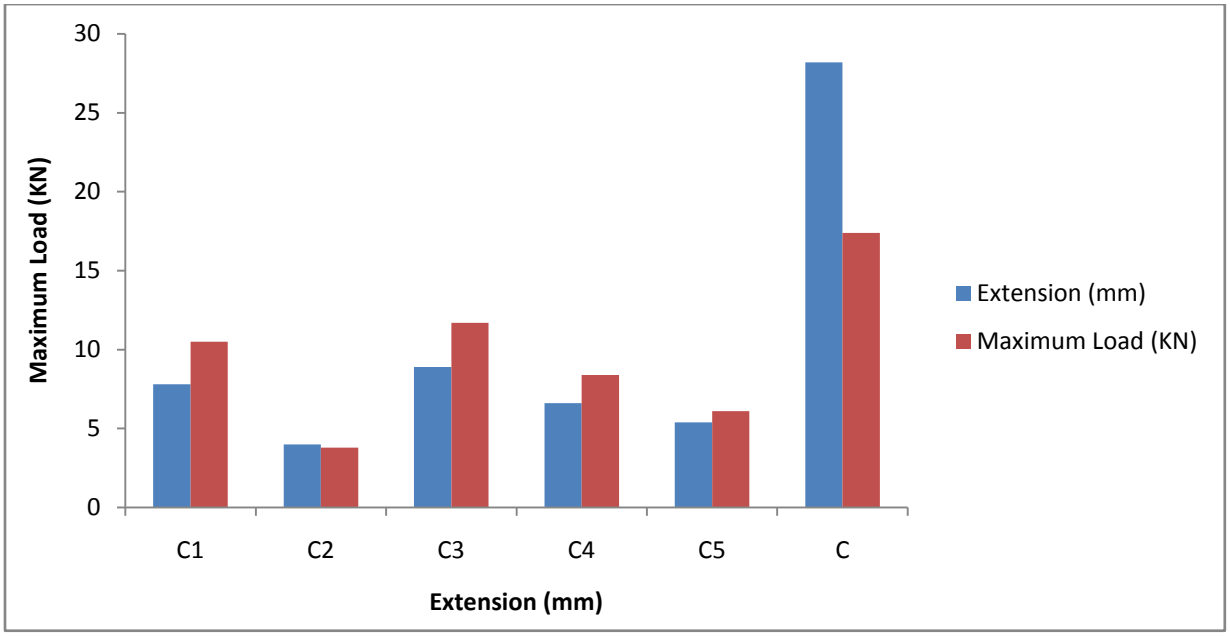

Figure 4.48: Load-Extension of tensile test on the samples of ASS immersed in HCl medium.

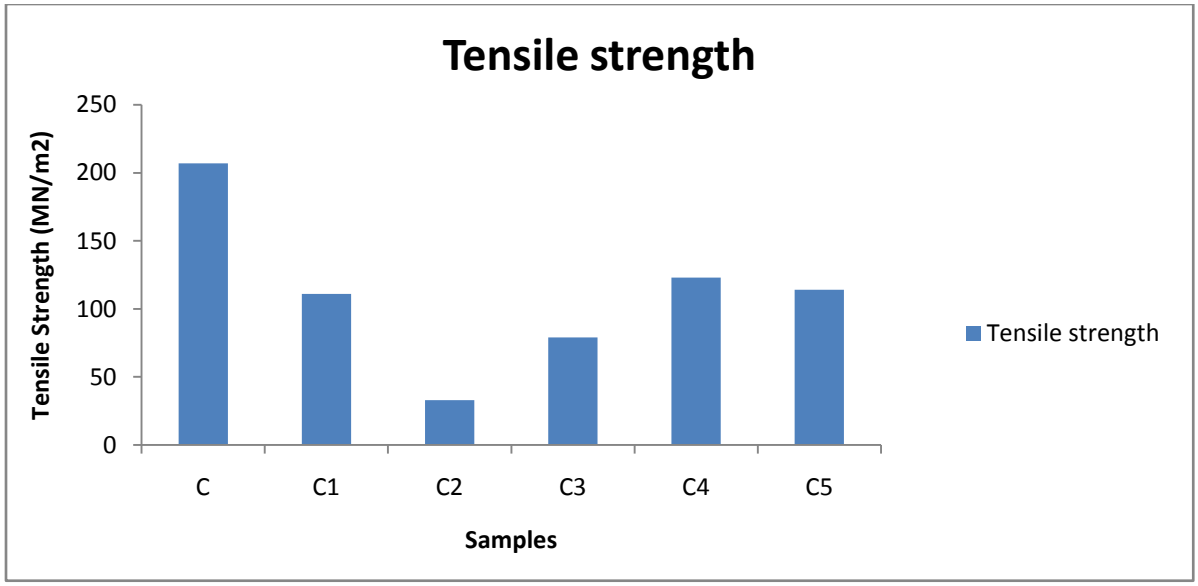

Figure 4.49: Tensile strength for welded (C_1-C_5) compared to unwelded control sample C.

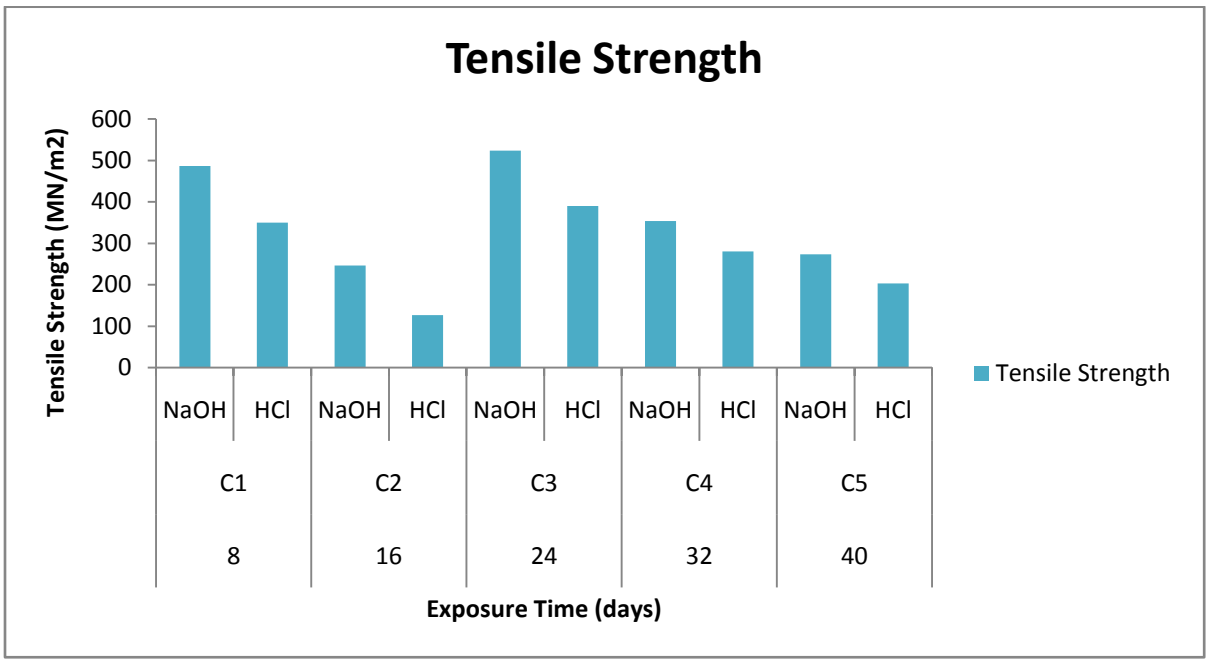

Figure 4.50: Comparison of the tensile strength for ASS samples immersed in sodium hydroxide and in hydrochloric acid media.

4.4.3 Impact properties of the samples

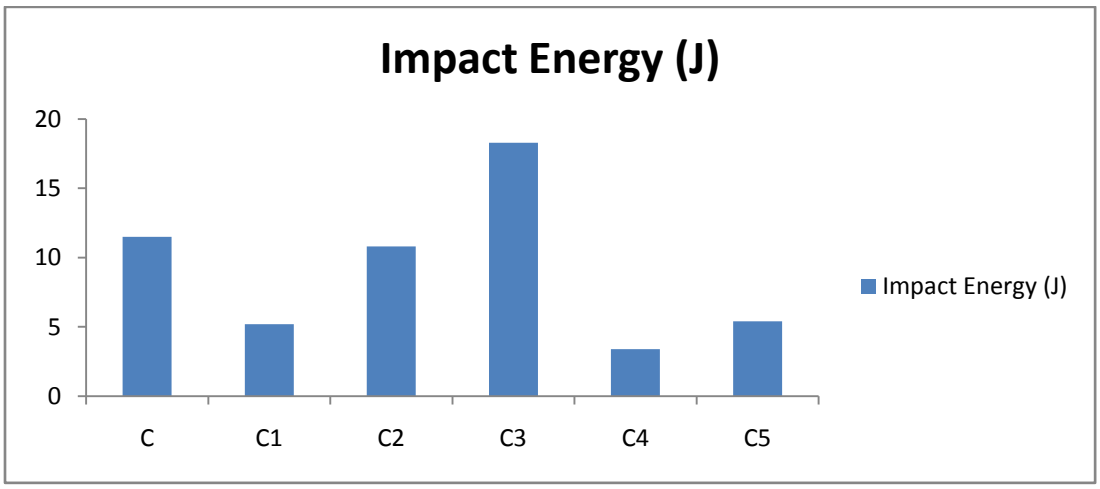

Figure 4.51: Impact test for the control; welded and unwelded control

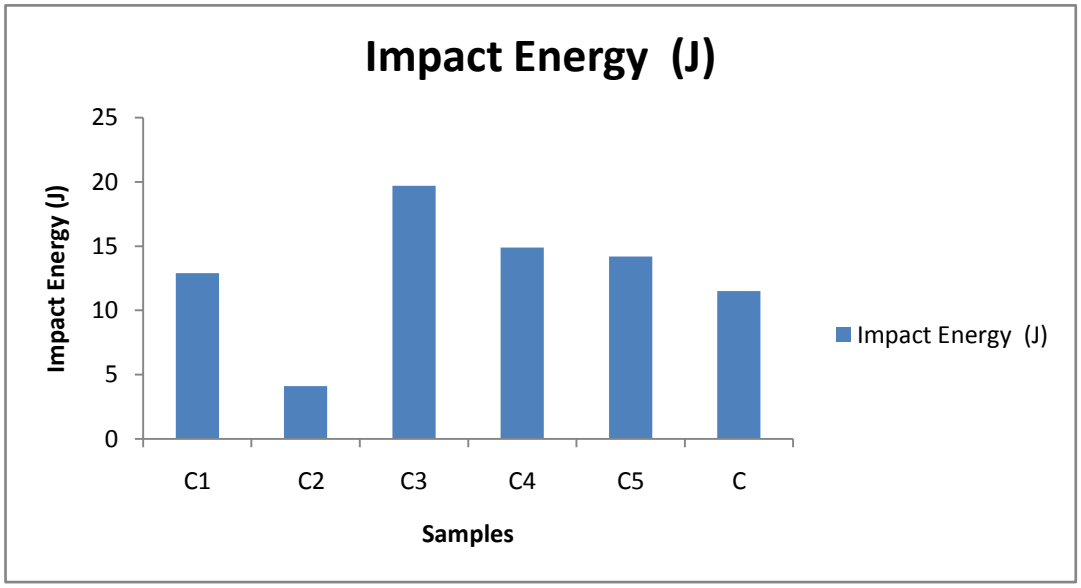

Figure 4.52: Impact Energy for ASS immersed in NaOH for 8 days as compared to control

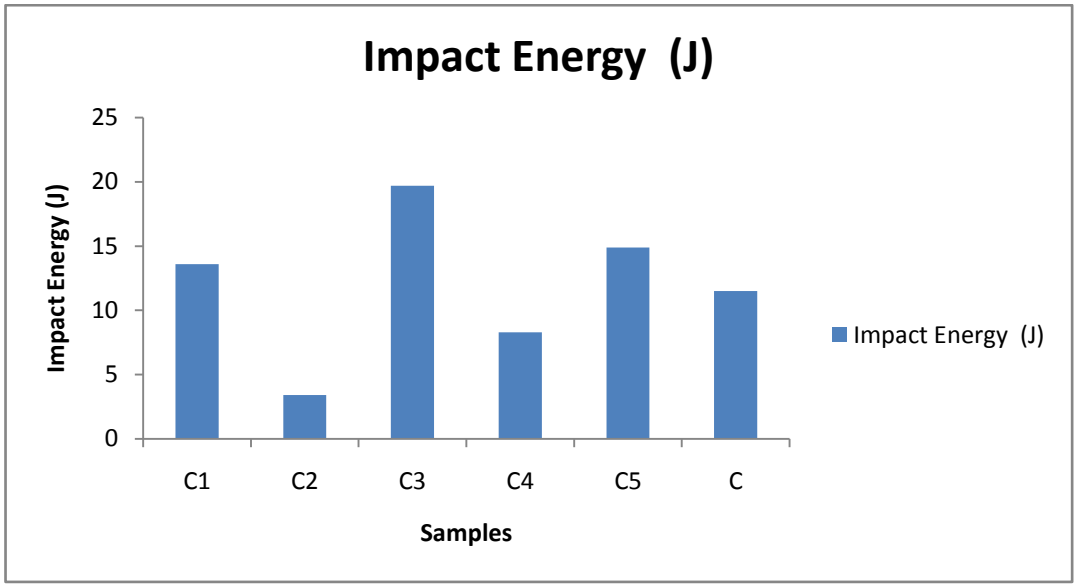

Figure 4.53: Impact Energy for ASS immersed in NaOH for 16 days as compared to control

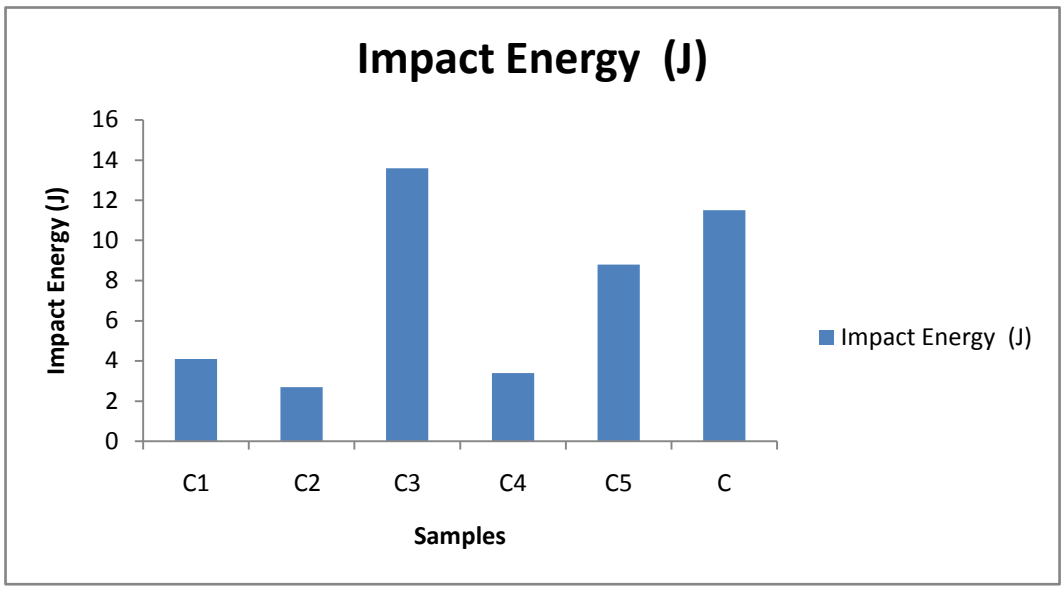

Figure 4.54: Impact Energy for ASS immersed in NaOH for 24 days as compared to control

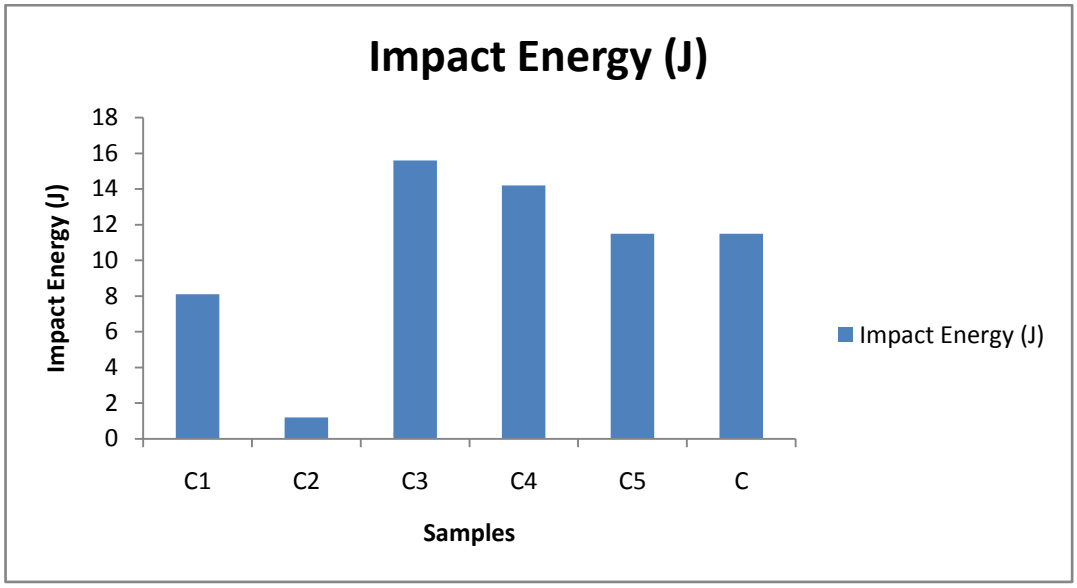

Figure 4.55: Impact Energy for ASS immersed in NaOH for 32 days as compared to control

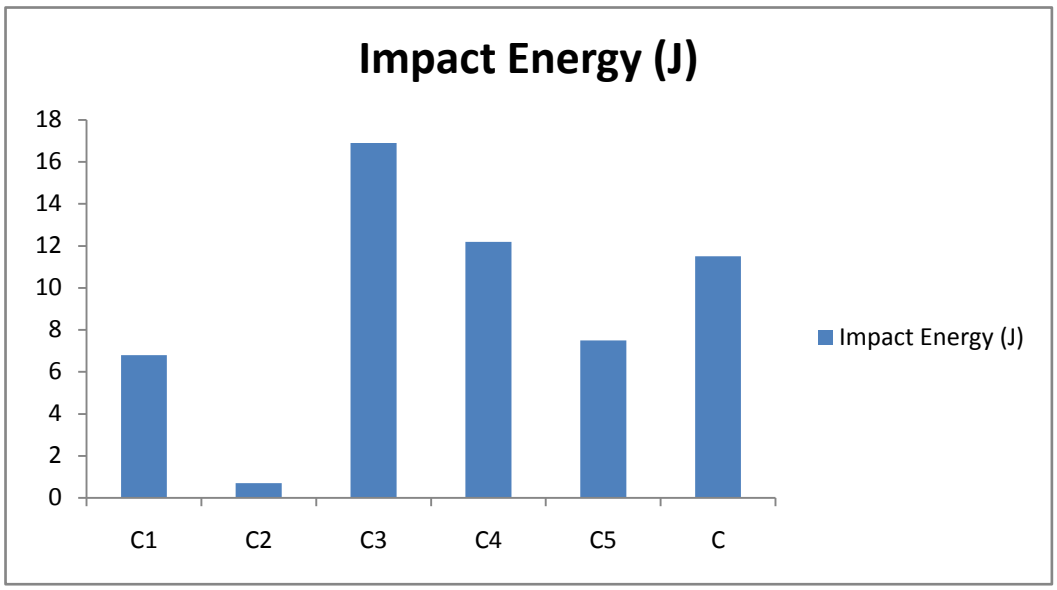

Figure 4.56: Impact Energy for ASS immersed in NaOH for 40 days as compared to control

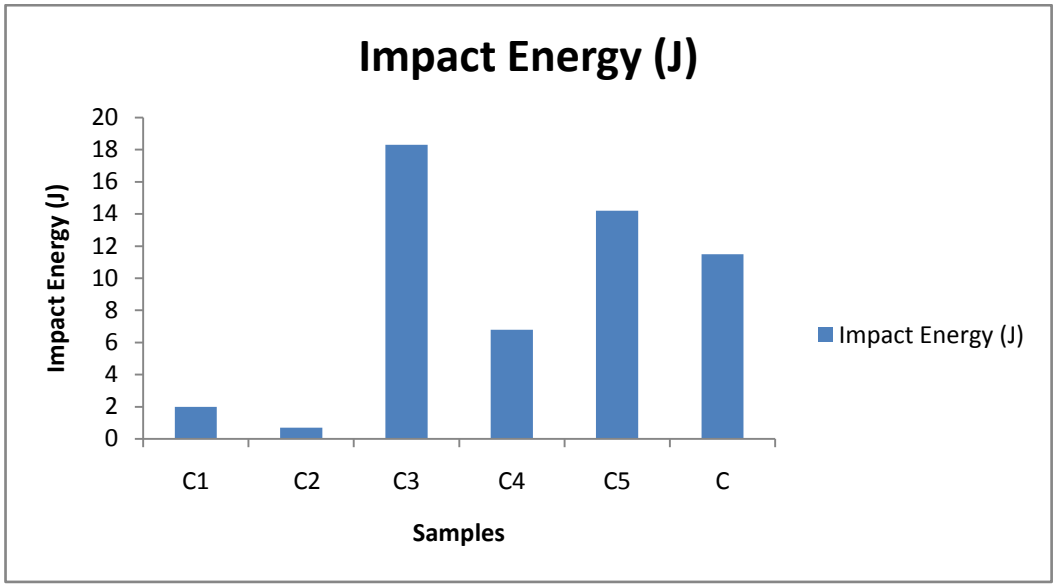

Figure 4.57: Impact Energy for ASS immersed in HCl for 8 days as compared to control

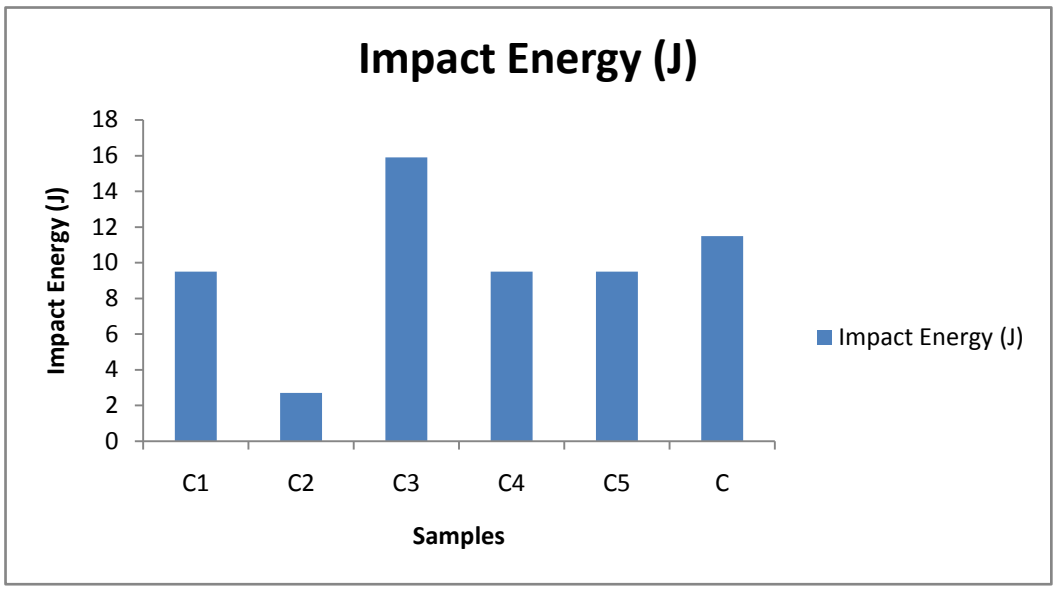

Figure 4.58: Impact Energy for ASS immersed in HCl for16 days as compared to control

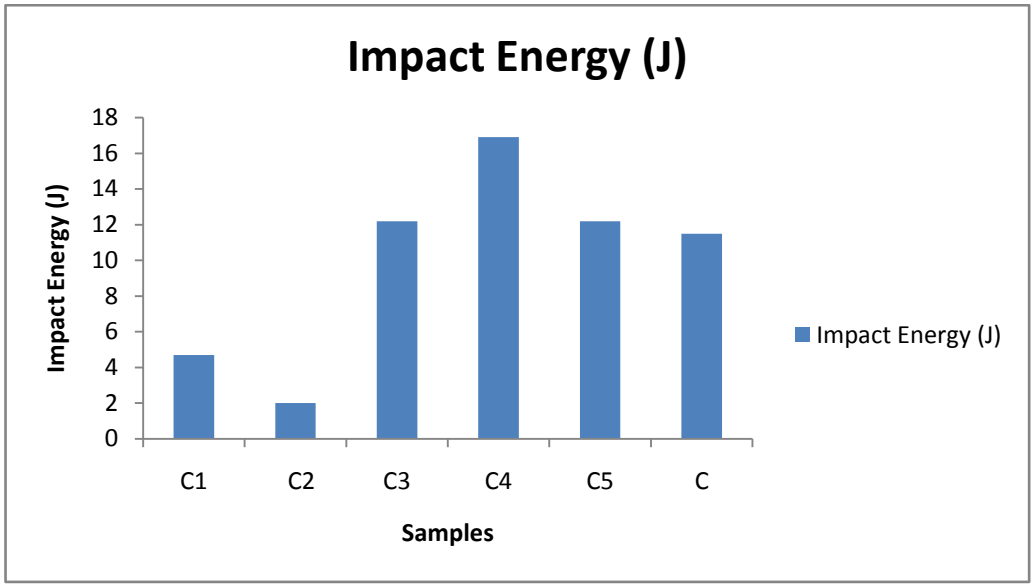

Figure 4.59: Impact Energy for ASS immersed in HCl for 24 days as compared to control

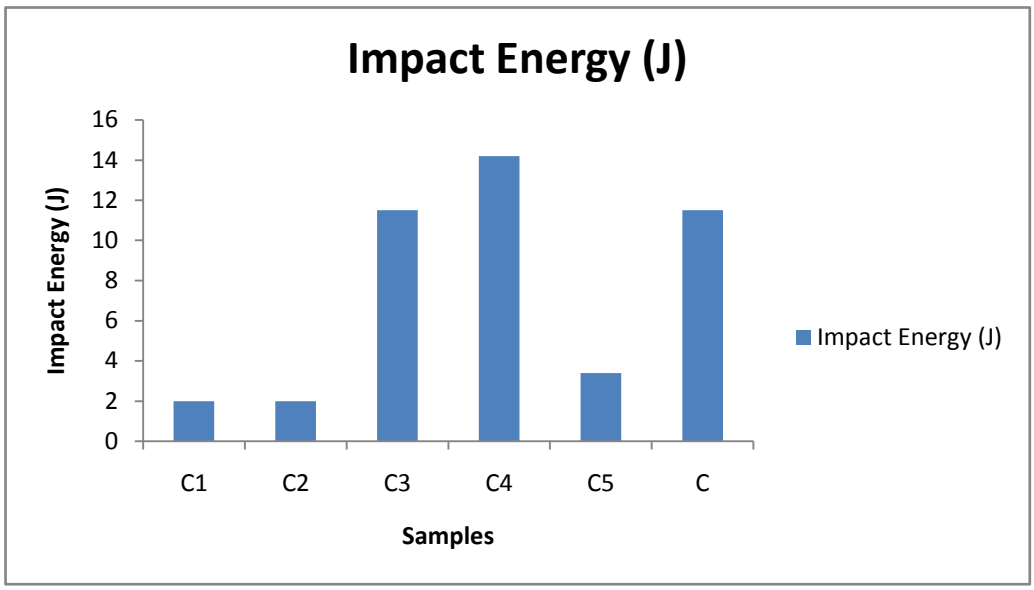

Figure 4.60: Impact Energy for ASS immersed in HCl for 32 days as compared to control

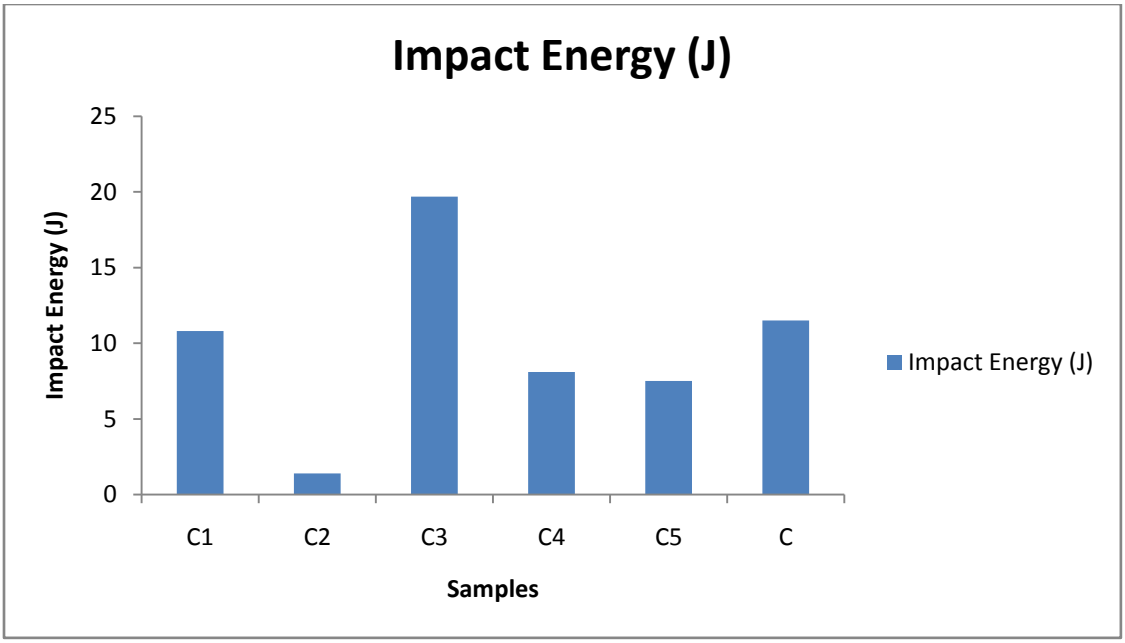

Figure 4.61: Impact Energy for ASS immersed in HCl for 40 days as compared to control

4.5 Scanning Electron Photo-Micrograph of the Samples

The photo-micrographs of the samples, using scanning electron microscope, are presented in plates III to XII as well as the EDS profiles of first three samples.

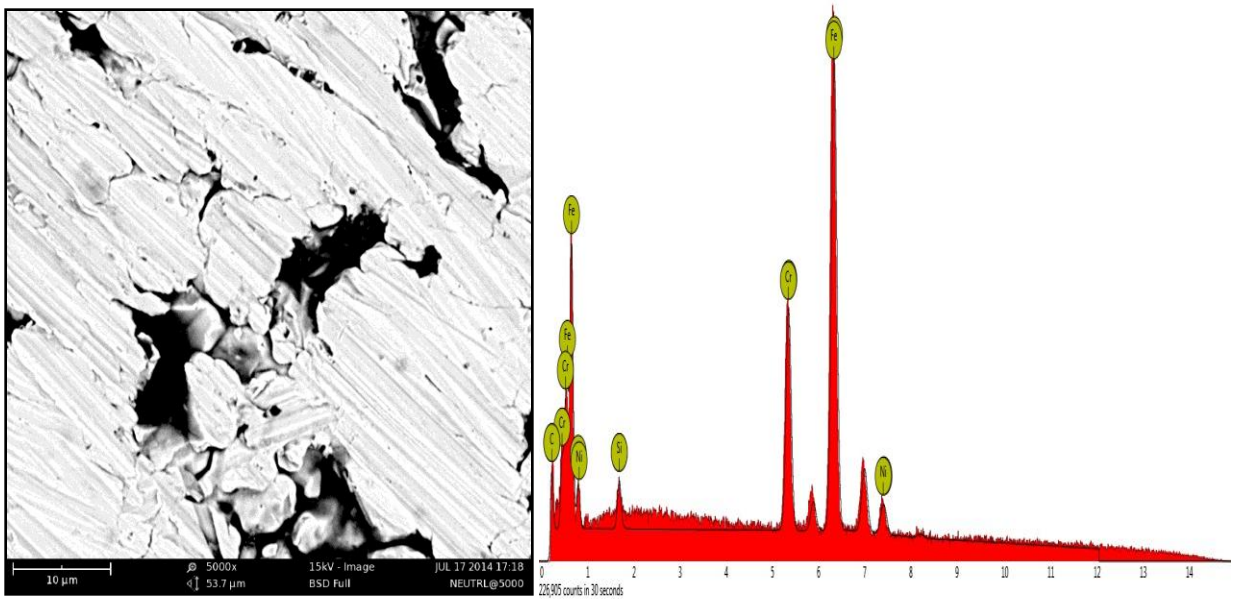

Plate III: Micrograph of the control sample (as received) with EDS profile

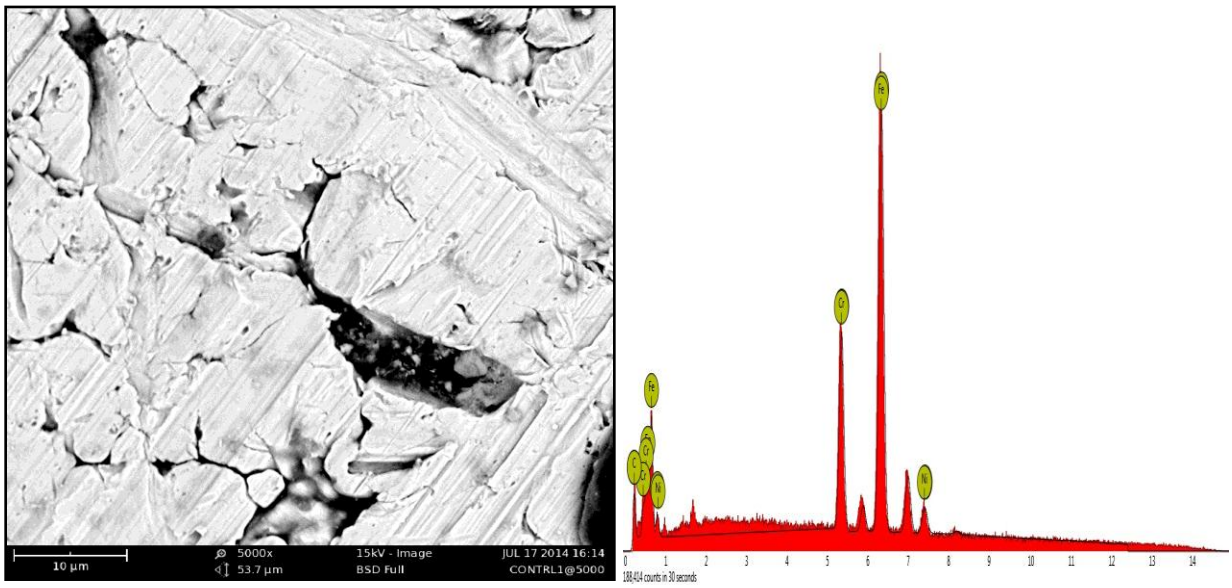

Plate IV: Micrograph of the control sample immersed in NaOH for 40 days with EDS profile

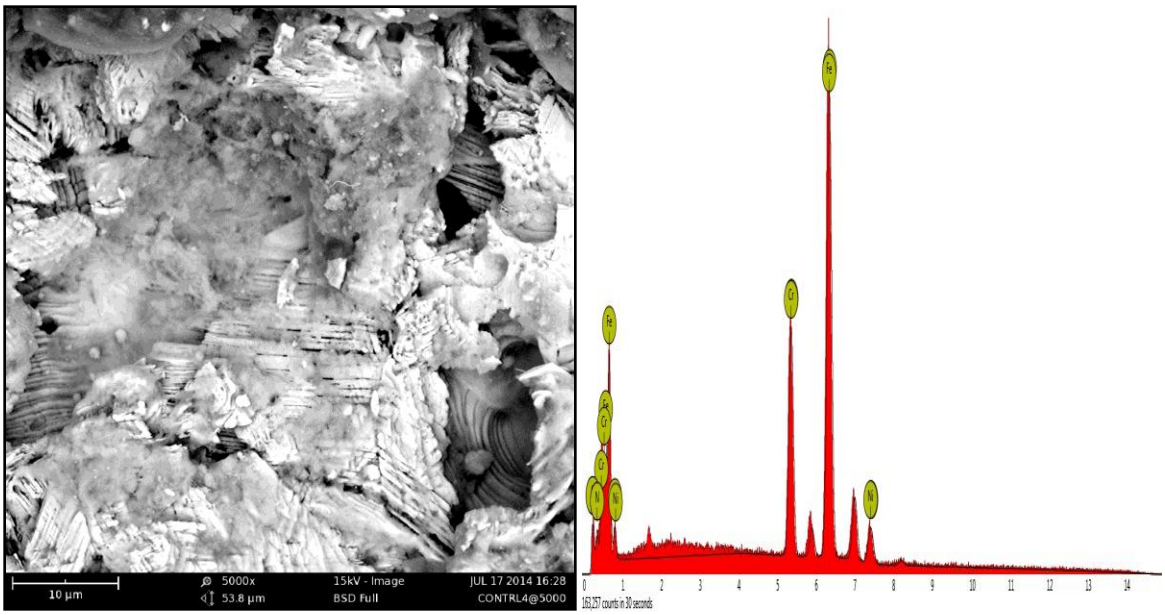

Plate V: Micrograph of the control sample immersed in HCl for 40 days with EDS profile

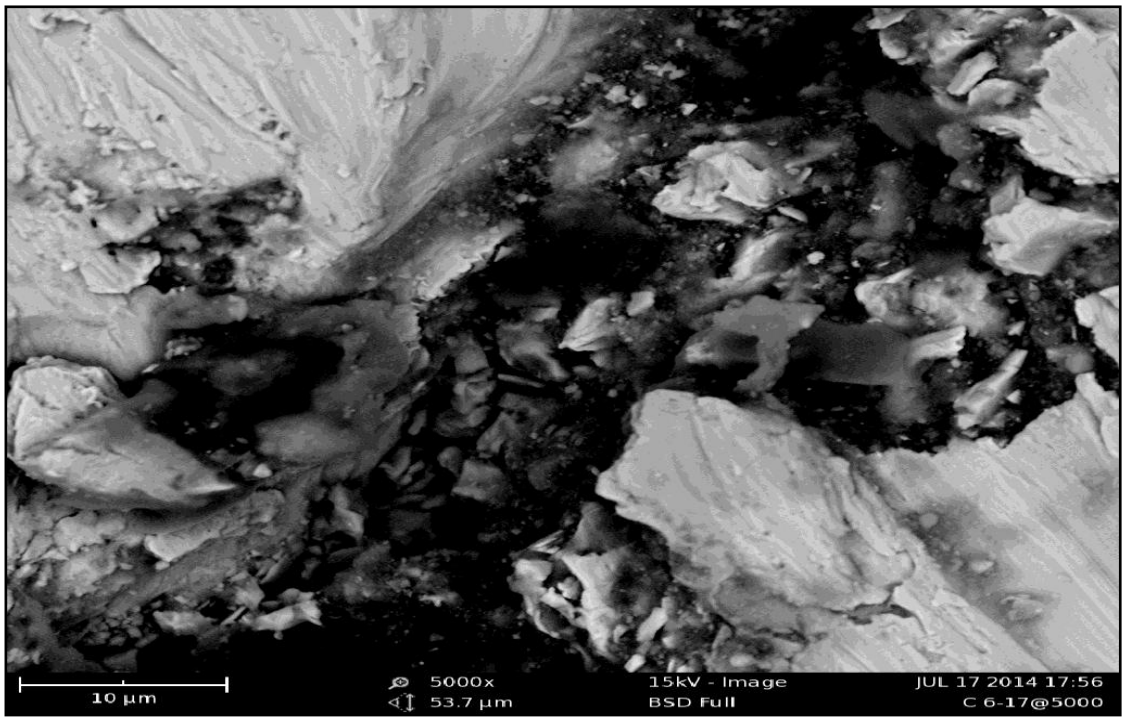

Plate VI: Micrograph of the FZ of sample C_3 welded but not immersed

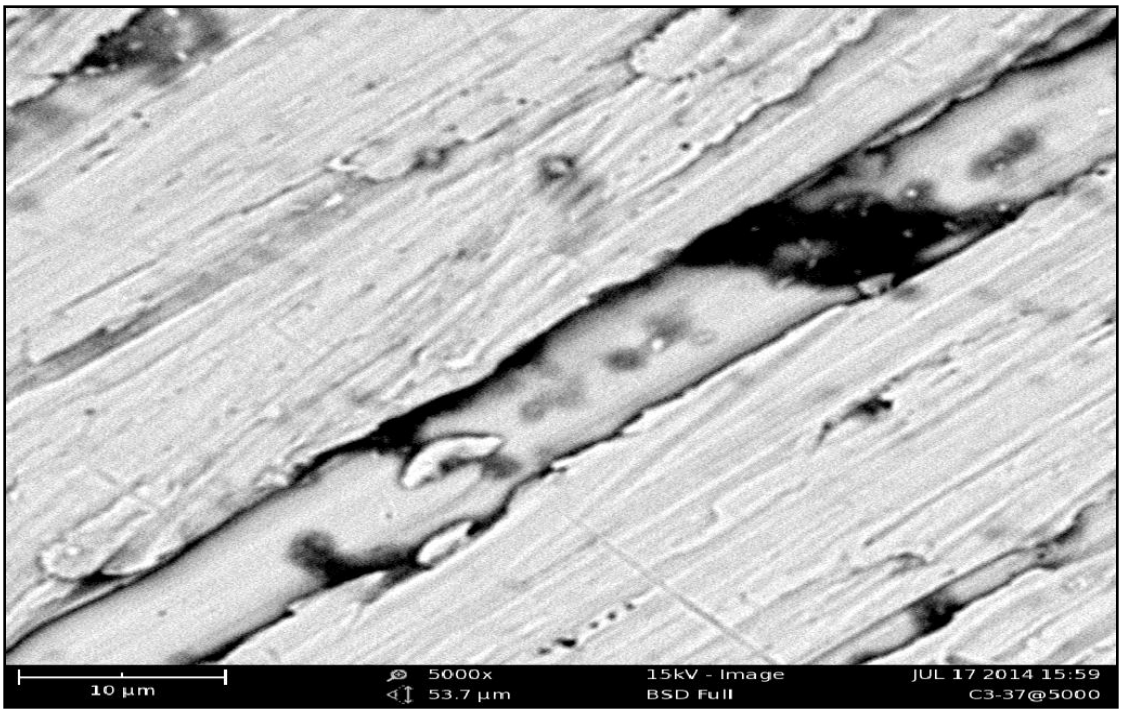

Plate VII: Micrograph of the HAZ and FZ of sample C_3 welded and immersed in HCl for 8 days

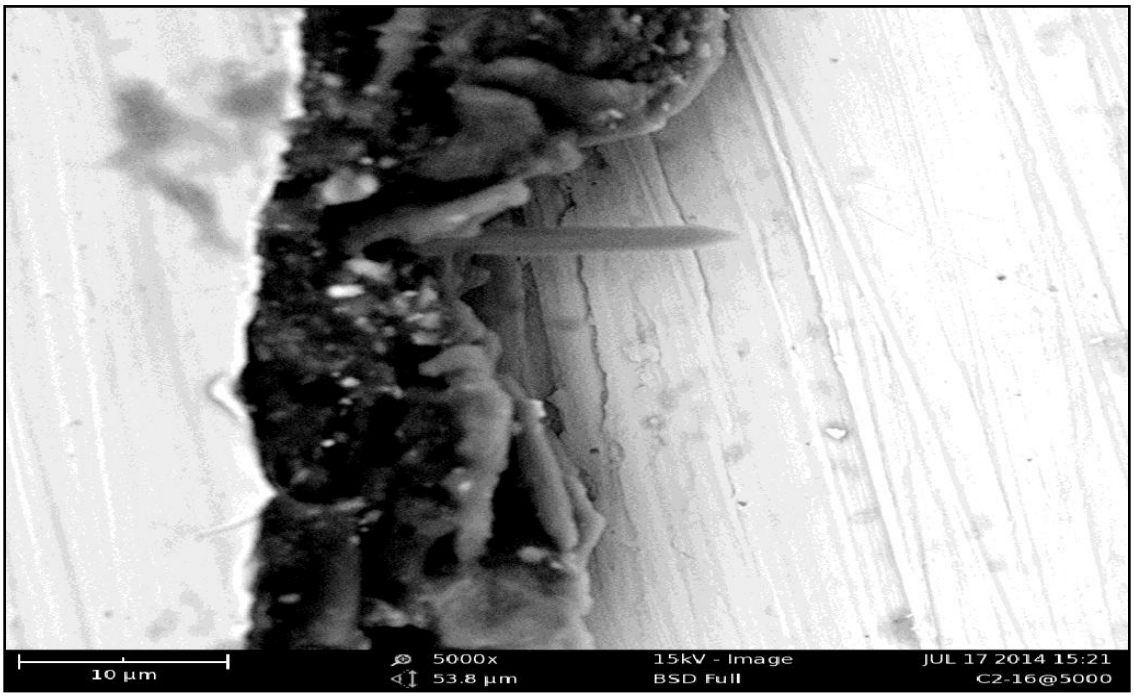

Plate VIII: Micrograph of the HAZ and FZ of sample C_2 welded and immersed in NaOH for 8 days

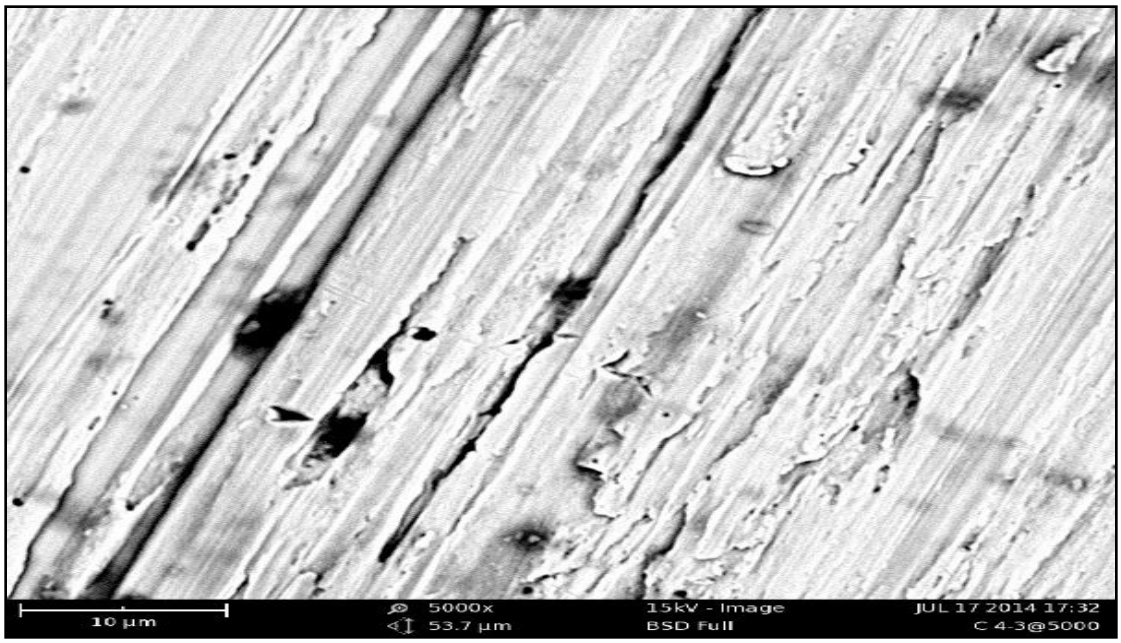

Plate IX: Micrograph of the HAZ of sample C_4 welded and immersed in NaOH for 24 days

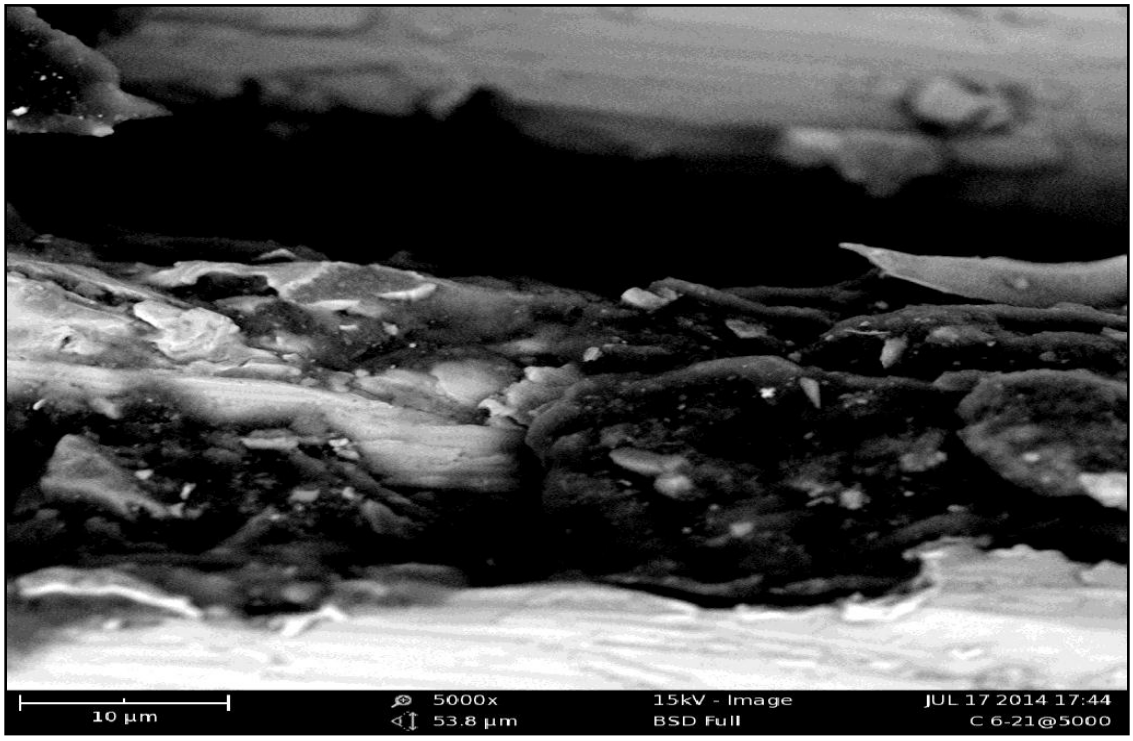

Plate X: Micrograph of the FZ of sample C_3 welded and immersed in HCl for 24 days

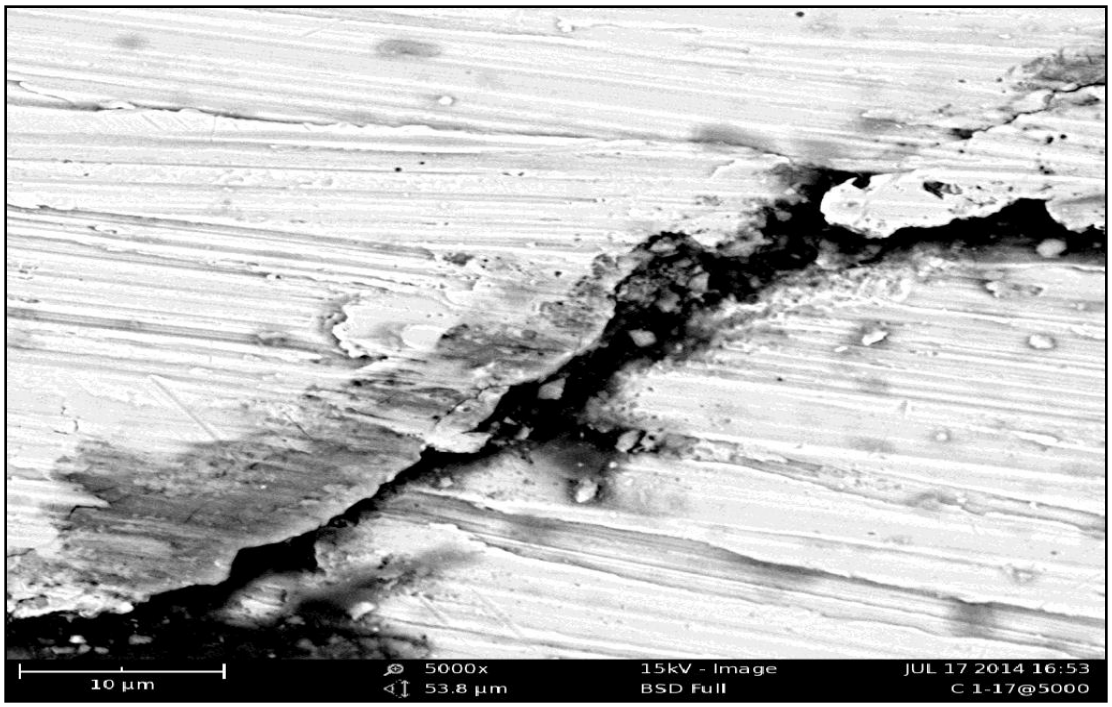

Plate XI: Micrograph of the HAZ of sample C_1 welded and immersed in HCl for 40 days

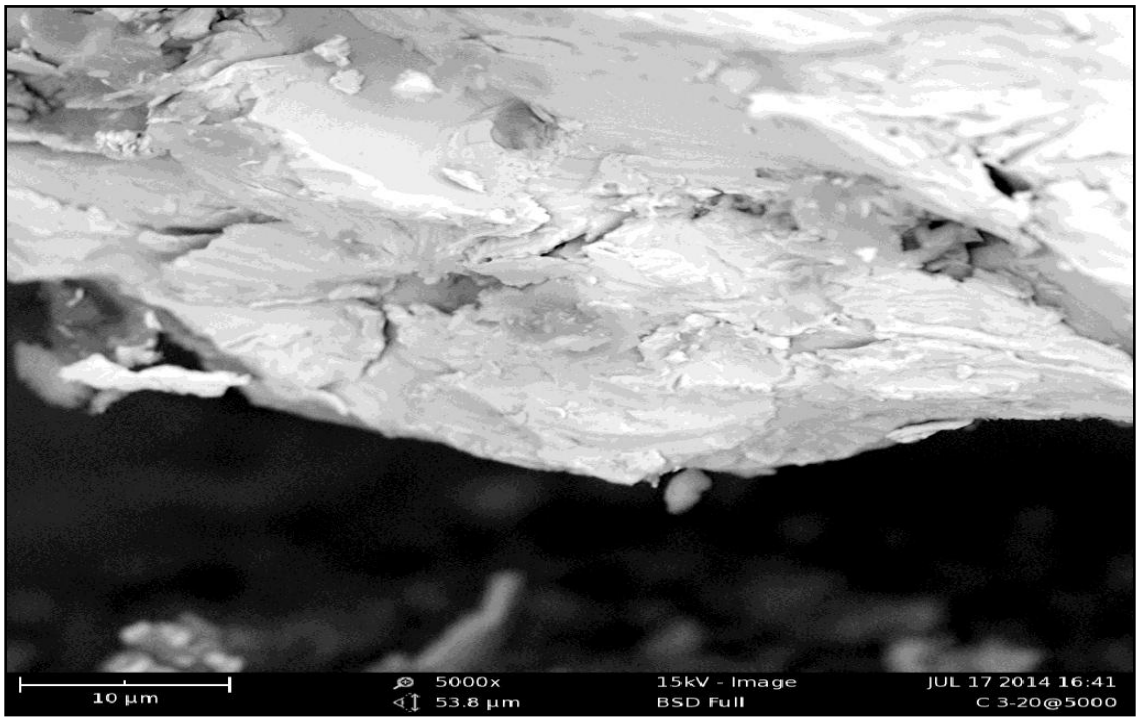

Plate XII: Micrograph of the FZ of sample C_3 welded and immersed in NaOH for 40 days

CHAPTER FIVE

5.0 DISCUSSION OF RESULTS

5.1 Elemental Analysis of Austenitic Stainless Steel

The X-ray florescence test was used to determine the actual chemical composition of the stainless steel. Table 4.1 shows the result of XRF test carried out on the stainless steel. The result in table 4.1 shows that the material is an austenitic stainless steel type 304. This is due to the presence of high percentage composition of iron (Fe) 68.7% as the base material, chromium (Cr) 20.12% and nickel (Ni) 8.34% as major alloying elements, low percentages of Carbon (C) 0.12% and other elements in accordance with the AISI standard grade.

5.2 Responses and ANOVA for the Factorial Model for Speed and Current at a Constant Voltage for NaOH Environment

Presented in Table 4.4 is the variation of the selected welding parameters (factors) affecting the behaviour of ASS in 0.5M concentration of sodium hydroxide environment and the corresponding weight loss in milligrams obtained after each experimental run performed on the welded ASS immersed for 40 days in an interval of 8 days. The results show that experimental run four (4) gave the least weight loss values for eight (8) days, sixteen (16) days, twenty-four (24) days, thirty-two (32) days and forty (40) days as 0.0008mg, 0.0002mg, 0.0006mg, 0.0004mg and 0.0020mg respectively at a welding speed of 40cm/min, welding current of 110 Amperes at a constant voltage of 230 volts. This implies that the best welding parameters setting that gave the best optimal welding performance of the ASS in 0.5M concentration of sodium hydroxide medium was when the speed is set at 40cm/min and the current at 110 Amperes. This shows a good corrosion resistance of the steel to the environment since the least weight loss was observed

with it, while experimental run five (5) gave the highest weight loss values for eight (8) days, sixteen (16) days, twenty-four (24) days, thirty-two (32) days and forty (40) days as 0.0016mg, 0.0059mg, 0.0053mg, 0.0040mg and 0.0094mg respectively. This implies that at low current, poor weldment was achieved.

The analysis of variance (ANOVA) for the factorial model for speed and current at constant voltage for NaOH is presented in Table 4.2. From the results of the ANOVA, model F-value of 50.44implies that the model is significant. There is only a 1.95% chance that a "Model F-Value" this large could occur due to noise.Values of "Prob > F" less than 0.0500 indicate model terms are significant. Since model terms A, B and AB are all less than 0.0500, it therefore means that they are all significant model terms. The " Curvature F-value" of 50.44 implies that there is significant curvature (as measured by the difference between the average of the centre points and the average of the factorial points) in the design space. A mean of 0.187%, C.V. of 20.25, Std. Dev. of 3.780 $X10^{-4}$, R^2 of 0.9870 and R^2_{Adj} of 0.9674 were obtained at 95% confidence limit.

Consequently, the "R^2_{Pred}" of 0.8927 is in reasonable agreement with the "R^2_{Adj}" of 0.9674. The value of R^2 calculated for this model was 0.9870, i.e., reasonably close to unity, and thus acceptable. It concluded that 98.70% of the data can be explained by this model. It shows that this model provides reasonably good explanation of the relationship between the independent factors and the responses.

The "Adeq Precision" measures the signal to noise ratio (Signal-to-noise ratiois a measure used in science and engineering that compares the level of a desired signal to the level of background noise. It is defined as the ratio of signal power to the noisepower). Since a ratio greater than 4 is

desirable Okibe (2014), therefore the ratio of 18.466 indicates an adequate signal. This made the model useful to navigate the design space. The equations that defines each of the responses obtained in the factorial design for speed and current at a constant voltage for NaOH medium for forty (40) days are given by Equation 5.1 to 5.5 below;[That is, the weight loss (WL) for eight (8) days, sixteen (16) days, twenty-four (24) days, thirty-two (32) days and forty (40) days];

$WL_8 = +0.013108\ 1.97500 \times 10^{-4}A - 1.10000 \times 10^{-4}B + 1.75000 \times 10^{-6}AB$…..……...…5.1

$WL_{16} = -0.022008 + 1.33750 \times 10^{-3}A + 2.05000 \times 10^{-4}\ B - 1.22500 \times 10^{-5}AB$…..……5.2

$WL_{24} = -0.010267 + 9.10000 \times 10^{-4}A + 1.05000 \times 10^{-4}B - 8.50000 \times 10^{-6}AB$ …….5.3

$WL_{32} = -0.013317 + 8.40000 \times 10^{-4}A + 1.40000 \times 10^{-4}B - 8.00000 \times 10^{-6}AB$…….....5.4

$WL_{40} = -0.038017 + 2.00500 \times 10^{-3}A + 3.90000 \times 10^{-4}B - 1.90000 \times 10^{-5}AB$…..……5.5

Where;

A Represents Speed (cm/min).

B Represents Current (Amperes).

5.3 Responses and ANOVA for the Factorial Model for Speed and Current at a Constant Voltage for HCl Medium

Presented in Table 4.5 is the variation of the selected welding parameters (factors) affecting the behaviour of ASS in 0.5M concentration of hydrochloric acid medium and the corresponding weight loss in milligrams obtained after each experimental run performed on the welded ASS immersed for 40 days in an interval of 8 days. The results show that experimental run four (4) gave the least weight loss values for eight (8) days, sixteen (16) days, thirty-two (32) days and forty (40) days as 0.0470mg, 0.0546mg, 0.0974mg and 0.0759mg respectively at a welding speed of 40cm/min, welding current of 110 Amperes at a constant voltage of 230 volts. This implies that experimental run four (4) gave the least average weight loss value. This further shows that in a

corrosive hydrochloric acid medium, ASS is susceptible to corrosion than in a corrosive alkali medium (NaOH). While experimental run five (5) and two (2) gave the highest average weight loss values. This implies that at low current and low speed, poor weldment was achieved.

The analysis of variance (ANOVA) values are presented in table 4.3. From the results of the ANOVA, model F-value of 63.66implies that the model is significant. There is only a 1.55% chance that a "Model F-Value" this large could occur due to noise. Values of "Prob > F" less than 0.0500 indicate model terms are significant. In this case B, AB are significant model terms while A is not significant. The "Curvature F-value" of 63.66implies that there is significant curvature (as measured by the difference between the average of the centre points and the average of the factorial points) in the design space. There is only a 1.55% chance that a "Model F-Value" this large could occur due to noise. A mean of 0. 7.6%, C.V. of 3.04, Std. Dev. of 2.301 $X10^{-3}$, R^2 of 0.9896 and R^2_{Adj} of 0.9741 were obtained at 95% confidence limit.

Consequently, the "R^2_{Pred}" of 0.7613 is in reasonable agreement with the "R^2_{Adj}" of 0.9741. The value of R^2 calculated for this model was 0.9896, i.e., reasonably close to unity, and thus acceptable. It concluded that 98.96% of the data can be explained by this model. It shows that this model provides reasonably good explanation of the relationship between the independent factors and the responses.

The "Adeq Precision" measures the signal to noise ratio. Since a ratio greater than 4 is desirable, therefore the ratio of 23.522 indicates an adequate signal. The equations that defines each of the responses obtained in the factorial design for speed and current at a constant voltage for HCl medium for forty (40) days are given by Equations 5.6 to 5.10.[That is, the weight loss (WL) for eight (8) days, sixteen (16) days, twenty-four (24) days, thirty-two (32) days and forty (40) days];

$WL_8 = -0.10801+5.98750 \times 10^{-3}A+1.80500 \times 10^{-3}B - 6.52500 \times 10^{-5}AB$……..……..5.6

$WL_{16} = -0.21847 + 0.012920A + 2.89000 \times 10^{-3}B -1.27500 \times 10^{-4}AB$……..5.7

$WL_{24} = -0.37328 + 0.017160A + 4.45000 \times 10^{-3}B - 1.59500 \times 10^{-4}AB$…….5 .8

$WL_{32} = -0.72201 + 0.036358A+7.94500 \times 10\text{-}3B - 3.45750 \times 10^{-4}AB$…….....5.9

$WL_{40} = -2.11827 + 0.091910A+0.021765B - 8.86500 \times 10^{-4}AB$ …….……5.10

Where;

A Represents Speed (cm/min).

B Represents Current (Amperes).

5.4 Interaction between Two Welding Variables and the Effect on ASS Immersed in NaOH and HCl Media

5.4.1 Effects of the interaction of two welding variables on the ASS immersed in NaOH

Presented in figures 4.1- 4.5 are the response surface plots to show the interactions between the speed and current at constant voltage on the ASS immersed in 0.5M concentration of sodium hydroxide for eight (8) days, sixteen (16) days, thirty-two, twenty- four (24) days, (32) days and forty (40) days. From the results obtained, the interactions of these two variables on the ASS were clearly shown. Increase in welding current and welding speed at constant voltage gave the optimum performance of the ASS in this environment since the materials' deterioration was minimal. These were clearly shown at the weight loss level of the metal (ASS) at different current and speed. That is, when current were set at 90Amp and speed at 20cm/min, the weight losses were 0.0024mg, 0.0058mg, 0.0050mg, 0.0041mg and 0.0089mg for eight (8) days, sixteen (16) days, twenty- four (24) days, thirty-two (32) days and forty (40) days respectively as compared

with when current were set at 110Amp and speed were at 40cm/min that gave a weight loss of 0.0008mg, 0.0001mg, 0.0003mg, 0.0005mg and 0.0015mg for eight (8) days, sixteen (16) days, twenty-four (24) days, thirty-two (32) days and forty (40) days respectively. This observation is supported by the interaction effect of speed and current at constant voltage on ASS immersed in 0.5M concentration of sodium hydroxide for 8 days, sixteen (16) days, thirty-two (32) days and forty (40) days in Appendices I to V. The plots indicate that the least weight loss values are at the highlighted points in the design space.

5.4.2 Effects of the interaction of two welding variables on the ASS immersed in HCl

Presented in figures 4.6- 4.10 are the response surface plots to show the interactions between the speed and current at constant voltage on the ASS immersed in 0.5M concentration of hydrochloric acid for eight (8) days, sixteen (16) days, twenty-four (24) days, thirty-two (32) days and forty (40) days. From the results obtained, the interactions of these two variables on the ASS were clearly shown. Increase in welding current and welding speed at constant voltage gave the optimum performance of the ASS in this environment since the materials' deterioration was minimal (that is, at speed of 40cm/min and current of 110Amp). This established the fact that, the best welding parameter's value to obtaining an optimum performance of an ASS is when the current and the speed are relatively high. Nevertheless, the rate of deterioration was high in this environment (HCl) as compared to NaOH medium. The least weight loss values for eight (8) days, sixteen (16) days, thirty-two (32) days and forty (40) days were 0.0430mg, 0.0552mg, 0.0849mg and 0.0517mg respectively at a welding speed of 40cm/min, welding current of 110 Amperes at a constant voltage of 230 volts. While the highest weight loss value for eight (8) days, sixteen (16) days, thirty-two (32) days and forty (40) days were 0.0667mg, 0.0994mg, 0.2026mg, and 0.3256mg respectively. This observation is supported by the interaction effect of speed and

current at constant voltage on ASS immersed in 0.5M concentration of hydrochloric acid medium for 8 days, sixteen (16) days, thirty-two (32) days and forty (40) days in Appendices VI, VII, IX and X. The plots also indicate that the least weight loss values are at the highlighted points in the design space.

5.5 Interaction between Three Welding Variables and the Effect on ASS Immersed in NaOH and HCl Media

5.5.1 Effects of the interaction of three welding variables on ASS immersed in NaOH medium

Shown in figures 4.11 – 4.15 are the cube plots of the effect of the interactions of current, speed and constant voltage on corrosion behaviour of the ASS immersed in 0.5M concentration of sodium hydroxide for eight (8) days, sixteen (16) days, twenty-four (24) days, thirty-two (32) days and forty (40) days. In application, an ASS has a high corrosion resistance in an alkali medium because ASSs exhibit active-passive behaviour in sodium hydroxide solution. At room temperature and concentration up to 50%, sodium hydroxide exhibit low uniform corrosion rate (Khatak and Balev, 2002). The results show that at constant voltage of 230V, a varied speed from 20cm/min to 40cm/min and a varied current from 90Amp to 110Amp, weight losses for eight (8) days, sixteen (16) days, twenty-four (24) days, thirty-two (32) days and forty (40) days were obtained as follows;

Results obtained for eight (8) days are; 0.16% (C+, B-, A+), 0.08% (C+, B+, A+), 0.24% (C+, B-, A-) and 0.09% (C+, B+, A-). For sixteen (16) days are; 0.58% (C+, B-, A+), 0.01% (C+, B+, A+), 0.11% (C+, B-, A-) and 0.03% (C+, B+, A-). For twenty-four (24) days are; 0.50% (C+, B-, A+), 0.03% (C+, B+, A+), 0.21% (C+, B-, A-) and 0.08% (C+, B+, A-). For thirty-two (32) days are; 0.41% (C+, B-, A+), 0.05% (C+, B+, A+), 0.17% (C+, B-, A-) and 0.13% (C+, B+, A-). For forty

(40) days are; 0.89% (C+, B-, A+), 0.15% (C+, B+, A+), 0.30% (C+, B-, A-) and 0.32% (C+, B+, A-). Hence, for the interaction of speed and current at constant voltage of 230V, the optimum performance of the ASS were achieved at the least weight loss values in percentages at 0.08% (C+, B+, A+), 0.01% (C+, B+, A+), 0.03% (C+, B+, A+), 0.05% (C+, B+, A+) and 0.15% (C+, B+, A+) for eight (8) days, sixteen (16) days, twenty-four (24) days, thirty-two (32) days and forty (40) days respectively. It was observed at the end of this analysis that ASS has a strong corrosion resistance in an alkali environment since the percentages of deterioration for the days observed for the corrosion process was non-uniform and it was minimal. This clearly shows that sodium hydroxide solution causes stress corrosion cracking (SCC) on ASS since the rate of deterioration is gradual as reported by Prawoto et al., (2012).

5.5.2 Effects of the interaction of three welding variables on ASS immersed in HCl medium

Shown in figure 4.16 – 4.20 are the cube plots of the effect of the interactions of current, speed and constant voltage on corrosion behaviour of the ASS immersed in 0.5M concentration of hydrochloric acid for eight (8) days, sixteen (16) days, twenty-four (24) days, thirty-two (32) days and forty (40) days. The results show that at constant voltage of 230V, a varied speed from 20cm/min to 40cm/min and a varied current from 90Amp to 110Amp, weight losses for eight (8) days, sixteen (16) days, twenty-four (24) days, thirty-two (32) days and forty (40) days were obtained as follows;

Results obtained for eight (8) days are; 5.90% (C+, B-, A+), 4.29% (C+, B+, A+), 5.67% (C+, B-, A-) and 6.67% (C+, B+, A-). For sixteen (16) days are; 9.94% (C+, B-, A+), 5.52% (C+, B+, A+), 7.05% (C+, B-, A-) and 7.73% (C+, B+, A-). For twenty-four (24) days are; 13.94% (C+, B-, A+), 10.08% (C+, B+, A+), 8.33% (C+, B-, A-) and 10.85% (C+, B+, A-). For thirty-two (32) days

are; 20.26% (C+, B-, A+), 8.49% (C+, B+, A+), 9.78% (C+, B-, A-) and 11.84% (C+, B+, A-). For forty (40) days are; 32.56% (C+, B-, A+), 5.17% (C+, B+, A+), 8.31% (C+, B-, A-) and 16.38% (C+, B+, A-).

Hence, for the interaction of speed and current at constant voltage of 230V, the optimum performance of the ASS in this medium were achieved at the least weight loss values in percentages at 4.29% (C+, B+, A+), 5.52% (C+, B+, A+), 8.33% (C+, B-, A-), 8.49% (C+, B+, A+) and 5.17% (C+, B+, A+), for eight (8) days, sixteen (16) days, twenty-four (24) days, thirty-two (32) days and forty (40) days respectively. It was also noted that hydrochloric acid causes a general corrosion in ASS (Claus, 2011).

5.6 Comparative Effects of Sodium Hydroxide and Hydrochloric Acid Media on ASS

Comparing the least weight loss of ASS immersed in 0.5M concentration of sodium hydroxide and in 0.5M concentration of hydrochloric acid media, it was clearly observed that ASS deteriorated more in HCl medium than in NaOH environment. Here, the corrosion behaviour of the austenitic stainless steel in acidic solution depends considerably on the concentration of chloride ions and the acidity of the environment caused by the hydrogen ion (H^+) (Ferwerda, 2014). The presence of chloride ions produces and enhances the metal corrosion through the passive layer, and decreases the passivity breakdown potential (Albrimi et al., 2011).

It can also be seen from these Figures (4.11 – 4.15 and 4.16 – 4.20) that ASS show less susceptibility to corrosion in sodium hydroxide medium in comparison to the hydrochloric acid environment. Figures 4.6 - 4.10 reveals a progressive weight loss in the ASS throughout the

exposure time in hydrochloric acid medium than in hydroxide medium. This could be attributed to the aggressive chloride ion which continuously breaks down the protective film on the metal. Protective chromium oxide formed on the surface of the ASS in the presence of aerated concentration of hydrochloric acid couldhave been too weak or thin to prevent further penetration of chloride ion which is known for its aggressiveness and depassivation effect which usually lead to pitting corrosion (Refaey et al., 2005).

5.7 Hardness Properties of the Samples

Figure 4.21 to 4.30 shows that the hardness value is high in the heat affected zone of the material than at the weld zone. This could be due to the residual stresses at the HAZ caused by the heat generated during welding. Also from the figures (4.21 to 4.30), it could be observe that the variations of hardness value at different days of immersions in the two media (NaOH and HCl). This clearly shows that some external factors during welding operation like handling of the welding torch, lack of constant supply of shielded gas to shield the weld pool from atmospheric contaminations and other related factors must have contributed immensely to the low hardness at the fusion zone.

It can also be observed that the foreign ASS (welded but not immersed) produced the highest average value of hardness test (Appendix XVI) and of the five different parameters; C_3 produced a relatively high hardness value than other parameters. Also, of the five different intervals of immersions, 24 days and 40 days of immersion produced a relatively high hardness value than other intervals. A similar trend was observed in the result of the hardness test conducted in relation to tensile test result. The variation in the hardness values of the samples also agreed with observations made by Mishra et al, (1999), Kock, (2000) and White andAnsell (1993). They

showed that hardness is a function of grain size of the weldment and the integrity of the welded joints.

5.8 Tensile Properties of the Samples

Figures 4.31 to 4.46 show the variation of load against extension of the tensile test of the weld joint of the ASS. it can be observed generally that with a gradual increase in load, there is a corresponding increase in extension of the specimen, that is the extension produced is directly proportional to the load, this continues until the maximum load is reached. At this point of maximum load, a neck is formed. The reduced area was not able to sustain the load being applied, hence the specimen finally fractured at this new point which is called the breaking load point.

From figure 4.47 it can be seen that for samples immersed in 0.5M of NaOH the parameters has a significant role in the tensile strength of the welded ASS joint. The variation on the maximum load and extension is a function of the weld parameter and it is observed that the highest values are obtained at weld parameter C_3 which is current, I = 100A, speed = 30mm/s followed closely by weld parameter C_1. It is seen that the immersion of the ASS metal in 0.5M of NaOH has a sizable deteriorative effect on steel which in turn affects the tensile strength when compared to the control. For samples immersed in 0.5M of HCl medium as seen in figure 4.48, the observations of weld parameter on tensile strength is similar to samples immersed in 0.5M of NaOH. The results show that weld parameter C_3(15.7KN) has maximum values of load and extension followed by C_1(14.6KN).

Figure 4.50 shows the comparative effect of exposure time of ASS in 0.5M of HCl and NaOH media on its tensile strength. This gives information on the corrosion behaviour of the ASS when

immersed in the two media used in this research. It can be seen that samples immersed in 0.5M of HCl medium has lower tensile strength compared to samples in 0.5M of NaOH for all exposure time. This implies that HCl medium has greater corrosive effect on the integrity of the welded joint when subjected to tensile stresses. This may be due to the aggressiveness of the chloride ion (Cl^-) in the medium (Claus, 2011). Also it is noted from the figure 4.50 that there is a gradual decrease in the tensile strength of the immersed ASS in both media with increasing exposure time.

The results obtained from the tensile test of the welded austenitic stainless steel are in agreement with those obtained by other researchers Grassel, et al (2000) and Clyne, (2000). They show that the tensile strength increases as the grain size decreases and also tensile strength depends on the integrity of welded joint.

5.9 Impact Properties of the Samples

Table 4.10 to 4.12 shows the results of the impact test conducted on some samples (control samples, welded and immersed samples and also unwelded samples). It can be observed from figure 4.51 that the control sample C_3 among others has the highest impact energy. Also from figure 4.52 to 4.56 for samples immersed in NaOH medium from 8 days to 40 days for sample C_3, there is an observed effect of weld parameter used in welding the metal joint on the energy absorbed by the ASS. It can be seen that weld parameter C_3 gave the metal with highest absorbed energy followed by parameter C_4, after immersion in 0.5M of NaOH for 8 days to 40 days, compared to the other weld parameters. This clearly shows that better weld deposit and stronger weldment was effected at C_3 (19.7J) and C_4(14.9J) parameters.

Figure 4.57 to 4.60 for samples immersed in 0.5M of HCl acid medium from 8 days to 40 days, sample C_3 C_4 and C_5 were the parameters that produce weld with highest absorbed energy. Also, the results showed that samples that are welded and immersed immersed in NaOH produced high impact energy than those immersed in HCl. This could be due to the high deterioration of the steel in HCl medium than in NaOH. It could also be as a result of the coarse microstructure in the GMAW process. The impact energy absorbed by C_3 immersed in NaOH and HCl are close to that of the sample C_3 welded but not immersed which absorbed energy 21.70J before it fails.

The variation in the impact strength is in agreement with the variation of their elongation at failure during tensile and hardness tests carried out. The result obtained from this test is in agreement with those obtained by these researchers Bonnefois et al., (1991) and Gunn (1997).

5.10 Correlation of Hardness, Tensile and Impact Strength Tests

It was observed from the mechanical destructive tests carried out on the ASS when immersed in the media used for this research work that when the properties are compared with varying weld parameters adopted in joint's weld operations, there was a pattern displayed among the weld parameters with C_3(19.7HRA, 203N/mm^2 and 19.7J)and C_4(14.9 HRA, 189N/mm^2 and 14.9J) consistently coming out as the parameter producing an ASS weld joint with the best mechanical properties of hardness, tensile and impact strength.

5.11 Scanning Electron Micrograph of Samples

SEM was used to study the morphology of all the welded and as received samples. Plate III shows the SEM micrograph of as received sample of ASS (not welded and not immersed)with EDS profiles. It was observed here that the microstructure clearly showed a fine grain boundary

and is an indication of a better blending of parent material and the alloying elements. The pore spaces observed in the microstructure suggest non uniformity of the ASS material.

Plate IV to V shows the SEM micrographs of unwelded ASS sample immersed in 0.5M of sodium hydroxide medium (NaOH) and hydrochloric acid (HCl) media for 40 days with EDS profiles, indicating iron to have the highest percentage as the base metal followed by chromium as the highest alloy element. Plate IV shows uniform corrosion of the ASS while plate V shows signs of dissolution of metallic structure and grain boundaries due to the aggressiveness of chloride ion (Cl^-) in the medium. It was observed that HCl medium had higher corrosion attack on the ASS. Plate VI shows the SEM micrograph of the FZ of sample C_3 welded and not immersed. The little blackening in the metal shows the source of the part of ASS used to produce a non-reflective black oxide surface.

Plate VII to VIII show the SEM micrographs of the HAZ and FZ of samples C_3 and C_2 welded and immersed for 8 days in 0.5M of hydrochloric acid and sodium hydroxide media respectively. Plate VIImicrograph shows a better weldment with the presence of pitting corrosion effect (dark area) along the grain boundaries of the parent metal than plate VII. This actually supports the corrosion susceptibility of ASS in hydrochloric acid medium a reported by Claus, (2011).

Plate IX to X shows the SEM micrographs of the HAZ of samples C_4 and FZ of sample C_3 welded and immersed for 24 days in 0.5M of sodium hydroxide medium and hydrochloric acid media respectively. Plate IX shows a good weldment of ASS immersed in 0.5M of NaOH for 24 days indicating a high integrity weldment that has less corrosion attack in comparison with plate X immersed in HCl acid medium for 24 days which shows a sign of pitting corrosion. Some

blackening in plate X micrograph suggests lack of adequate shielded gas during welding operation which must have given room for atmospheric contaminant.

Plate XI to XII shows the SEM micrographs of the samples immersed for 40 days. Plates XI show the SEM micrographs of the HAZ of sample C_1 welded and immersed for 40 days in 0.5M of hydrochloric acid medium. It can be observed from the scanned image of the ASS sample C_1 the crack propagation on the parent metal resulting in stress induced corrosion on the microstructure which arises as a result of internal stresses from non-uniform cooling during welding. This resulted to the poor tensile strength and hardness values of C_1. While plate XII shows the SEM micrograph of the FZ of sample C_3 welded and immersed for 40 days in 0.5M of sodium hydroxide. A scan image of the welded region (FZ) shows a homogenous weldment free of corrosion effects. This could be as a result of the alloying elements such as nickel in the electrode which reduces the effect of corrosion on the welded joint.

Morphological analysis using SEM clearly shows differences in the morphologies of the heat affected zone, fusion zone and the parts that are not affected, causing the grains of the heat affected zone to be more coarse than those of the unaffected zone (Plate III). The microstructure clearly shows that there will be great influence of this change in morphology to the properties of the welded samples.

However, the grain sizes of the heat affected zone for samples immersed in NaOH medium are shown to be finer as compared to other samples immersed in HCl medium. This is expected to give them better mechanical properties. The basic information obtained from the SEM

micrograph is in agreement with observations raised by other researcher Whitehouse, et al (1991), while the relationship between the microstructure and the properties of the welded ASS agrees with the conclusions of Mohanty, et al (2002) and Madugu, et al (2010). These researchers showed that the grain size has a measurable effect on most of the mechanical properties such as hardness, tensile strength, impact strength and these properties increases as the grain size decreases.

CHAPTER SIX

6.0 CONCLUSIONS AND RECOMMENDATIONS

6.1 Conclusions

The following conclusions can be drawn from the studies conducted on the effects of GMAW parameters on the corrosion and mechanical behavior of ASS in sodium hydroxide and hydrochloric acid media using design expert 6.0.6 software.

1. The austenitic stainless steel can be welded successfully using gas metal arc welding process depending on the application or service life which the material will be subjected to. The tensile test, impact test and the hardness test show that welding has a negative effect on the mechanical properties of this alloy.
2. Corrosion of ASS occurred in both sodium hydroxide and hydrochloric acid media due to the aggressiveness of hydroxyl ion (^{-}OH) and chloride ion (Cl^{-}) in the media respectively. Also, Surface passivation of ASS observed only in sodium hydroxide is attributed to film stability in the compound.
3. Corrosion susceptibility of ASS is more pronounced in hydrochloric acid medium than in sodium hydroxide for all the exposure time studied. This could be attributed to the aggressive chloride ion which continuously breaks down the protective film on this metal. The corrosion behaviour of austenitic stainless steel in acidic solution depends considerably on the concentration of chloride ions and the acidity of the environment.
4. The effects of GMAW parameters on the corrosion behaviour of ASS in sodium hydroxide and hydrochloric acid media were successfully optimized by the application of factorial design of experiments. The interaction effect of speed and current at constant voltage on ASS immersed in sodium hydroxide medium and hydrochloric acid medium was evaluated,

which is not possible with the conventional univariate technique that is time-consuming, requiring a large number of experimental runs and it is expensive.

5. Low welding speed and low welding current concurrently gave a low weldment of the material as observed with C_1(speed 20cm/min, current 90A), C_2(speed 20cm/min, current 110A)and C_5(speed 40cm/min, current 90A)while relatively high welding speed and current gave a better weldment of the steel as observed with C_3 (speed 30cm/min, current 100A) and C_4(speed 40cm/min, current 110A).The best welding paramenters that gave optimum mechanical properties were when the current was set between 100A to 110A and speed set between30cm/min to 40mm/sec at a constant voltage of 230V.

6.2 Recommendations

5. Further work should be done on the fracture toughness of this alloy because of its exceptional mechanical properties.
6. Full factorial design of experiment at other levels and factors above three to include heat input, postweld heat treatment and arc length may be investigated.
7. Study should be carried out on this steel (ASS) at different concentrations of the corrosive environments in order to determine its behaviours.

6.3 Contribution to Knowledge

Some of the contribution to knowledge of the research are;

1. High current between 100A to 110A, high speed between 30cm/min to 40cm/min at constant voltage of 230V improved the mechanical properties of the steel (ASS) at optimal values of 35.1HRA at HAZ and 30.2HRA at the FZ for hardness, 225MN/m^2 for the tensile and 21.7J for impact.

2. Design-Expert Software of 6.0.6 used in the variation of the welding parameters (current 90A to 110A, speed 20cm/min to 40cm/min and constant voltage 230V) in determining the corrosion behavior of the ASS structure, gave an optimal performance of the steel (ASS) at the points where the weight loss were WL_{40} = 0.0020mg for NaOH and WL_{40} = 0.0759mg forHCl media.

REFERENCES

Abdel-Monem, E. (2012). Laser Beam Welding of Austenitic Stainless Steels – Similar Butt and Dissimilar Lap Joints. *Manufacturing Technology Department, Central Metallurgical R & D Institute, Cairo, Egypt pp 94-116.*http://dx.doi.org/10.5772/48756.

Abdel-Monem, E., Abdel-Fattah, K. and Thoria, S. (2011) "Effect of Laser Beam Welding Parameters on Microstructure and Properties of Duplex Stainless Steel," *Materials Sciences and Applications*, Vol. 2 No. 10, 2011, pp. 1443-1451.

Abdul, G.O. (1990). The Effect of Post Weld Heat Treatment and Distribution of Residual Stress in Weld Repaired High Chromium Steel (AISI 410) Components. *M.Eng Thesis submitted to Dublin City University, Scientific Studies & Research Centre Damascus – Syria*.pp 1-12

Adebayo, S.M. and Odepidan, E.O. (2002). Effects of Welding Speed on Mechanical Properties of an Arc Welded Steel Plater. *Journal of Applied Science and Technology*, Vol 2, No 1: pp40-43.

Afolabi, A.S. (2008). Effect of Electric Arc Welding Parameters on Corrosion Behaviour of Austenitic Stainless Steel in Chloride Medium.*AU J.T.* 11(3): 171-180.

Afolabi, A.S.,Alaneme, K. K. and Bada, S.O. (2009). Corrosion Behavior of Austenitic and Duplex Stainless Steels in Lithium Bromide. *Leonardo Electronic Journal of Practices and Technologies*.pp 1-10

Albrimi, A. Y., Eddib, A., Douch, J., Berghoute, Y., Hamdani, M. and Souto, R.M. (2011). Electrochemical Behaviour of AISI 316 Austenitic Stainless Steel in Acidic Media Containing Chloride Ions. *International Journals of Electrochemical Science* Vol.6, pp.4614 – 4627.

Aleksandra, K. and Marjetka, C. The Corrosion Behaviour of Austenitic and Duplex Stainless Steels in Artificial Body. *Materials and Technology*, Vol.44, No 1, pp 21–24.

Almubarak, A., Abuhaimed, W. and Almazrouee, A (2013). Corrosion Behavior of the Stressed Sensitized Austenitic Stainless Steels of High Nitrogen Content in Seawater. *International Journal of Electrochemistry*, Volume 2013, pp 1-7

Aluko, O.S. (2014). Corrosion Fatigue and Microstrural Behaviours of Welded Austenitic Stainless Steel in Different Environments. M.Sc Thesis in Mechanical Engineering

Atamert, S.A.K., and King, J.E (1993). Sigma-Phase Formation and its Prevention in Duplex Stainless Steels. *Journal of Materials Science Letters*, 12(14): pp1144-1147.

Avery, C.H. (1963). Heat Treatment of Stainless Steel. Metal Handbook, 8th edition. *America Society of Metals, Ohio*, pp 200-243.

Balmforth, M.C. and Lippold, J.C. (2000). A New Ferritic-Martensitic Stainless Steel Constitution Diagram. *Welding of Research Journal, December, 2000*. pp339-345.

Bernard, M. and Jack, H. (1999). Determining the Parameters for GTAW. *Published in the July/August 1999 Issues of Practical Welding Today*www.pro-fusiononline.com. Retrieved on the 16th of March, 2013.

Bonnefois, B., Charles, J.,Dupoiron, F. and Soulignac, P. (1991). How to Predict Welding Properties of Duplex Stainless Steels. *In Duplex Stainless Steels* . 1991.

Box, G.E.P. and Wilson, K.N. (1951). On the experimental attainment of optimum conditions. J. Roy statist. Soc. Ser. B Method 13: 1-45.

Callister, W.D. Jnr (1997). Material Science and Engineering, Fourth Edition, *John Wiley and Sons, New York*, pp 349-353.

Callister, W.D. (2007). Material Science and Engineering, Seventh Edition, *John Wiley and Sons, Incorporation, New York.*

Chamberlain, J. and Trethewey, A.R. (1988). Corrosion for Students of Science and Engineering. *Longman Scientific and Technology Books, Londan, England*.

Charles J. (1991) Welds in Duplex Stainless Steels, Proc. *Duplex Stainless Steels '91, Beaune, France*, 151-168.

Charles, J. (1997). Why and Where Duplex Stainless Steels. *Duplex Stainless Steels '97 Maastricht, Netherlands 1(1997)* pp 29-42.

Charles, J., Mithieux, J.D., Santacreu, P.O. and Peguet L. (2007). Retrieved 2nd May, 2013 from www.aperam.com.

Chris, S. and Alan, L (2007). Precipitation Hardening P/M Stainless Steels *Roger Doherty Drexel University Philadelphia, PA 19104* pp1-13

Claes-Ove, P. and Sven-Aven, F. (1995). Welding Practice for the Sandvik Duplex Stainless Steels SAF2304, SAF2205 and SAF2507.

Claus, Q.J. (2011). Stainless Steel and Corrosion. First edition, *Damstahl.* Retrieved on 25th September, 2014 from http://www.damstahl.com/Files/Billeder/2011/PDF/BOOK/book.pdf .pp 81-84

Clyne, T. W. (2000). Comprehensive Composite Materials. *Journal of Metal Matrix Composite*,3:1-8.

Cornu J. (1988). 'Advanced Welding Systems-Part2'. *London, IFS Limited*. pp 168.

Crawford, S. (2011). Functionally Graded Martensitic Stainless Steel Obtained Through Partial Decarburization. Retrieved 2nd May, 2013 from www.materials.mcmaster.ca

Daisuke, K. Saxhiko, H., Takoa, H. and Yasuyuki, K. (2002). Corrosion Behaviour of Nickel-Free High Nitrogen Austenitic Stainless Steel in Simulated Biological Environments. *Materials Transactions*, Vol. 43, No.12, pp3100-3104.

Damian, K. and Armao, F. (2003). Stainless Steels Properties –How To Weld Them Where To Use Them. Retrieved 7th May, 2013 from www.lincolnelectric.com

Dauda, E.T. (2008). Weldability Assessment of Some Locally Sourced Steels, *PhD Dissertation, Department of Metallurgical Engineering, A.B.U Zaria, Nigeria.*

Dı´az-Cedre, E., Cruz-Crespo, A., Morales, F.R., Rico, M.T., Gonza´les, J.C., Pe´rez, M.R., Morejo´n, J.A.P., Puchol, R.Q. and Pino, N.M.P. (2010). Effect Of The O_2/Co_2 Ratio and Welding Current on The Geometry of Square Groove Weld Joints in Low Carbon Steels Obtained with GMAW. *Welding International* 24 (7): 499–508.

Duane, K.M. (2003). Preheat and Interpass Temperature. Retrieved on 17th September, 2013 fromwww.weldinginnovation.com.

Elibol, M. (2002). Response surface methodological approach for inclusion of perfluorocarbon in actinorhodin fermentation medium. *Process Biochemistry*, 38:667-773.

Ferwerda, E. (2004). "Chemistry: Objectives - Chapters 20 and 21." Chemistry Teacher's Work Site.

Retrieved November, 2014 fromhttp://water.me.vccs.edu/courses/env211/lesson7_print.htm

Fraser, K. (2009). Corrosion Resistance of Austenitic and Duplex Stainless Steels in Environments Related to UK Geological Disposal. Pp1-29. www.nda.gov.uk.

Galal, A., Atta, N.F. and Al-Hassan, M.H.S. (2005). Effect of some thiophene derivatives on the electrochemical behaviour of AISI 316 austenitic stainless steel in acidic solutions containing chloride ions. *Mater.Chem.Phys.* 89: 38-48.

Gooch, T.G. (1996). Corrosion Behavior of Welded Stainless Steel. *American Welding Journal, May, 1996*; pp 135-154. Retrieved on 4th September, 2013 from www.americanweldingsociety.org.

Gooch, T.G. (1991). Corrosion resistance of welds in Duplex Stainless Steels.

Grassel, O., Kruger, L., Frommeye, G. and Meyer, L.W. (2000). High Stregth Fe-Mn-(Al,Si) TRIP?TWIP Steels Development, Properties and Application. *International Journal of Plasticity, vol 16, Issues 10-11*. pp 1391–1409

Gunn, R. (1997). Duplex Stainless Steels-Microstructure, Properties and Applications. *Abington publishing: Cambridge, England.*

Habsah, M., Ishak, M, Misbahul, A. and Mohd, N. D.(2008). Effect of Temperature on Corrosion Behavior of AISI 304 Stainless Steel with Magnesium Carbonate Deposit.*Journal of Physical Science*, Vol. 19(2), 137–141

Ibhadode, A. A. O. (2001). Introduction to Manufacturing Technology. *Ambik Press, Benin City, Nigeria. Second Edition*. pp 505.

Ibrahim, O. H. (2010). Impact behaviour of different stainless steel weldments at low temperatures. *Engg. Fail. Anal* 17(1):1069-1076. www.ijaiem.org

Iliyasu, I., Yawas, D. S. and Aku, S.Y. (2012). Corrosion Behavior of Austenitic Stainless Steel in Sulphuric Acid at Various Concentrations. *Advances in Applied Science Research*, 3 (6):3909-3915 (www.pelagiaresearchlibrary.com).

Internet link: www.sppusa.com (Accessed 2nd May, 2013).

Internet link: www.stoprust.com (Accessed 23rd April, 2013).

Internet link: www.aws.org/w/a/wj/1998/11/kotecki.com (Accessed 9th September, 2013).
Internet link:www.stainlesssteelbiz.com (Accessed 23rd August, 2013).

Internet link:www.outokumpu.com/SiteCollectionDocuments/Duplex_Stainless_Grade_Datasheet (Accessed 19th March, 2013).

Internet link: www.jansinc.com/welding.html (Accessed 21st May, 2015).

Internet link: www.lincolnelectric.com (Accessed 3rd September, 2013).

Internet link:www.bssa.org.uk/topics.php?article=20 (Accessed 3rd September, 2013).

Internet link:www.bssa.org.uk/about_stainless_steel.php?id=31 (Accessed 21st May, 2015)

Internet link:www.metals.about.com, (Accessed 6th September, 2013).

Internet link: www.aws.org/standards/page/standard-welding-procedure-specifications-swps (Accessed 27th May, 2015)

Internet link:http://www.gowelding.com/wp/wps.htm (Accessed 27th May, 2015)

Internet link:www.avestawelding.com (Accessed 23rd April, 2013).

Internet link: www.zhweijun.wordpress.com/2010/07/01/resistance-welding-benefits-and-limitations (accessed 2015)

Internet link:practicalmaintenance.net (Accessed 26th April, 2013).

Internet link:www.anconbp.com.au (Accessed 3rd July, 2013).

Internet link:www.boc.com.au (Accessed 3rd June, 2013).
Internet link:www.asminternational.org (Accessed 3rd June, 2013).
Internet link:www.nickelinstitute.org (Accessed 11th September, 2013).
Internet link: www.businessdictionary.com/definition/ferritic-stainless-steels.html (Accessed 26th March, 2013).
Internet link:www.arcelormittalstainless.com (Accessed 20th April, 2013).
Internet link:www.calphad.com/iron-carbon.html (Accessed 25th April, 2013).
Internet link: www.keytometals.com (Accessed 23rd August, 2013).
Internet link: www.bssa.org.uk/topics.php?article=20 (Accessed 3rd September, 2013).
Internet link:www.techtrain123.com (Accessed 9th September, 2013).
Internet link: www.nace.org/Pitting-Corrosion (Accessed 5th September, 2014).

Internet link:http://www.totalmateria.com (Accessed 5th September, 2014).
Internet link:www.azom.com/article.aspx?ArticleID = 2819 (Accessed 1st April, 2013).
Internet link: www.smt.sandvik.com/en/products/welding-products/shielding-gases/shielding-gases-for-mig (Accessed 2nd October, 2013).
Internet link: www.engtips.com/viewthread.cfm?qid=226701 (Accessed 19th September, 2013).

Internet link: www.toolingu.com/definition-650110-110539-gas-metal-arc-we (Accessed 9th September, 2013).

Ives, E., (2001). A Guide to wood micotermy; making quality microslides of wood sections, Ipswich, Suffolk IP8 3 AY, UK.

James, G.K. (2000). Chronology of Corrosion Disasters. *America Metal Society Handbook5, New York, NY, USA.*

Jeff, N. Gas Metal Arc Welding Guidelines. Retrieved 6th May, 2013 from www.lincolnelectric.com

Jonathan, B. and Gordon, J. (1999). Introduction to Stainless Steels 3rd Edition. *ASM International.*

Khatak, H.S. and Balev, R. (2002). Corrosion of Austenitic Stainless Steels: Mechanism, Mitigation and Monitoring. Woodhead Publishing, Elsevier. Retrieved on 20th August, 2014 from http://books.google.com.ng/books?id=f_4QdX8F_TAC&source=gbs_navlinks

Kobe, S. (1995). "Essential Factors in Gas Metal Arc Welding," Retrieved 14th August, 2014 from http://www.kobelco.co.jp/english/welding/events/files/2011GMAW.pdf.

Kock, J .W. (2000). Physical and Mechanical Properties of Chicken Feather Materials. *Msc Thesis Presented to the Academic Faculty Georgia Institute of Technology.*

Kondapalli, S.P., Chalamalasetti, S.R. and Damera, N.R. (2013). Effect of welding parameters on pitting corrosion rate of pulsed current micro plasma arc welded AISI 304L sheets in 1N HCl *Journal of Computational and Applied Research in Mechanical Engineering Vol. 3, No. 1, pp. 1-11*

Loto,R. T., Loto, C. A., Popoola, A. P. I. and Ranyaoa, M. (2012).Corrosion Resistance of Austenitic Stainless Steel in Sulphuric Acid.*International Journal of Physical Sciences* Vol. 7(10), pp. 1677 – 1688. (www.academicjournals.org/IJPS)

Luo, X., Tang, R., Long, C., Miao, Z., Peng Q. and Cong L. (2007). Corrosion Behavior of Austenitic and Ferritic Steels in Supercritical Water. *Nuclear Engineering and Technology,* Vol.40 No.2. Special Issue on the 3rd International Symposium on SCWR, pp 147-154.

Madugu, I. A, Abdulwahab, M. and Aigbodion, V.S. (2010). Effect of Iron Filings on the Properties and Microstructure of Cast Fibre-Polyester/Iron Filings Particulate Composite. Journal of Alloys and Compounds, :808-811.

Majumder, A (2011). Study of the effect of bevel angle and welding heat input on mechanical properties of mild steel weldment. International *Journal of Mechanical and Materials Engineering* 6(2): 280-290.

Manoj, S., Dharminder, S. and Dharmpal, D. (2010). Parametric Optimization of Gas Metal Arc Welding Processes by Using Factorial Design Approach. *Journal of Minerals & Materials Characterization & Engineering,* Vol. 9, No.4, pp.353-363

Mehmet, U., Bekir, S. Ü. and Mustafa, A. (2011). Determination of optimum welding parameters in connecting high alloyed X53CrMnNiN219 and X45CrSi93 steels by friction welding. *Bull. Mater. Sci.*, Vol. 34, No. 4, pp. 815–823.

Mishra, S. C., Nayak. N.B and Satapathy, a. (1999). Investigation on Bio-waste Reinforced Epoxy Composites, *Metallurgical and Materials Engineering Department, National Institute ofTechnology, Rourkela, India*. pp 119-123.

Mohanty, A.K., Misra M., and Drzal L.T., (2002). Sustainable Bio-composites from Renewable Resources: Opportunity and Challenges in the Green Materials World. *Journal of Polymer nad Environment;* 10:19–26.

Mohd, N.C.W., ,Khalid, S., Nurazilla, M.A.M. and Abdul-Majeed, M. (2011). Effect of Arc Voltage and Current on Mechanical and Microstructure Properties of 5083-Aluminium Alloy Joints Used in Marine Applications. *UMTAS 2011*. pp 169-178.

Munoz, A.I., Anton, J.G.,Nuevalos, S.L., Guinon, J.L., and Herranz V.P. (2004). Corrosion studies of austenitic and duplex stainless steel in aqueous lithium bromide solution at different temperatures. *Corrosion Science* Vol. 46, 2955-2974.

Murugan, N. (1993). Effect of submerged arc process variables on dilution and bead geometry in single wire surfacing. *Journal of Materials Processing Technology*. pp 1-3

Ojokuku, G.O. (2001). Practical Chemistry for Schools and Colleges. *Gbabeks Publishers Limited, 31, MKO Abiola's Way, Ibadan, Nigeria.* pp 197-199.

Okibe, F.G. (2014). Preparation and Characterization of Activated Carbons from Brachystegia eurycoma and prosopis Africana Seed Hulls for Solid Phase Adsorption of Dyes. *Ph.D Dissertation, Chemistry Department, ABU, Zaria, Nigeria.*

Parijslaan, R. (2002). Welding Stainless Steels: Techniques and Principles- *An electronic Manual* (www.cimeth.org\\stainless.htm). Retrieved 16th March, 2013.

Pascoe, K.J. (1982). An Introduction to the properties of Engineering. Materials *English language Book Society and Van Nostrand Reinhold (UK) Co.Ltd.*pp114-116.

Paul, S. (2006). Controlling the Heat Affected Zone (HAZ) in HF Pipe and Tube Welding Retrieved 23rd April, 2013 from www.thermatool.com/information/papers/welding

Paulo, M. O. S., Hamilton, F. G. A., Hugo, V. C. A. and Pedro, L. N. and João Manuel R.S. T,(2011). Cold Deformation Effect on the Microstructures and Mechanical Properties of AISI 301LN and 316L Stainless Steels. *Materials & Design* Vol. 32, Issue 2. Pp 605-614. Retrieved on 4th September, 2013 fromwww.sciencedirect.com/science/article.

Pierre, J.C. (2007). Welding of Stainless Steels. *Material and Application Series,* Vol 3. (www.euro-inox.org. Retrieved on 20th April, 2013).

Prawoto, Y., Sumeru, K. and Wan Nik, W. B. (2012). Stress Corrosion Cracking of Steel and Aluminum in Sodium Hydroxide: Field Failure and Laboratory Test. *Advances in Materials Science and Engineering Volume 2012.* Article ID 235028, pp1-8. Retrieved on 21st August, 2014 from http://www.hindawi.com/journals/amse/2012/235028/

Refaey, S. A. M, Taha, F. and El–Malak, A. M. (2005). Corrosion and inhibition of stainless stainless steel pitting corrosion in alkaline medium and the effect of Cl– and Br– anions,*Applied Surface Science 242*, pp. 114–120.

Sandvik, Your Guide to Easy Welding of Duplex Stainless Steels. Retrieved, 15th March, 2013 from (www.steel.sandvik.com).

Sathiya, P., Sudhakaran, A. and Soundararajan, R.(2012).Mechanical and Metallurgical Investigation on Gas Metal Arc Welding of Super Austenitic Stainless Steel. *International Journal of Mechanical and Materials Engineering (IJMME),* Vol. 7 No. 1, 107–112.

Scott, F. R. (1999). Key Concepts in Welding Engineering. *A Look at Heat Input. Welding Innovation* Vol XVI, NO 1.

Sedriks, A.J. (1996). Corrosion of Stainless Steels. Second Edition. *John Wiley, New York, NY*.

Shirali, A. A. and Mills, K.C. (1993). The Effect of Welding Parameters on Penetration in GTA Welds. *Welding Reseach Supplement,* 347-353. Retrieve on 12th September, 2013 from www.americanweldingsociety.org

Sieurin, H. (2006). Austenite reformation in the heat-affected zone of duplex stainless steel 2205. *Materials Science & Engineering*. Vol. 418.pp 250-256

Sridhar, N. and Kolts, J. (1987). *Corrosion Handbook* 43 (11) 647-651

Streicher, M.A. (1977). Stainless Steels: Past, Present and Future. *Proc. Symp. Stainless Steel. Climax Molybdenum Co, Ann Arbor, MI, USA.*

Suresh, K. L., Verma S.M., Radhakrishna, P.P., Kiran, K.P. and Siva, T.S. (2011). Experimental Investigation for Welding Aspects of AISI 304 & 316 by Taguchi Technique for the Process of TIG & MIG Welding. *International Journal of Engineering Trends and Technology*-Volume 2 Issue 2. pp 28-32.

Tanimu, I. (2013). Effects of Welding and Heat Treatment on the Mechanical Properties of Duplex Stainless Steels. *M.Sc Thesis in Mechanical Engineering Department, Ahmadu Bello University, Zaria , Nigeria*.pp 1-25.

Taylor, R. (1994). Duplex Stainless Steel Production. In SFSAT&O Conference.

Tewari, S. P., Gupta, A and Prakash J. (2010).Effect of Welding Parameters on the Weldability of Material. *International Journal of Engineering Science and Technology.* Vol. 2(4), pp 512-516.

Ugur, S., Osman, I., Fehim, F., Cemil, O. and Yasar, K. (2011). Determination of Welding Parameters for Shielded Metal Arc welding.*Scientific Research and Essays* Vol. 6(15), pp. 3153-3160

Vannevik, H., Nilsson, J.O., and Kangas, P. (1996). Effects of Elemental Partitioning on Pitting Resistance of High Nitrogen Duplex Stainless Steels. *ISIJ International, 1996*. 36 (7):pp807-812.

Vikas, D. P. and Stephen M. (1995).Stress Relief Guidelines for Stainless SteelMaterials for saline water, desalination and oilfield brine pumps"—*Nickel Institute reference book series* No. 11 004, 2nd edition, 1995. pp 1- 12,

White, D., Nuhn, N. and Kiefer, G. (1996). Effects of Moisture Contamination and Welding Parameters on Diffusible Hydrogen. *Welding Journal* 75(5); 155-161.

White, N.M .and Ansell, M.P. (1993). Straw Reinforced Polyester Composites. *Journal of Material Science,* 18:1549–56.

Whitehouse, A. F, Shahani, R. A. and Clyne, T. W. (1991). Metal Matrix Composites: Processing, Microstructure and Properties. *National Laboratory, Denmark*: 741-748.

Yawas, D.S (2005). Suitability assessment of some plant extracts and fatty acid vegetable oil as corrosive inhibitors. *Ph.D Dissertation, Mechanical Engineering Department, ABU, Zaria, Nigeria.*

APPENDICES

Appendix I: Interaction effect of speed and current at constant voltage on ASS immersed in NaOH for 8 days

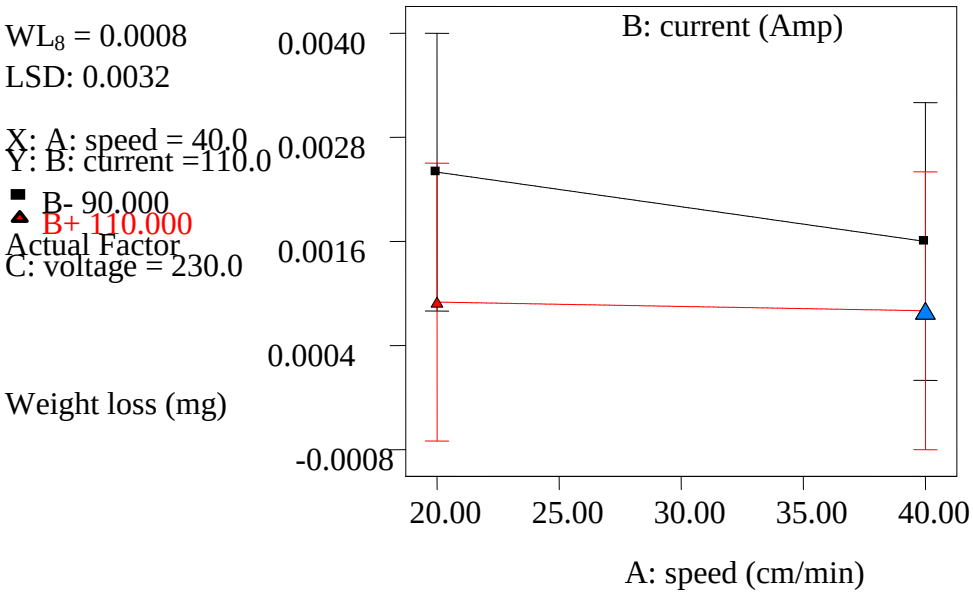

Appendix II: Interaction effect of speed and current at constant voltage on ASS immersed in NaOH for 16 days.

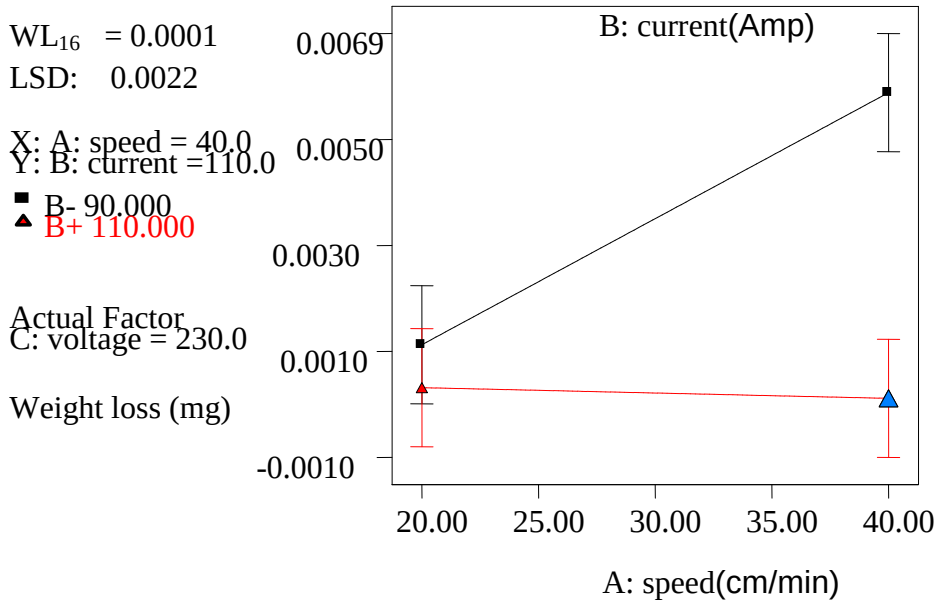

Appendix III: Interaction effect of speed and current at constant voltage on ASS immersed in NaOH for 24 days.

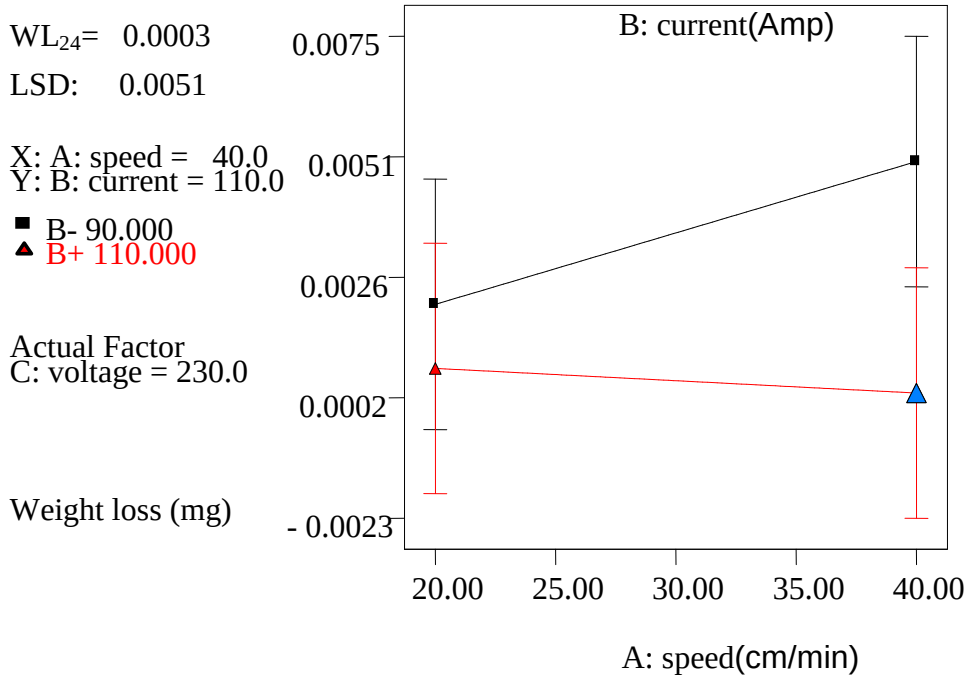

Appendix IV: Interaction of speed and current at constant voltage on ASS immersed in NaOH for 32 days.

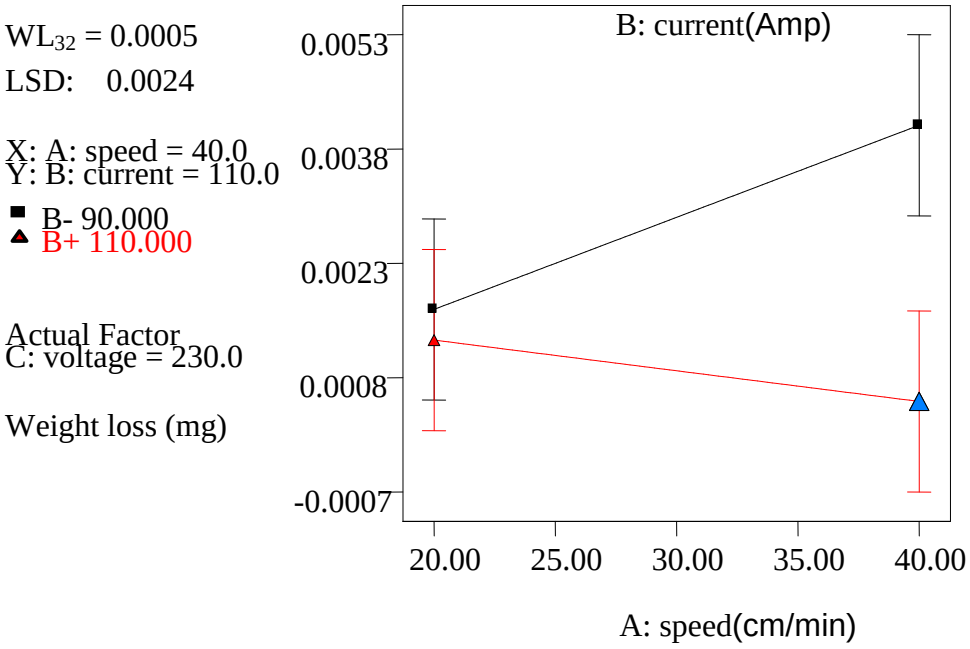

Appendix V: Interaction effect of speed and current at constant voltage on ASS immersed in NaOH for 40 days

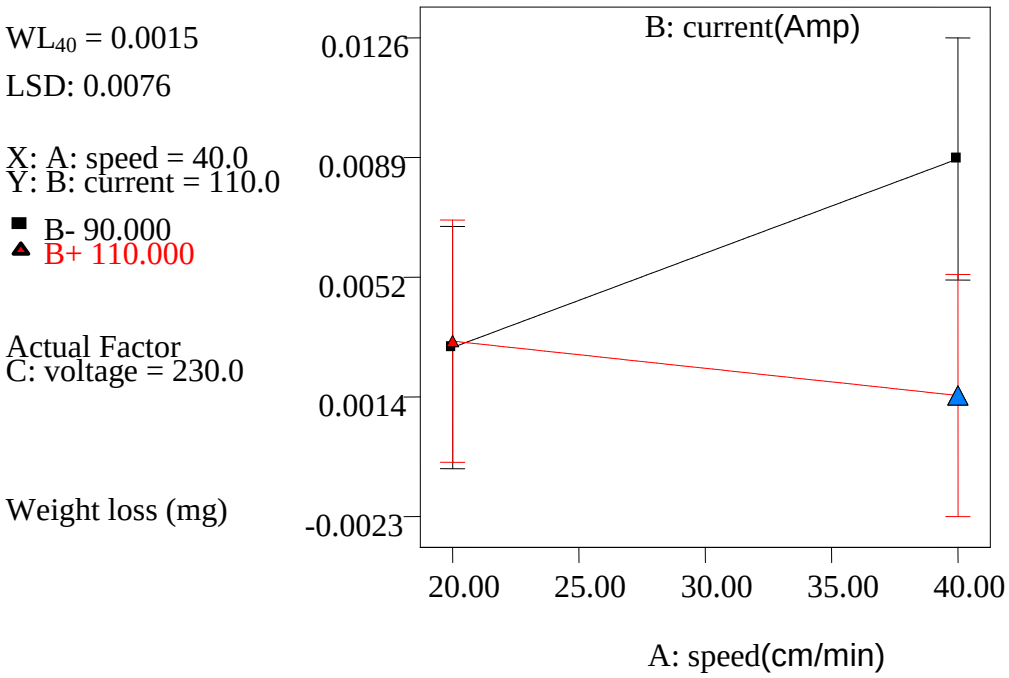

Appendix VI: Interaction effect of speed and current at constant voltage on ASS immersed in HCl for 8 days.

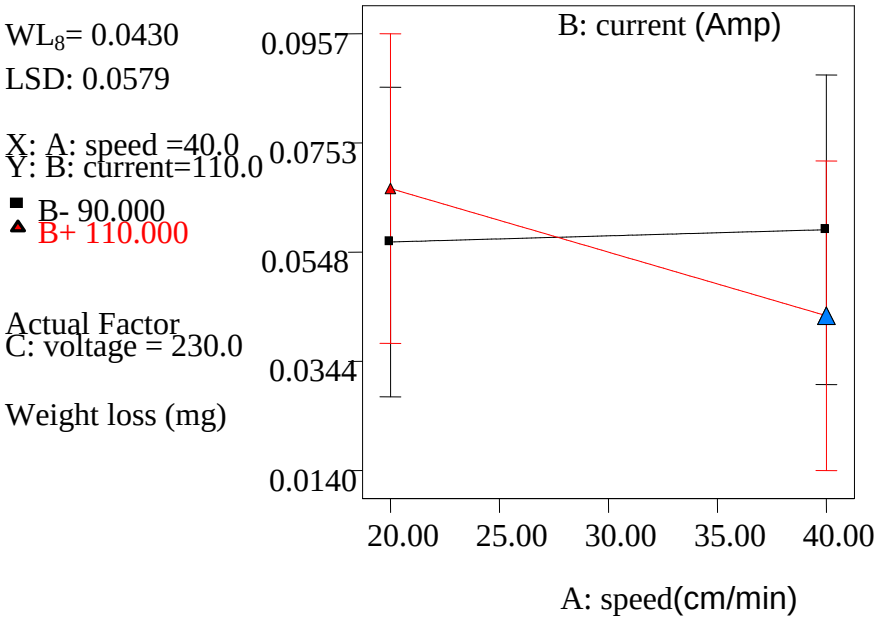

Appendix VII: Interaction effect of speed and current at constant voltage on ASS immersed in HCl for 16 days.

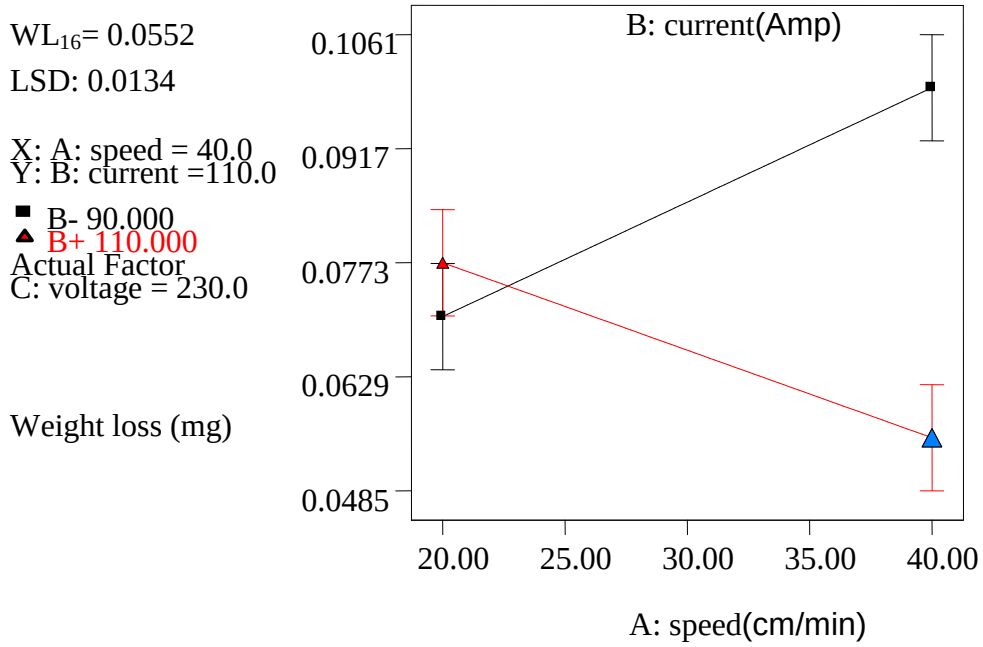

Appendix VIII: Interaction effect of speed and current at constant voltage on ASS immersed in HCl for 24 days.

WL_{24}= 0.0833

LSD: 0.1585

X: A: speed = 20.00
Y: B: current = 90.00

B- 90.000
B+ 110.000
Actual Factor
C: voltage = 230.0

Weight loss (mg)

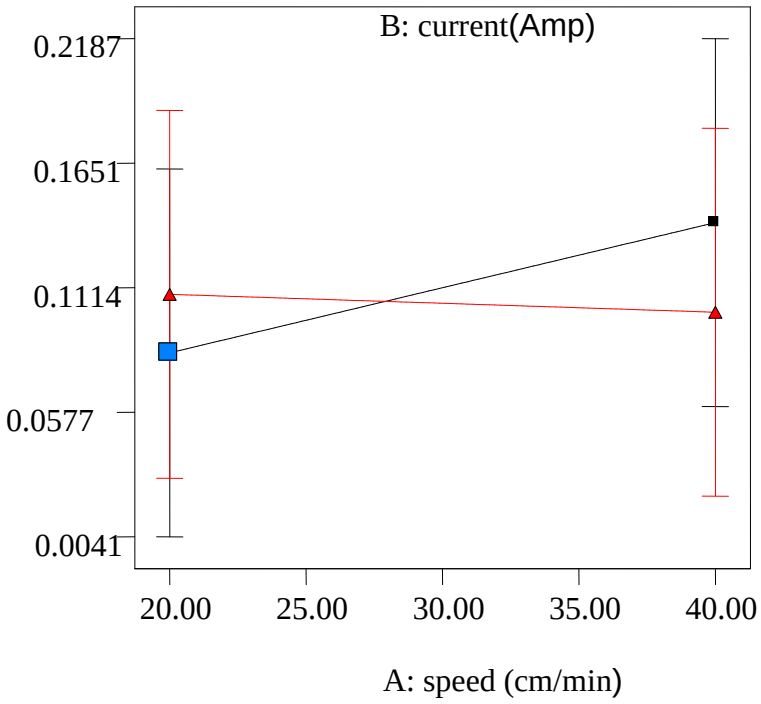

Appendix IX: Interaction effect of speed and current at constant voltage on ASS immersed in HCl for 32 days.

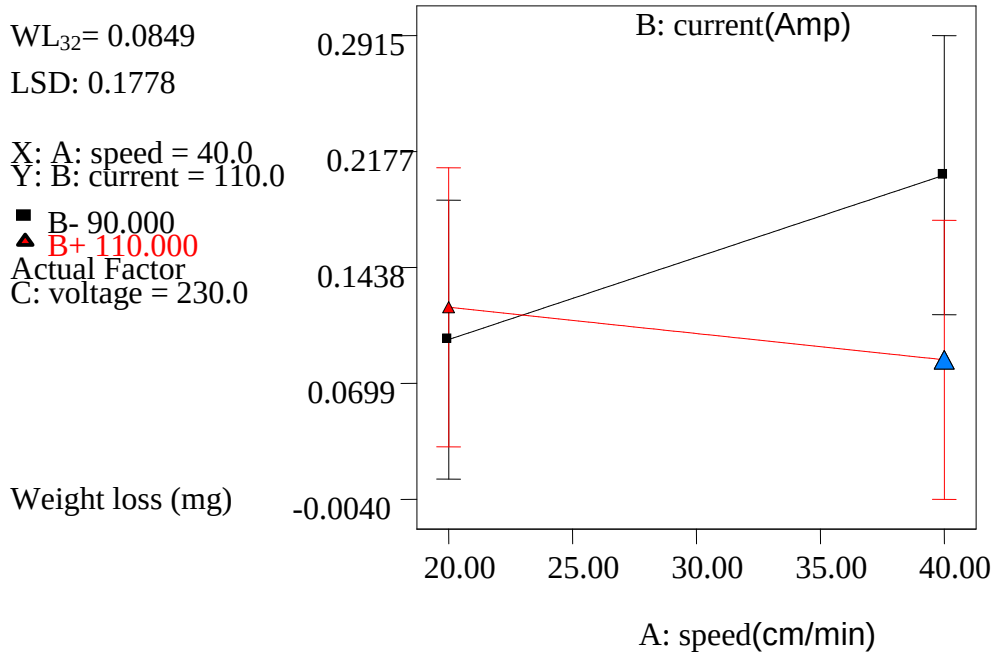

Appendix X: Interaction effect of speed and current at constant voltage on ASS immersed in HCl for 40 days

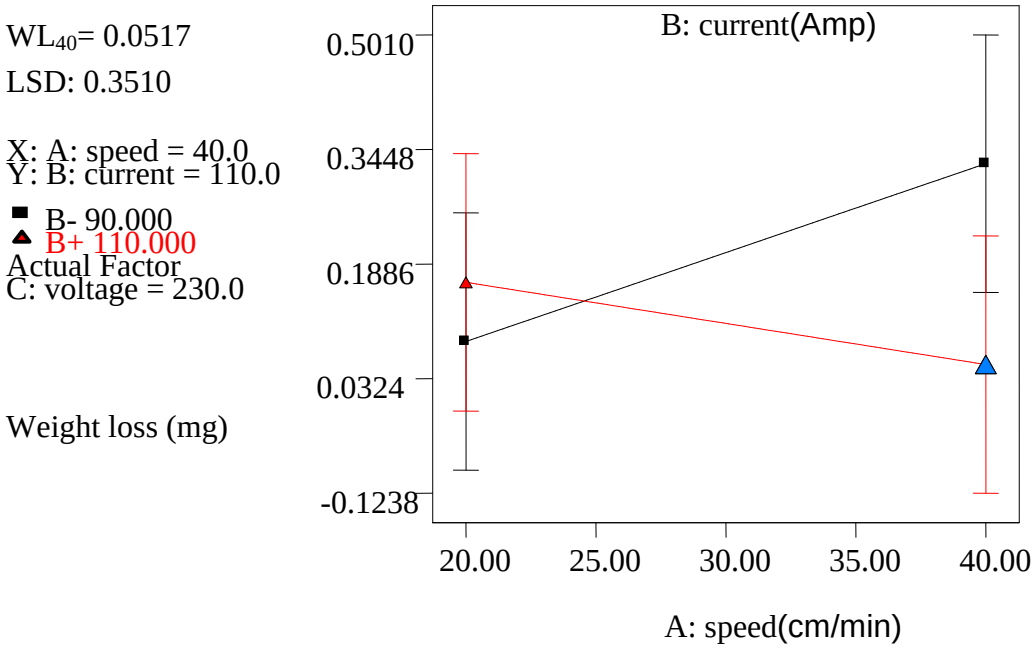

Appendix XI: (a) Grinding machine (b) GMAW machine

a

b

Appendix XII: (c) GMAW machine with welding wire spool and wire feeder (d) Tensile sample preparation on a milling machine**.**

c d

Appendix XIII: Welded and unwelded samples for impact, hardness and tensile test

Appendix XIV: Red-hot welded samples of ASS

Appendix XV: Hardness values from ASS samples immersed in NaOH

Sample	Location	Hardness Values, HRA					
		8 days	16 days	24 days	32 days	40 days	Control sample (C)
C1	FZ	21.3	26.0	24.4	23.3	23.8	28.6
	HAZ	29.5	31.1	31.7	30.8	30.8	33.2
C2	FZ	22.4	17.5	28.5	21.6	28.4	28.7
	HAZ	29.8	26.2	29.9	32.3	34.3	29.9
C3	FZ	25.3	27.7	28.7	24.1	28.0	30.2
	HAZ	32.8	31.4	33.0	30.6	37.1	35.1
C4	FZ	23.9	19.9	27.0	17.0	26.5	25.7
	HAZ	27.9	25.9	35.8	32.7	27.1	28.4
C5	FZ	28.4	23.3	26.7	20.3	17.8	26.0
	HAZ	34.2	31.4	36.9	33.4	30.4	28.1

Appendix XVI: Hardness test values from ASS samples immersed in HCl

Sample	Location	Hardness Values, HRA					
		8 days	16 days	24 days	32 days	40 days	Control sample (C)
C1	FZ	33.1	18.9	24.8	24.7	25.9	28.6
	HAZ	35.5	28.3	29.1	27.9	34.5	33.2
C2	FZ	17.4	25.7	18.0	15.2	26.5	28.7
	HAZ	34.9	29.7	27.4	24.1	31.2	29.9
C3	FZ	25.6	18.1	22.6	26.6	25.5	30.2
	HAZ	30.6	30.0	30.0	27.7	28.3	35.1
C4	FZ	23.5	24.2	25.1	30.1	24.0	25.7
	HAZ	27.4	30.1	27.1	32.2	32.9	28.4
C5	FZ	27.6	25.1	18.7	21.2	22.5	26.0
	HAZ	31.2	32.7	31.3	32.3	30.0	28.1

.

Appendix XVII: Tensile test from welded and unwelded control samples not immersed in media

Sample Label\Day	Maximum Load (KN)	Tensile strength (MN/m^2)	Extension (mm)	Strain	Percentage Elongation (%)
C	17.4	225	28.2	0.57	57
C_1	9.3	120	7.0	0.15	15
C_2	2.8	36	3.3	0.10	10
C_3	6.6	85	5.4	0.13	13
C_4	10.3	133	7.8	0.17	17
C_5	9.6	124	7.8	0.16	16

Key:

C = unwelded control sample

C_1 to C_5 takes their usual values as stated in figure 4.8

$$Tensile = \frac{Maximum\ load\ (N)}{Cross\ sectional\ area\ of\ the\ specimen\ (mm2)}$$

$$Strain = \frac{Change\ in\ length}{Guage\ length}$$

Percentage Elongation: Change in length over Original length x 100

Appendix XVIII: Tensile test values of welded samples immersed in sodium hydroxide and Hydrochloric acid environments.

Days of Immersion	Sample Label	Medium	Maximum Load (KN)	Tensile strength (N/mm^2)	Extension (mm)	Strain	Percentage Elongation (%)
8	C_1	NaOH	14.6	189	13.8	0.23	23
		HCl	10.5	136	7.8	0.14	14
16	C_2	NaOH	7.4	96	5.7	0.12	12
		HCl	3.8	49	4.0	0.09	9
24	C_3	NaOH	15.7	203	15.4	0.33	33
		HCl	11.7	151	8.9	0.19	19
32	C_4	NaOH	10.6	137	9.0	0.14	14
		HCl	8.4	109	6.6	012	12
40	C_5	NaOH	8.2	106	8.4	0.11	11
		HCl	6.1	79	5.4	0.10	10

Appendix XIX: Impact test of the samples immersed in NaOH medium

Sample	Impact test	8 days	16 days	24 days	32 days	40 days	Control sample (C)
C_1	Impact Energy (ft lb)	9.5	10.0	3.0	6.0	5.0	3.8
	Impact Energy(J)	12.9	13.6	4.1	8.1	6.8	5.2
C_2	Impact Energy (ft lb)	3.0	2.5	2.0	0.9	0.5	7.5
	Impact Energy(J)	4.1	3.4	2.7	1.2	0.7	10.2
C_3	Impact Energy (ft lb)	14.5	14.5	10.0	11.5	12.5	13.5
	Impact Energy(J)	19.7	19.7	13.6	15.6	16.9	18.3
C_4	Impact Energy (ft lb)	11.0	6.1	2.5	10.5	9.0	2.5
	Impact Energy(J)	14.9	8.3	3.4	14.2	12.2	3.4
C_5	Impact Energy (ft lb)	10.5	11.0	6.5	8.5	5.5	4.0
	Impact Energy(J)	14.2	14.9	8.8	11.5	7.5	5.4

Appendix XX: Impact test of the samples immersed in HCl medium

Sample	Impact test	8 days	16 days	24 days	32 days	40 days	Control sample (C)
C_1	Impact Energy (ft lb)	1.5	7.0	3.5	1.5	8.0	3.8
	Impact Energy(J)	2.0	9.5	4.7	2.0	10.8	5.2
C_2	Impact Energy (ft lb)	0.5	2.0	1.5	1.5	1.0	7.5
	Impact Energy(J)	0.7	2.7	2.0	2.0	1.4	10.2
C_3	Impact Energy (ft lb)	13.5	10.0	9.0	8.5	14.5	13.5
	Impact Energy(J)	18.3	13.6	12.2	11.5	19.7	18.3
C_4	Impact Energy (ft lb)	5.0	7.0	12.5	10.5	6.0	2.5
	Impact Energy(J)	6.8	9.5	16.9	14.2	8.1	3.4
C_5	Impact Energy (ft lb)	10.5	7.0	7.5	2.5	6.0	4.0
	Impact Energy(J)	14.2	9.5	10.2	3.4	8.1	5.4